CHALMERS

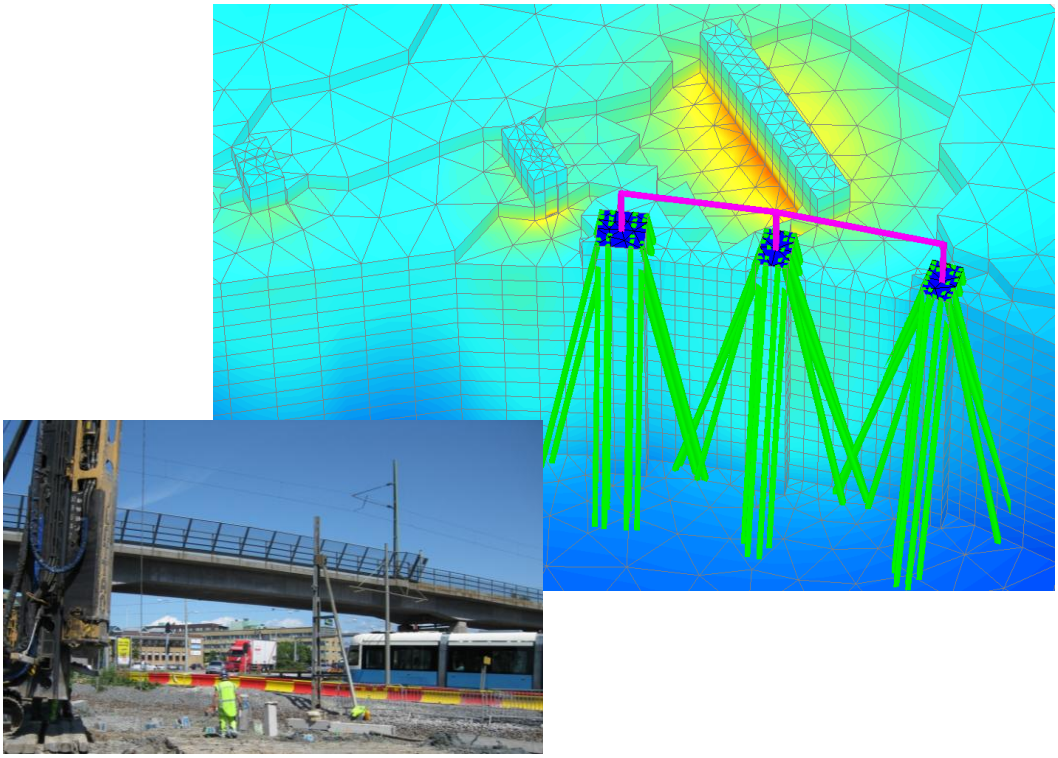

Environmental impact of pile driving

-An FE-analysis of the displacement of the Skäran bridge

Master of Science Thesis in the Master's Programme Structural Engineering and Building Performance Design

PAULINA NENONEN
JOHANNA RUUL

Department of Civil and Environmental Engineering
Division of GeoEngineering
Geotechnical Engineering
CHALMERS UNIVERSITY OF TECHNOLOGY
Göteborg, Sweden 2011
Master's Thesis 2011:38

MASTER'S THESIS 2011:38

Environmental impact of pile driving

-An FE-analysis of the displacement of the Skäran bridge

Master of Science Thesis in the Master's Programme Structural Engineering and Building Performance Design

PAULINA NENONEN

JOHANNA RUUL

Department of Civil and Environmental Engineering
Division of GeoEngineering
Geotechnical Engineering
CHALMERS UNIVERSITY OF TECHNOLOGY
Göteborg, Sweden 2011

Environmental impact of pile driving
-An FE-analysis of the displacement of the Skäran bridge

Master of Science Thesis in the Master's Programme Structural Engineering and Building Performance Design

PAULINA NENONEN
JOHANNA RUUL

Examensarbete / Institutionen för bygg- och miljöteknik,
Chalmers tekniska högskola 2011:38

Department of Civil and Environmental Engineering
Division of GeoEngineering
Geotechnical Engineering
Chalmers University of Technology
SE-412 96 Göteborg
Sweden
Telephone: + 46 (0)31-772 1000

Cover:
Soil displacements adjacent to bridge Skäran after four piling phases of the bridge Partihallsbron from simulation in PLAXIS 3D Foundation. Photograph taken by Anders Hansson 24 June 2009.

Reproservice, Chalmers University of Technology
Göteborg, Sweden 2011

Environmental impact of pile driving
-An FE-analysis of the displacement of the Skäran bridge

Master of Science Thesis in the Master's Programme Structural Engineering and Building Performance Design

PAULINA NENONEN
JOHANNA RUUL
Department of Civil and Environmental Engineering
Division of GeoEngineering
Geotechnical Engineering
Chalmers University of Technology

ABSTRACT

This thesis investigates the environmental impact, in terms of ground displacements, of pile driving. In particular the case of the railway bridge Skäran is analyzed. When constructing the bridge Partihallsbron in Göteborg several of the supports were placed very close to Skäran. The piling for the foundation of Partihallsbron caused ground displacements that in turn displaced Skäran. The movements of Skäran were predicted using a hand calculation method, Hellman/Rehnman, and the development of the displacements was closely monitored during construction by daily measurements at each of the supports. In this thesis, the soil movements and consequent impact on the piles of the foundation of Skäran are investigated using a finite element program; PLAXIS 3D Foundation. The effect of changing e.g. soil model and amount of pre-boring in the program is studied and the results are verified using the measurements of the displacements of Skäran. This study showed that a linear elastic soil model is easy to use and gives satisfactory results. The bridge deck and supports of Skäran are simplified to a beam-column system and the piles are modelled individually using a predefined element in PLAXIS 3D Foundation; embedded pile. The pile driving for Partihallsbron is simulated by lateral expansion of soil volume. The first four pile driving stages are modelled and the effects on the piles of support 3 of Skäran are examined. The analysis shows that the distance between existing piles and pile driving area, as well as the direction of inclination of the piles, has a noticable effect on the displacements. The piles placed closest to the piling area, together with an inclination towards the new piles, are subjected to large axial tension forces resulting in cracking of the concrete. Because the piles can only be modelled as linear elastic, the behaviour after cracking cannot be evaluated in PLAXIS 3D Foundation. When the construction is finished and the soil movements cease, the piles will go back to compression due to the loading from the bridge and the cracks may close again. A comparison of the FE-analysis and different hand calculation methods shows that the finite element analysis gives the best accordance with measured surface soil displacements. The hand calculation methods are fast and simple, but with a relatively simple model in Plaxis, a more advanced analysis can be done without an unreasonable time effort.

Key words: soil movement, ground displacement, pile driving, FE-analysis, PLAXIS 3D Foundation

Omgivningspåverkan orsakad av pålning
- En FE-analys av förskjutningarna av Skäranbron
Examensarbete inom Structural Engineering and Building Performance Design

PAULINA NENONEN
JOHANNA RUUL
Institutionen för bygg- och miljöteknik
Geologi och geoteknik
Geoteknik
Chalmers tekniska högskola

SAMMANFATTNING

I det här examensarbetet har omgivningspåverkan i form av massundanträngning på grund av pålning undersökts. Järnvägsbron Skäran har använts för att studera detta. Partihallsbron i Göteborg byggdes så att flera av stöden är i anslutning till den befintliga järnvägsbron Skäran. Pålningen för Partihallsbron orsakade jordrörelser som i sin tur orsakade rörelser utav bron Skäran. Skärans rörelser förutspåddes genom en handberäkningsmetod, Hellman/Rehnman. Skärans verkliga rörelser kontrollerades noggrant genom daglig inmätning av de olika stöden. I det här examensarbetet har jordrörelserna och påverkan på pålarna hos bron Skäran studerats i det finita elementprogrammet PLAXIS 3D Foundation. Effekten av ändring av t.ex. jordmodeller och mängd förborrning i programmet har studerats och verifierats med de uppmätta rörelserna av Skäran. Det har visats att linjär elastisk jordmodell är lätt att använda och ger tillfredsställande resultat. Brofarbanan och dess stöd är modellerade som ett pelare-balk system och pålarna är modellerade individuellt med det i PLAXIS fördefinierade elementet; embedded pile. Pålningen för Partihallsbron har simulerats med en lateral volymexpansion av jorden. De fyra första pålningsfaserna är modellerade och effekten på pålarna i Skärans stöd 3 har studerats. Analysen visar att avståndet mellan de befintliga pålarna och pålningsområdet är en viktig faktor tillsammans med riktningen på lutningen på de befintliga pålarna. Pålarna som ligger närmast pålningsområdet och som lutar så att pålfoten är närmast pålningsområdet utsätts för stora axiella dragkrafter och sprickor kommer uppstå. Eftersom pålarna endast kan modelleras som linjärelastiska så fångas inte beteendet hos det spruckna tvärsnittet i PLAXIS 3D Foundation. Pålarna kommer dock, när jordrörelserna avstannat, bli tryckta på grund av lasten från bron och sprickorna kommer troligtvis gå igen. Jämförelsen mellan FE-analysen och handberäkningsmetoder visar att finita elementmetoden ger bäst överrensstämmelse med uppmätta jordrörelser i ytan. Handberäkningsmetoderna är snabba och enkla att använda, men med en relativt enkel modell i PLAXIS kan en mer avancerad analys göras utan orimlig tidsåtgång.

Nyckelord: jordrörelse, omgivningspåverkan, pålning, FE-analys, PLAXIS 3D Foundation

Contents

Preface

This master's thesis has been carried out at the division of GeoEngineering at Chalmers University of Technology as a part of the master's program Structural Engineering and Building Performance Design. The study was initiated by Skanska Teknik as an extension of the research project "Skäranbron-rörelser vid påslagning för den närliggande Partihallsbron" (The bridge Skäran – movements due to pile driving of the adjacent bridge Partihallsbron) and the work was carried out at Skanska, the division of Geotechnics in Gothenburg. Claes Alén, at the division of GeoEnginnering at Chalmers, has been the examiner.

First of all we would like to thank our supervisor Anders Kullingsjö for making our work a priority and always taking time for us. We would also like to give our thanks to Torbjörn Edstam for his support and valuable thoughts.

Thanks also to Anders Hansson for helping us gathering information about the construction procedure of the bridge Partihallsbron. Gunnar Holmberg and Per-Ola Svahn have contributed with their knowledge which we are very grateful for.

Last but not least, we would like to thank our opponents, Fredrik Berg and David Johansson, for looking at our work from a different point of view and giving their comments.

Göteborg, May 2011

Paulina Nenonen and Johanna Ruul

Notations

Roman upper case letters

A	[m^2]	Area
E	[Pa]	Young's modulus
G	[Pa]	Shear modulus
I	[m^4]	Moment of inertia
K	[Pa]	Bulk/Volumetric modulus
M_{cr}	[Pa]	Cracking moment
N	[N]	Axial force
N_{cr}	[N]	Cracking axial force
N_{Rd}	[N]	Structural resistance to axial force
OCR	[-]	Over consolidation ratio
V	[m^3]	Volume
V_{cr}	[N]	Cracking shear force

Roman lower case letters

c	[Pa]	Cohesion
c_u	[Pa]	Undrained shear strength
$f_{ctk0,05}$	[Pa]	Fifth percentile tensile strength of concrete
f_{ctm}	[Pa]	Mean tensile strength of concrete
f_{syk}	[Pa]	Critical tensile strength of reinforcement
g	[m/s^2]	Gravity constant
u	[Pa]	Pore pressure
w_L	[%]	Liquid limit
w	[m]	Displacement
z	[m]	Depth in soil

Greek letters

γ	[-]	Shear strain
γ	[N/m^3]	Unit weight
γ_i	[N/m^3]	Unit weight of soil
γ_w	[N/m^3]	Unit weight of water
ε	[-]	Strain
ε_1	[-]	Strain in major principal stress direction
ε_3	[-]	Strain in minor principal stress direction
μ	[-]	Correction factor, shear strength
ν	[-]	Poisson's ratio
ρ	[kg/m^3]	Density
σ_0	[Pa]	In-situ stress
σ'_0	[Pa]	Effective in-situ stress
σ'_C	[Pa]	Pre consolidation pressure
σ_1	[Pa]	Major principal stress
σ_3	[Pa]	Minor principal stress
τ	[Pa]	Shear stress
τ_f	[Pa]	Shear stress, failure
φ	[˚]	Friction angle

1 Introduction

1.1 Background

The project Parthallsförbindelsen aims to connect the major roads E20 and E45 in central Göteborg and thereby decrease the traffic on highway E6 between Gullbergsmotet and Olskroksmotet. The project was initiated by the Swedish road administration in 1998 and Skanska Sverige AB started the construction in 2008.

During construction of Partihallsförbindelsen, the project "Massundanträngning vid pålslagning" (Ground displacements due to pile driving) was an additional research-project. The purpose was to evaluate different methods used to predict soil movements due to pile driving. The Hellman/Rehnman method, which currently is the most commonly used method in Sweden, was compared to a cavity expansion method proposed by Sagaseta. Some simulations were also made in three dimensional finite element analyses. The methods were compared to measurements of evolving ground displacements during piling for one of the bridge supports. (Edstam et al, 2010)

The comparison showed that the Sagaseta method was more accurate than the Hellman/Rehnman method (Edstam & Kullingsjö, 2010). Considering these results it is interesting to see if the Sagaseta method is applicable also for more complex surroundings. A new research-project "Skäranbron-rörelser vid påslagning för den närliggande Partihallsbron" (The bridge Skäran – movements due to pile driving of the adjacent bridge Partihallsbron) has been initiated to investigate this. (Edstam, 2010) A further step could be to compare the results from the comparatively simple method to those from a finite element analysis to find out if the extra resources spent on a FE-analysis are justifiable.

Large parts of the foundation for Partihallsförbindelsen were constructed in areas with existing structures. For one of the bridges, Partihallsbron, several of the supports were placed very close to existing infrastructure. Constructing the foundation of six of the supports were especially challenging because they are placed very close to the bridge Skäran. (Edstam et al., 2010)

The bridge Skäran is a railway bridge and therefore extra sensitive to dislocation and distortion. Since Skäran was in use during construction for the new bridge, it was necessary to take actions to minimize the movements. The relative displacement between two bridge supports was limited to 10 mm. Because of this, extensive measurements were made of the ground movements. The piling for the new bridge was also planned to ensure an even displacement of the whole bridge. For this, the ground movements were predicted using the Hellman/Rehnman method.

1.2 Purpose

The purpose with this thesis is to analyze the environmental impact, in terms of ground displacements, caused by pile driving for the new bridge "Partihallsbron". A finite element program is used to analyze the ground movements due to pile driving as well as the stresses created in the piles in the foundation of Skäran due to the displacements. The purpose is also to compare a finite element analysis to hand calculation methods used today.

1.3 Method

A literature study has been done to gain knowledge of the different methods for calculating ground displacements. Data from field measurements and pile protocols have been compiled and reviewed.

A study of the soil displacements during the piling for the foundation of one of the supports for Partihallsbron further away from Skäran has been done. This support is placed in an area with simple geotechnical conditions and extensive measurements were done during the piling. The results have been used to compare different models and input parameters in PLAXIS and to see how changing them affects the accuracy of the calculated displacements.

Using 3D PLAXIS Foundation, a simplified model of a part of the foundation of Skäran was created. A simplified model of the bridge has also been created to connect the supports. Thereafter, a simulation of the process of the pile driving for the new bridge was accomplished. The measurements of the movements were used to verify the model.

1.4 Scope

The ground movements have been calculated using PLAXIS 3D Foundation with focus on movements at Skäran. To simplify the calculations and get a reasonable calculation time only support 2, 3 and 4 have been modelled. The bridge has been simplified to a column-beam system due to the limitations of PLAXIS 3D Foundation. For Partihallsbron piling for support A17, and partially for A18 and A19, are modelled in four piling stages.

2 Theory

This chapter explains the theoretical background to this thesis, including the soil properties and ways of evaluating and modelling them, different methods for modelling ground displacements and some theory about how piles can be affected by ground displacements. Since the soil in the studied area consists of clay, this will be the material presented in this chapter. The piles in the studied bridge are precast reinforced concrete piles and the theory presented here applies to this specific kind of piles.

2.1 Soil properties

Soil is a material consisting of three phases; grains, water and gas. The grains build up a skeleton with pores in between, filled with water, gas or both. The shape and size of the grains as well as the material are important for the properties of the soil. The stress history is also important for the soil properties. (Sällfors, 2001)

2.1.1 Clay properties

Clay particles, which are the smallest grain size, less than 0,002 millimetres, have different properties compared to the larger grain sizes. Clay particles are connected by chemical bounds which give the soil its special properties compared to frictional soils e.g sand. (Sällfors, 2001)

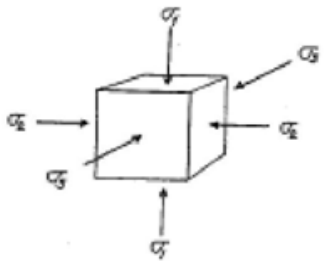

Figure 2.1 Stresses in positive main directions. (Sällfors, 2001)

The soil particles are subjected to stresses in three main directions, see Figure 2.1. When there is a horizontal soil surface, the principal stresses will be vertical and horizontal. The vertical stress is normally the largest and increases with depth and can be determined as follows (Sällfors, 2001):

$$\sigma_0 = \sum_{i=1}^{N} g \cdot \rho_i \cdot z_i \tag{2.1}$$

and

$$\gamma_i = g \cdot \rho_i \tag{2.2}$$

The total vertical stress is divided into effective stress, the stress carried by the particles or grains, and the pore pressure, see equation (2.3) (Sällfors, 2001).

$$\sigma_0 = \sigma_0' + u \tag{2.3}$$

If the pore pressure is hydrostatic, as in the studied area, it is described as:

$$u = g \cdot \rho_w \cdot z = \gamma_w \cdot z \tag{2.4}$$

For clay, its properties and behaviour are strongly connected to its stress history. All principal stresses, together with the water content, will affect the properties of the soil. When the soil is subjected to load, the load is carried by the grain skeleton and by the water. The water will gradually be squeezed out of the clay and more of the load will be carried by the grain skeleton. This phenomenon is called consolidation. The pre consolidation pressure is the maximum pressure the soil has been subjected to. The creep will also affect the pre consolidation pressure, for further information see e.g. Meijer & Åberg (2007). The rate of consolidation is important for the behaviour of the clay.

If the effective stress is below the pre consolidation pressure, σ_c, there will be small deformations and if the effective stress is higher than the pre consolidation pressure there will be large deformations due to the consolidation. Since clay is a low permeable soil, the consolidation will be time dependent. (Sällfors, 2001)

The deformation of soil can be divided into two parts; volumetric and deviatoric. The volumetric deformation is, for an isotropic homogenous material, depending on an, in all main stress directions, equal additional stress, see Figure 2.2. The deviatoric deformation depends on a deviatoric stress, when the horizontal and vertical stress unequal, see Figure 2.2. The deviatoric deformation can either be pure or simple shear. (Sällfors, 2001) Pure deviatoric deformation is when vertical and horizontal stresses are equal but have opposite signs and it will appear in undrained conditions. Pure volumetric deformation is unusual in nature, due to the anisotropic properties of soil. (Larsson, 2008)

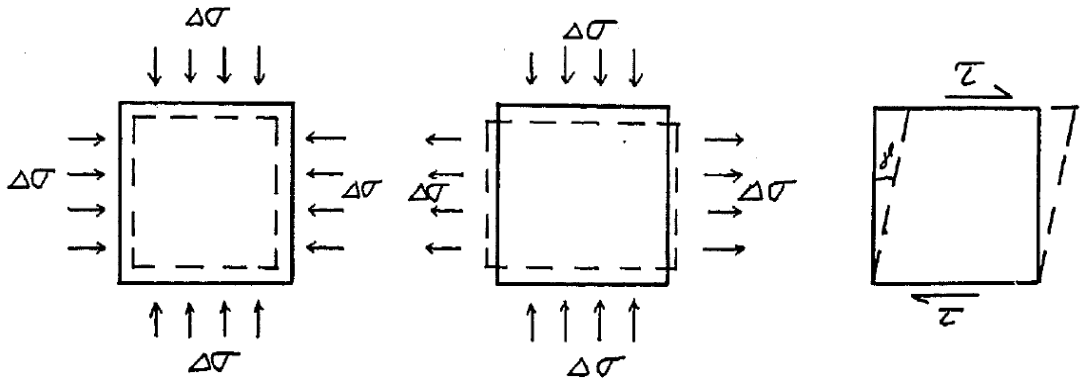

Figure 2.2 a) Volumetric deformation, b) deviatoric deformation due to pure shear and c) deviatoric deformation due to simple shear. (Sällfors 2001)

Volumetric modulus, *K*, and shear modulus, *G*, are two parameters that connect the stress to the deformation, see equations (2.5) and (2.8) (Larsson, 2008).

$$K = \frac{\delta p'}{\delta V} \tag{2.5}$$

where

$$p' = \sigma_1' = \sigma_2' = \sigma_3' \tag{2.6}$$

and

$$V = \varepsilon_1 + \varepsilon_2 + \varepsilon_3 \quad (2.7)$$

$$G = \frac{\delta\tau}{\delta\gamma} \quad (2.8)$$

For explanation see Figure 2.2 and Figure 2.3.

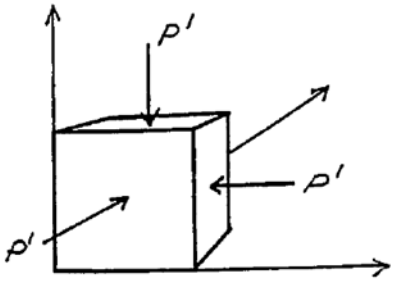

Figure 2.3 Volumetric change. (Sällfors 2001)

Poisson's ratio, *v*, describes the response of the material in compression and tension. It defines the relationship between the strains in the principal directions (Lundh, 2007). In the short term scenario, clay acts like water due to its low permeability. For an incompressible material, like water, Poisson's ratio is 0.5 (Sällfors. 2001). Poisson's ratio can be given as (Lundh, 2007):

$$\nu = -\frac{\varepsilon_3}{\varepsilon_1} \quad (2.9)$$

The elastic modulus can be described by a relationship between the bulk modulus, *K*, and the shear modulus, *G*, as equation (2.10) (Sällfors, 2001) or as equation (2.11) (Larsson, 2008).

$$E = \frac{3G}{1+{}^{G}/_{3K}} \quad (2.10)$$

$$E = 2G(1+\upsilon) \quad (2.11)$$

The elastic modulus and Poisson's ratio can be determined by triaxial tests while the shear modulus can be determined by simple shear test. (Sällfors, 2001)

2.1.2 **Shear behaviour**

Shear stresses occur when the soil is under non-isotropic pressure. The resistance to shear stress is called shear strength and can, in a simplified manner, be divided into drained and undrained shear strength. Since clay has a very low permeability, undrained conditions can be assumed, except for very slow loading where no excess pore pressure develops (Sällfors, 2008). Since the soil in the area considered in this thesis consists of clay, the shear behaviour described in this chapter will be the undrained. The undrained shear strength can be divided into three main cases depending on the direction of loading; active, direct and passive shear see Figure 2.4.

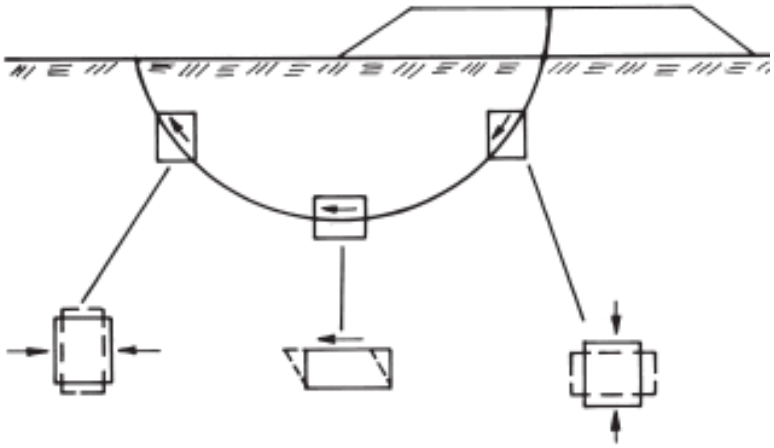

Figure 2.4 Stress situations in a slip surface. (Larsson et al., 2007. Modified)

These three stress situation can be simulated in soil tests. Active and passive shear can be said to correspond to active and passive triaxial tests respectively and direct shear to direct simple shear tests. (Larsson et al., 2007) However, in most modelling applications the value of the shear strength is treated as independent of loading direction (Kullingsjö, 2007). It is therefore important to determine which value is best suited for the modelled situation, and results from different tests must be corrected correspondingly, see Section 2.2.1-2.2.4.

2.2 Soil tests

When evaluating the undrained shear strength of a soil profile from different tests and empirical relations it is important to distinguish between the results from active and passive triaxial tests and results from other tests. The corrected values of the undrained shear strength from vane tests and fall-cone tests are assumed to correspond to the direct shear strength while the active and passive triaxial test results are normally the highest and lowest undrained shear strengths when taking anisotropic effects into account. (Larsson et al., 2007)

2.2.1 **Vane test**

Vane test is one way of measuring the shear strength in soil. The test is performed in the field with a rotating vane, see Figure 2.5. While the vane is rotating, the torsional moment is measured and when the moment exceeds the resistance in the soil, the soil will fail. The relationship between rotation and moment is recorded as well as the maximum required moment and from this the shear strength can be evaluated. (Sällfors, 2001)

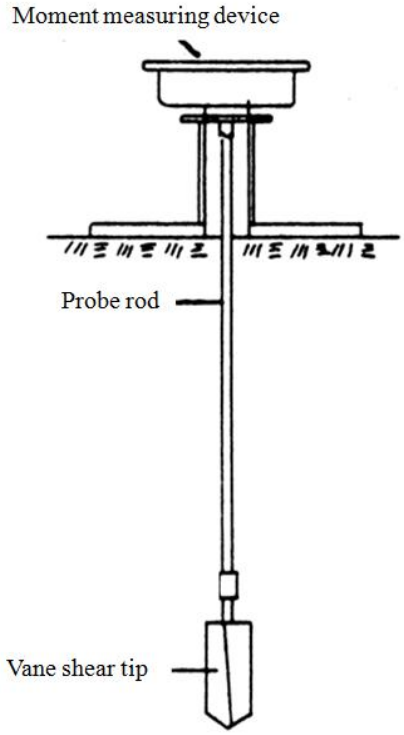

Figure 2.5 Principal sketch of a vane test instrument. (Larsson, 2008, Modified)

The results from the vane shear test, as well as the fall-cone test see Section 2.2.2, are corrected with regard to the liquid limit, w_L, of the soil, and correspond to the direct shear strength. For normally consolidated or slightly over consolidated clay the shear strength is evaluated according to equation (2.12) (Larsson et al., 2007).

$$c_u = \mu \cdot \tau \tag{2.12}$$

where $$\mu = \left(\frac{0{,}43}{w_L}\right)^{0{,}45} \geq 0{,}5 \tag{2.13}$$

Empirical values for the shear strength can be used to validate the results from the tests. The shear strength is a function of the pre consolidation pressure and the over consolidation ratio, *OCR*, according to (Larsson et al., 2007):

$$c_{u,empirical} = a \cdot \sigma_c' \cdot OCR^{-(1-b)} \tag{2.14}$$

where *a* and *b* are material parameters. The factors both vary depending on the loading situation and factor *a* also vary with the soil type. Normally it is assumed that *b*=0,8 and *a* for clay depends on stress situation as shown in Table 1 below.

Table 1 Material parameter a for calculation of empirical shear strength.

	$a \approx$
Active shear	$\mathbf{0,33}$
Direct shear	$\mathbf{0,125 + 0,205 \cdot \frac{w_L}{1,17}}$
Passive shear	$\mathbf{0,055 + 0,275 \cdot \frac{w_L}{1,17}}$

When the value for the liquid limit is unknown a = 0,22 is a reasonable estimation. (Larsson et al., 2007)

2.2.2 **Fall-cone test**

The undrained shear strength can be determined by the fall-cone test. The fall-cone test can be performed either with disturbed or undisturbed specimens. In the test, a weight formed as a cone is placed just touching the specimen, see Figure 2.6. The cone will then fall freely and the impact is measured. Depending on the cone and the impact, the shear strength can be determined using a diagram. (Sällfors, 1993) The results must be corrected in the same manner as for the vane shear test, see Section 2.2.1.

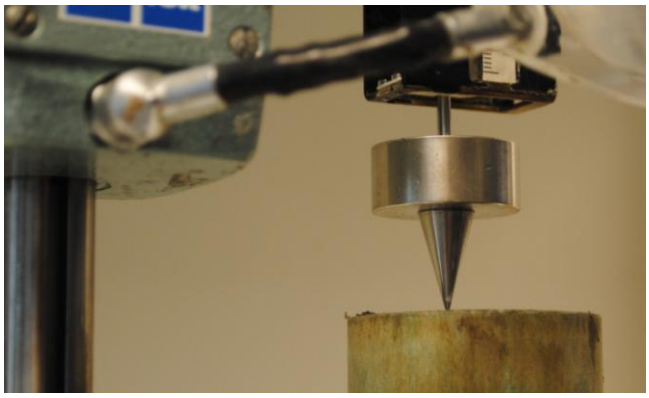

Figure 2.6 Fall-cone test.

2.2.3 **Direct simple shear test**

The direct shear strength can be evaluated using direct simple shear test (DSS). An undisturbed cylindrical specimen from the field is used for the test. The specimen is subjected to a normal force for consolidation after which the specimen is subjected to a shear force at the surface of the specimen. The specimen is enclosed in a rubber membrane and steel rings which prevents it from any volume change, see Figure 2.7. (Larsson, 2008)

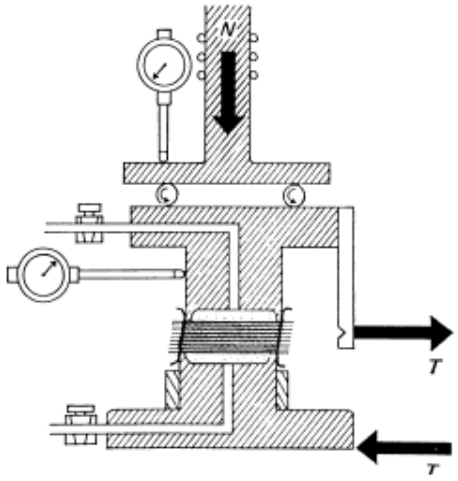

Figure 2.7 Principal sketch of a DSS device. (Larsson, 2008).

2.2.4 **Triaxial test**

In a triaxial test, the sample is placed in a cell filled with a liquid. The test could be performed either drained or undrained. The specimen is subjected to a pressure which results in an isotropic pressure. The relationship between vertical and horizontal stresses can be adjusted by tension or compression in a pole, see Figure 2.8. If the vertical load is increased, there will be an active failure and if the vertical load is decreased the fail will be passive. (Kompetenscentrum, -)

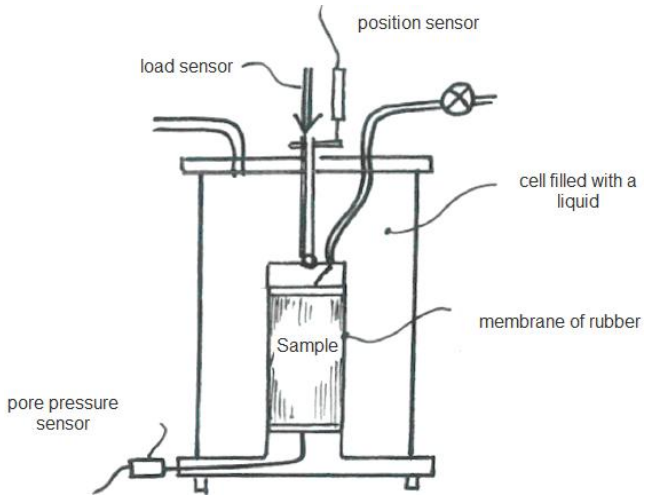

Figure 2.8 Triaxial test. (Kompetenscentrum, Triaxialförsök, 2011-03-07, Modified)

2.2.5 **Oedometer test**

In an oedometer test a sample is placed in a ring with filters below and above as in Figure 2.9. A load is applied from above, either incrementally or to ensure a constant deformation rate of the sample. A test where the deformation rate is kept constant is called CRS, or Constant Rate of Strain, test and is the most commonly used oedometer test today in Sweden. In the case with traditionally incremental loading the vertical load is doubled every 24 hours. The deformation during the test is measured

at certain time intervals and this results in time-settlement and load-deformation curves. From these curves the pre-consolidation pressure, σ'_c, and the consolidation coefficient, c_v, can be evaluated as well as the modulus. (Larsson, 2008)

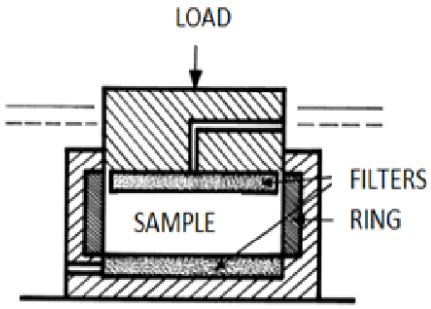

Figure 2.9 Principal sketch of an oedometer test device. (Larsson, 2008, Modified)

2.3 Modelling soil behaviour

When modelling the mechanical behaviour of soil the complexity of the model seems to relate to the accuracy with which the real behaviour is captured, according to Brinkgreve et al. (2007). To find a suitable model, the accuracy must be acceptable without getting a model too complex to work with. In this chapter the two different models used in the analysis in this thesis are described; the simple linear elastic model and the somewhat more complex ideal elastic-plastic model.

2.3.1 Linear elastic model

Linear elastic material is favourable to use for a simplified model. If the material is linear elastic, the deformation can be described knowing the elastic modulus, *E*, and Poisson's ratio *v*. Linear elastic models are applicable when the strains are relatively small, and when the material is homogenous and isotropic. Even though soil is more complicated due to its anisotropy, soil is often modelled as a linear elastic material. (Larsson, 2008)

In a linear elastic model the material has a linear relationship between stresses and strains as in Figure 2.10. When the material is subjected to a stress, the material will deform elastically. To deform elastically means that the material will regenerate its original shape when unloading.

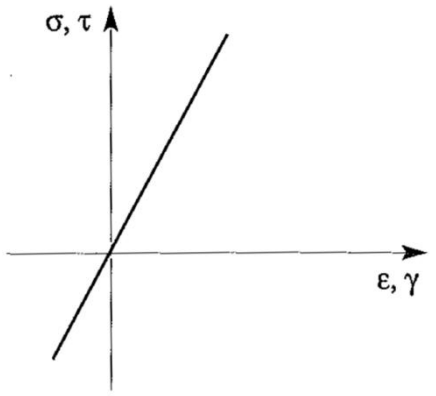

Figure 2.10 Linear-elastic material model. (Sällfors, 2001)

When using a linear elastic model and studying shear behaviour the material parameters can be exchanged to shear modulus, *G*, instead of elastic modulus, *E*, and Poisson's ratio, *v* (Kullingsjö, 2007).

2.3.2 **Elastic-plastic model with Mohr-Coulomb's failure criterion**

In an ideal elastic-plastic model the material behaviour is divided into two parts; elastic and plastic. In the elastic phase, the material behaves as described in the previous section while in the plastic phase the deformation will remain when unloading. The stress and strain relationship can be found in Figure 2.11.

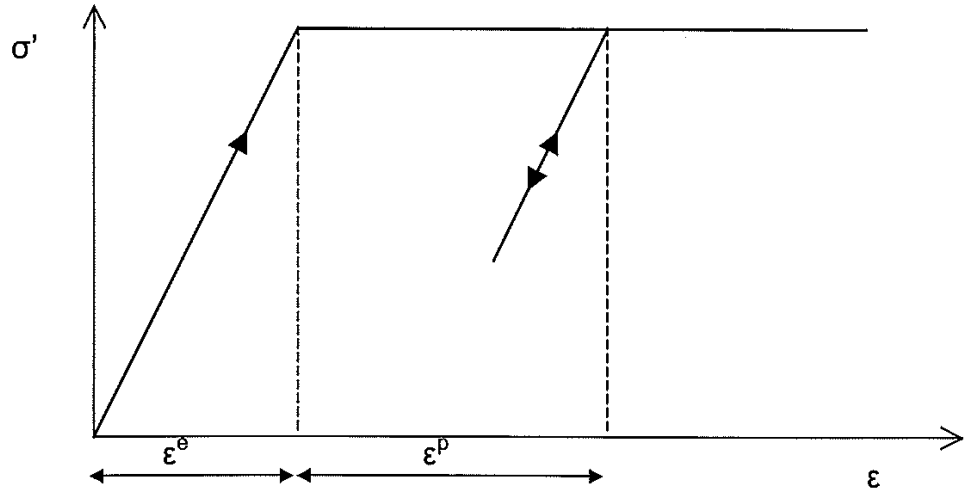

Figure 2.11 Elastic-perfectly plastic material model. (Brinkgreve et al. 2007)

A commonly used method for modelling soil is to use an elastic-plastic model with Mohr-Coulomb's failure criterion (Kullingsjö, 2007). The Mohr-Coulomb failure criterion is a model of the relation between the different strength parameters in soil; shear strength, cohesion and friction angle, see Figure 2.12. The Mohr-Coulomb failure criterion describes the border between linear elastic and plastic behaviour. The criterion states that:

$$\tau_f = c + \sigma \cdot \tan\varphi \tag{2.15}$$

The shear strength in the soil is determined by the cohesion, the stress and the friction angle.

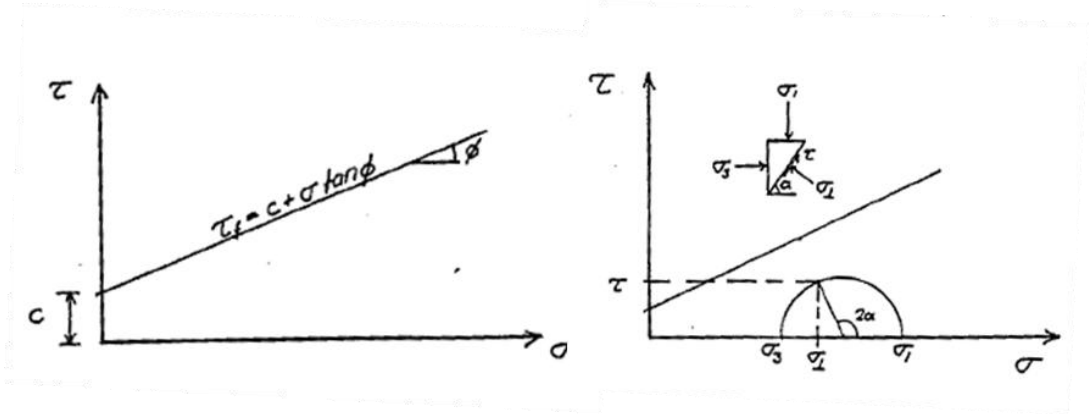

Figure 2.12 Mohr-Coulombs failure criterion and Mohr's circle. (Sällfors, 2001)

When the difference between the major principal stress, σ_1, and the minor principal stress, σ_3, see Figure 2.12, is increased, the radius of the circle will increase until the circle touches the line, or the failure envelope. This stress combination will result in shear failure. If σ_3 is negative the soil is in tension and soil has a very limited capacity in tension.

2.4 Methods for modelling ground displacements

Because clay is nearly incompressible in the short term scenario, every added volume, in form of e.g. piles, will cause soil displacements, see Figure 2.13. This can affect closely surrounding structures in negative ways such as uplift in adjacent piles or movements of nearby buildings (Sagaseta & Whittle, 2001). To compensate for the added volume, a commonly used action is to pre-bore the upper layer of the clay with a so called auger bore. The pre-augering can only be done to a certain depth, depending on the undrained shear strength and the *E*-modulus of the clay, otherwise the bore hole will collapse and the shear strength will be reduced due to the disturbance of the soil. (Olsson & Holm, 1993)

Figure 2.13 Soil movements due to pile driving. (www.tpub.com/eqopbas/163.htm, 2 May 2011)

2.4.1 **Hellman/Rehnman**

The Hellman/Rehnman method is a simple hand calculation method for calculating ground displacements and the most commonly used in Sweden. The theory is based on the assumption that the width of the affected area outside of the piling area is limited to one pile length, see Figure 2.14. In this method, the pre-boring is assumed to be to the same depth as the piles, even though it is not possible to pre-bore to large depths.

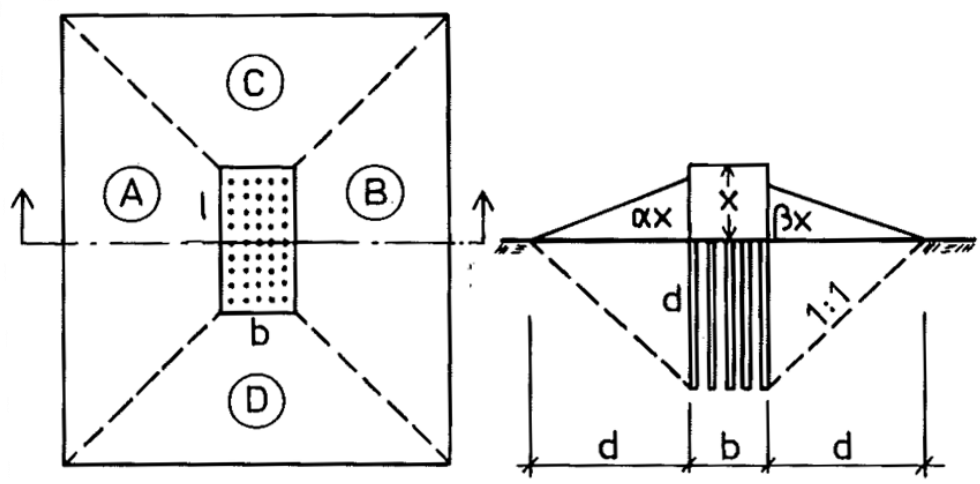

Figure 2.14 Soil displacements according to Hellman/Rehnman. (Olsson Holm, 1993)

The heave, displacement in vertical direction, is calculated using equation (2.16).

$$x = \frac{\eta(V_{piles} - V_{preauger})}{d\left[(\alpha+\beta)\left(\frac{l}{2}+\frac{d}{3}\right)+(\gamma+\delta)\left(\frac{b}{2}+\frac{d}{3}\right)+\frac{b \cdot l}{d}\right]} \quad (2.16)$$

x	heave [m]
η	heave factor [-]
V_{piles}	volume of piles [m^3]
$V_{preauger}$	volume of pre augering [m^3]
d	pile depth below ground surface [m]
l	length of piling area [m]
b	width of piling area [m]
α	heave factor of building [-]
β	heave factor of building [-]
δ	heave factor of building [-]
γ	heave factor of building [-]

The heave factor, η, describes the compressibility of the clay and can vary between 0.5 and 1. The heave factors, α- γ, are used to take the weight of the surrounding structures into consideration. The heave factors can vary between 0 and 1, where 0 is a heavy and 1 is a light structure. (Olsson & Holm, 1993)

The model can also be used to calculate the horizontal ground displacements. At the ground surface the horizontal and vertical displacements are considered equal. Below the surface the horizontal displacements decline linearly with depth, see Figure 2.15.

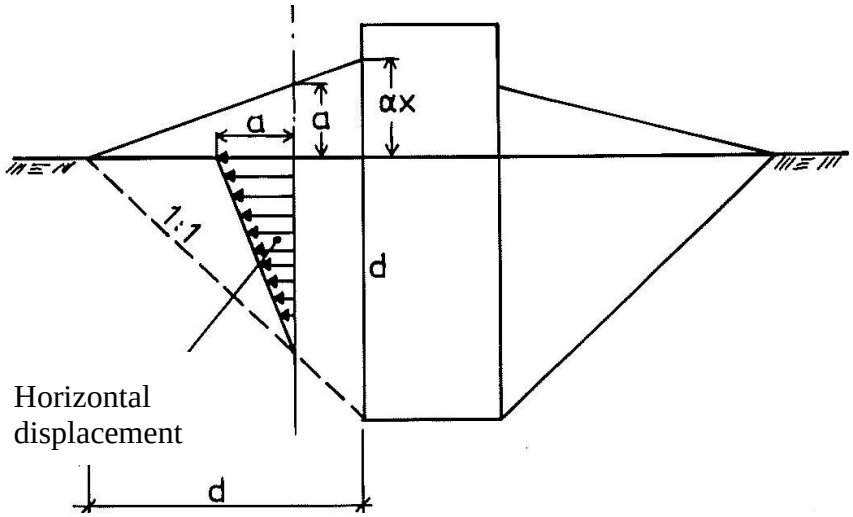

Figure 2.15 Horizontal displacements of the soil due to pile driving. (Olsson & Holm, 1993, modified)

2.4.2 **Cavity expansion, Sagaseta**

In the cavity expansion method, suggested by Sagaseta, the driving of a pile can be modelled in three steps, see Figure 2.16. This method is from here on referred to as the Sagaseta method. First the pile is modelled as a point-source, continuously emitting fluid in a spherical pattern while moving from the ground surface to the depth corresponding to the length of the pile, $z = L$. The surrounding is modelled as a non-viscous infinite media. In the second step a sink, absorbing the equal volume that is pumped out, is introduced. It moves in the opposite direction, up from the ground surface, to $z = -L$. This will cancel out the vertical displacements but double the horizontal, at the surface. In step three, to achieve a stress free surface, corrective surface tractions based on elastic theory are introduced.

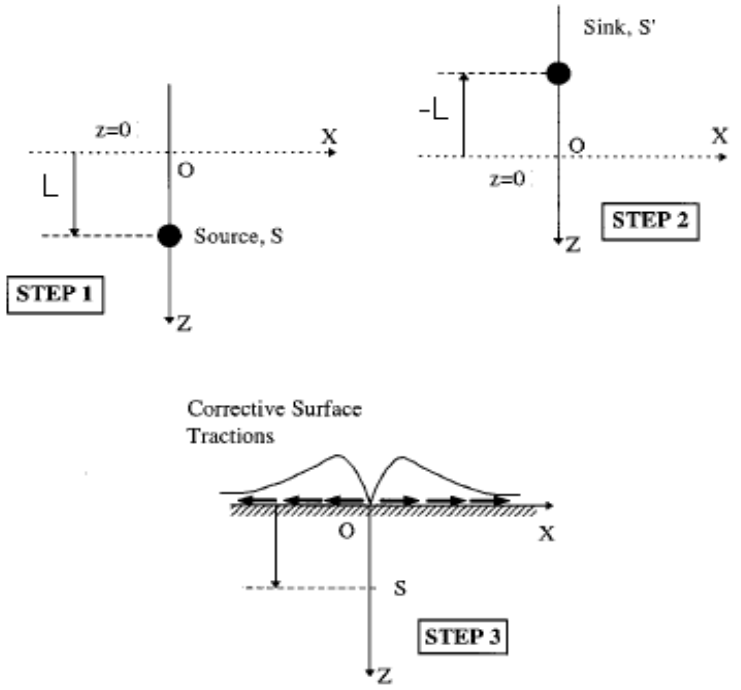

Figure 2.16 Conceptual model of the Sagaseta method. (Sagaseta et al., 1997, modified)

The velocities and strain rates from the three steps above is then numerically integrated to get the displacements. The soil movements in the surface can be calculated with equations (2.17) and (2.18):

$$\delta_r = \frac{R^2}{2} \cdot \frac{L}{r \cdot \sqrt{r^2+L^2}} \tag{2.17}$$

$$\delta_v = \frac{R^2}{2} \cdot \left(\frac{1}{r} - \frac{1}{\sqrt{r^2+L^2}}\right) \tag{2.18}$$

This method is not used for the analysis in this thesis, but results from another project where this method is used will be compared to the results from the finite element analysis in Section 8.3.1.

2.4.3 **FE-Analysis**

In the FE-analysis, mainly PLAXIS 3D Foundation is used. It is a numerical calculation program in three dimensions which uses two dimensional horizontal planes which are extruded in the depth direction to build up a three dimensional model. A horizontal layer is needed in all levels where there is a discontinuity. Boreholes are used to define the soil layers and pore pressure profile. The model used in this thesis is described in Chapter 6.

2.5 Effects on piles due to ground displacements

For lateral soil movements, moments and deflections develop in the piles. These vary with the soil properties, the stiffness and grouping of the piles. The section capacity, boundary conditions for the piles and the horizontal movement profile of the soil are also influential. For a very flexible pile, the deflection follow the movement of the soil, and small moments develop, while for a very stiff pile the deflections are small but the moments increase. (Poulos, 1973)

The response in passive piles is generally analyzed with either pressure-based or displacement-based methods. In the pressure-based methods, the calculated soil pressure is applied to the piles either directly or as an equivalent load. From the resulting pressure distribution the shear and bending forces can be calculated. In the displacement-based approach, the response in the pile is evaluated as a function of the relative displacements between soil and pile. (White et al., 2008)

To analyze the response of piles subjected to ground displacements either the finite element method or the finite difference method can be used (Poulos, 2005). In this thesis the finite element program PLAXIS 3D Foundation is used to find the displacements of the piles. The resulting moments and shear forces are evaluated using the equation of the elastic line (Lundh, 2007):

$$M(x) = -EI \cdot w''(x) \tag{2.19}$$

$$V(x) = -EI \cdot w'''(x) \tag{2.20}$$

The moment can be found by using the second derivative of the displacements along the beam, or in this case, pile. This will be compared to the cracking moment, M_{cr}, of the pile according to equation (2.21) (Al-Emrani et al., 2008b):

$$M_{cr} = \left(f_{ctk0,05} - \frac{N}{A_c}\right) \cdot \frac{I}{\left(\frac{h}{2}\right)} \tag{2.21}$$

There is also need to check the shear force in the pile. The shear force that causes cracking can be calculated according to equation (2.22) (Al-Emrani et al., 2008a):

$$V_{cr} = \frac{2}{3} \cdot f_{ctk0,05} \cdot A_c \tag{2.22}$$

The axial force can also cause cracking in the pile if the tensile force exceeds the axial cracking force, N_{cr}. This is calculated according to equation (2.23) (Al-Emrani et al., 2008a):

$$N_{cr} = f_{ctk0,05} \cdot A_c \tag{2.23}$$

The ultimate tensile strength in the piles can be approximated as the tensile strength of the reinforcement, since the cross-section will be cracked and the concrete therefore unable to resist any tensile force. The tensile strength of the reinforcement is evaluated according to equation (2.24) (Al-Emrani et al., 2008b).

$$N_{Rd} = f_{syk} \cdot A_{s,tot} \tag{2.24}$$

3 Description of the Area

The studied area is the area where the construction of Partihallsbron might affect the existing bridge, Skäran. The shortest distance in between the new and the existing bridge supports is about 10 meters. Six of the supports of Partihallsbron are placed in the area, considered as the effecting area of Skäran. The supports of Partihallsbron in the effecting area are called A16 to A21 (Edstam et al, 2010). However, in this thesis only A17 to A19 of Partihallsbron is of interest due to the order of the pile driving.

3.1 Properties of the soil

To find a suitable soil model for the calculations the results from soil surveys performed in the area have been analyzed. The soil consists of a deep layer of clay. Investigations have been performed both recently, for the construction of Partihallsbron, and before Skäran was built. Results from seven different boreholes near Skäran have been evaluated. For the borehole A4B, see Figure 3.1, vane shear tests and fall-cone tests have been performed. This was done in the geotechnical study for the construction of Skäran. More recent are the results from boreholes 32001, 32002, ST08-09, ST40 and ST42, see Figure 3.1. For borehole 32001 active triaxial, oedometer and direct simple shear (DSS) tests have been done, and for 32002 fall-cone and oedometer tests. For ST08 and ST40 the shear strength has been evaluated with both vane shear tests and fall cone tests, whereas for ST09 and ST42 only vane shear tests have been performed.

Borehole 32001 shows that the clay layer is thicker than 75 meters. The bedrock has not been reached in the tests.

Figure 3.1 Plan drawing; the bridge Skäran, supports A17-A21 for Partihallsbron and seven of the boreholes for the soil investigation.

3.1.1 **Undrained shear strength**

The behaviour of the soil in the area studied in the model is assumed to be something in between direct shear and passive shear, see Figure 2.13. The assumption is made due to the soil displacement where a horizontal displacement as well as a heave of the soil will occur. The undrained shear strength used as input in the model is chosen to correspond approximately to the direct shear strength.

The results from the fall-cone and vane tests are corrected according to equation (2.12) (see Section 2.2.1). The active triaxial shear test results are neglected since they correspond to the highest undrained shear strength and are not relevant. The results from the direct simple shear tests can be used directly.

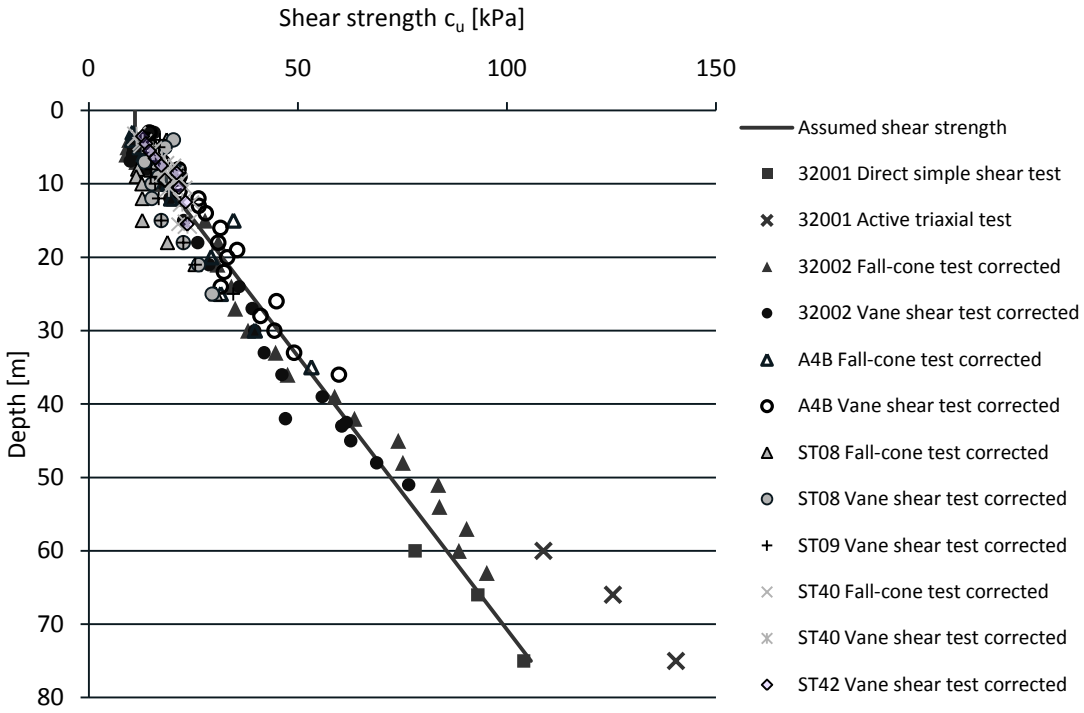

Figure 3.2 Shear strength from soil surveys in boreholes 32001, 32002, A4B, ST08-09, ST40 and ST42, and the assumed shear strength used in the soil model.

The results are plotted against the depth to find how the shear strength varies in the soil profile, see Figure 3.2. The outcome in input shear strength, an incremental value and a reference depth, where the strength starts increasing, are shown in Table 2.

3.1.2 **Shear modulus G_{50}**

Another strength parameter is the shear modulus at 50 % strength, G_{50}. From the DSS tests the modulus has been evaluated directly from the result curve, see Appendix 1. The elastic modulus, E, from the results from the active triaxial tests was used to find the corresponding shear modulus, see Appendix 1. Since these two tests have only been performed on soil samples from depths 60-75 m, the undrained shear strength was used to estimate an shear modulus for the rest of the soil profile, according to equation (3.1) (Kullingsjö, 2007).

$$G_{50} = 100 \cdot c_u \tag{3.1}$$

In the same way as for the shear strength the results are plotted in Figure 3.3 with the shear modulus assumed in the soil model.

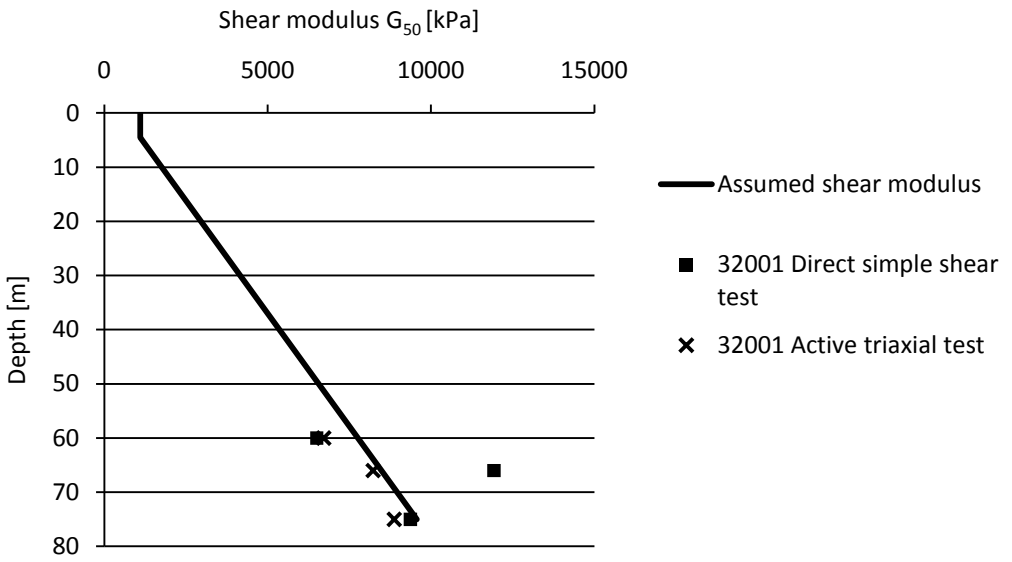

Figure 3.3 Shear modulus from soil surveys in boreholes 32001, 32002, A4B, ST08-09, ST40 and ST42, and the assumed shear modulus used in the soil model.

The value at depth 66 meters, from the direct simple shear test, shows a discrepancy compared with the rest of the values and was therefore disregarded. The resulting shear modulus, increment and reference depth is shown in Table 2.

Table 2 Evaluated input data for the shear strength.

Parameter	**Notation**	**Assumed value**
Shear strength [kPa]	c_u	**11**
Increment, shear strength [kPa]	$c_{increment}$	**1,5**
Shear modulus [kPa]	G_{50}	**1100**
Increment, shear modulus [kPa]	$G_{increment}$	**120**
Reference depth [m]	y_{ref}	**4,5**

3.2 Design of the Skäran bridge

The bridge Skäran is a continuous plate girder concrete railway bridge which was built during the 90s, see Figure 3.4.

Figure 3.4 Bridge Skäran. (Photo: Anders Hansson, 22 April 2009)

The bridge has 10 supports which are founded on piles. The bearings which the bridge deck is placed on have different movability; totally movable, partially movable or totally fixed. Generally, the bridge can be divided into two parts with one hinge in between, see Figure 3.5.

Figure 3.5 Hinge at support 4, bridge Skäran.

In order to prevent damage on the bridge bearings due to horizontal movements of the supports, the movable bearings are fixed with locks, see Figure 3.6. This horizontal movement will appear when piling for Partihallsbron and the locks are planned to be temporary. According to the designer of the locks, the maximum acceptable relative displacement between two adjacent supports is 10 mm.

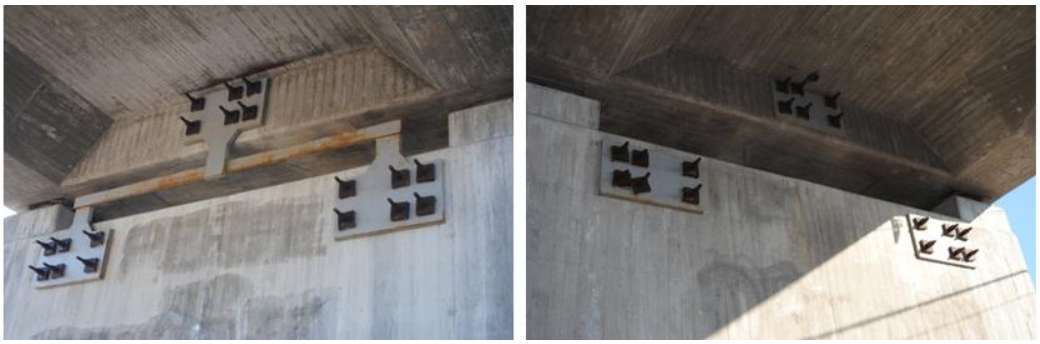

Figure 3.6 The lock of the bearings of Skäran, east and west side of the support.

The first five supports of the ten in total, counted from northwest, have cohesion piles. The sixth supports have both cohesion and end-bearing piles while the last four supports have end-bearing piles. Most of the piles are made of concrete and are of the type SP2 but some are SP3. SP2 and SP3 are standardized types of piles with the dimension 275x275 mm^2. The reinforcement of an SP2 is 8 ϕ 12 and made of the steel Ks60. The shear reinforcement is placed outside of the longitudinal reinforcement, see Figure 3.7, and made of steel with yield strength 390 MPa and diameter of 5 mm. The concrete is of the quality K50. The difference between SP2 and SP3 is the dimension of the longitudinal reinforcement, for SP3 the reinforcement is 8 ϕ 16.

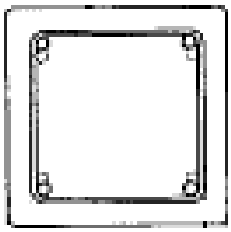

Figure 3.7 Cross-section of SP2 pile. (Olsson, Holm 1993)

In this thesis the focus is on support 2, 3 and 4. The lengths of the piles are varying but the supports of interest have piles which are between 59 and 71 meters, see Appendix 2.

The piles consist of jointed pile elements and the joints are so called ABB joints, see Figure 3.8. There is one part of the joint in the upper and one in the lower pile element and they are connected with four pegs.

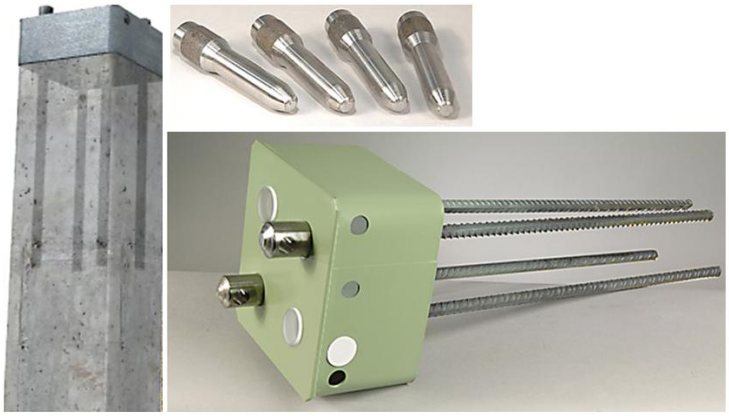

Figure 3.8 Pile joint. (http://www.leimet.fi/se/paalujatkos.php, 2011-04-04).

3.3 Design of Partihallsbron

The bridge Partihallsbron is a part of the connection Partihallsförbindelsen, a project to connect the two major roads E20 and E45. The bridge is about one km long and consists of four connected continuous plate girder bridges and two access ramp bridges, see Figure 2.1. The bridge is, at least partly, founded on 80-100 m deep layers of soft marine clay with ongoing settlements which makes the design of the foundation challenging. (Edstam et al., 2010)

The bridge is founded on five abutments and 40 intermediate supports. Most of the supports consist of two circular columns on a joint ground plate. The plate is in turn founded on steel kernel or concrete piles. (Edstam et al., 2010)

Figure 3.9 Photo montage of Partihallsbron. (www.trafikverket.se, 2011-05-10, Photo: Per Petersson)

Both cohesion and end bearing piles are used for the bridge foundation, but for the supports studied in this thesis, only concrete cohesion piles are used. The studied supports have piles with an inclination of 20:1 to 5:1 as well as some vertical piles, and the dimensions of the piles are 275x275 mm^2. The piles are mostly SP2 but some are SP3.

4 Pile-driving for Partihallsbron

To minimize the relative displacement between the supports of Skäran, the order of the pile driving for Partihallsbron was important. Relative displacement is here defined as the difference of the displacements of two adjacent supports. The intention was to move the whole bridge evenly instead of one support at a time. Before the construction was started the soil movements were predicted using the method Hellman/Rehnman and during the pile-driving the movements of the supports of Skäran were measured once each day.

4.1 Piling order

The purpose of the piling order was to cause an even displacement of Skäran, and thereby keeping the relative displacements at an acceptable level. Therefore not all the piles for each support were installed at the same time.

In this thesis, four piling phases are studied. For the section of Partihallsbron studied here, the first piling stage was in the south side of support A17. 24 piles were installed there before moving to support A18, where 24 piles were installed on the north side in stage two. In stage three 24 piles were installed on the north side of support A19 before going back to support A17 and installing the remaining 48 piles of that support in stage four. The areas of the different piling stages can be seen in Figure 4.2, where the different colours each represent one piling stage. In these four piling phases the pile length varies between 59 and 65 meters.

4.2 Pre-boring

Another measure that was taken to minimize the soil movements was pre-boring with an auger bore, which is shaped like a screw, see Figure 4.1. It is screwed into the ground to a depth of 10 meters and then the rotation of the screw is reversed. This makes the soil travel upwards along the screw to the surface. The diameter of the drill is 320 mm and the diameter of the core of the drill is 125 mm.

Figure 4.1 Preboring with auger bore. (Photo: Skanska, 28 January 2009)

For every installed pile in Partihallsbron, 10 meters pre-boring was done in the spot where the pile was to be installed. In some piling stages two holes were pre-bored for

each pile, and rows of holes, forming slits, were bored around the piling area. Because of lack of information of the exact procedure, two different interpretations of the quantity of pre-boring have been done; a maximum and minimum interpretation. There is also an uncertainty in the effective volume reduction when pre-boring with an auger-bore. In this thesis the volume reduction has been assumed to be the same as the volume for a pile, per unit length. It should be noted that this is an assumption and a possible source of error.

4.3 Calculated soil displacement according to Hellman/Rehnman

Initial calculations showed that the predicted movements were close to the limiting value; therefore the control of soil movements was important. The piling order was chosen according to the predicted movement by the method Hellman/Rehnman and the calculations were continuously updated during the construction according to the measurements made of the ongoing soil movements. (Edstam et al, 2010)

The predicted soil displacement due to the Hellman/Rehnman method can be found in Figure 4.2 and the calculations can be found in Appendix 3. In this method the heave and the absolute horizontal displacement at the surface are equal. The direction of the horizontal displacement is radial from the centre of the piling area. The colorized areas in Figure 4.2 represent the piling area in the particular piling phase. The black vectors show the total displacement after four phases.

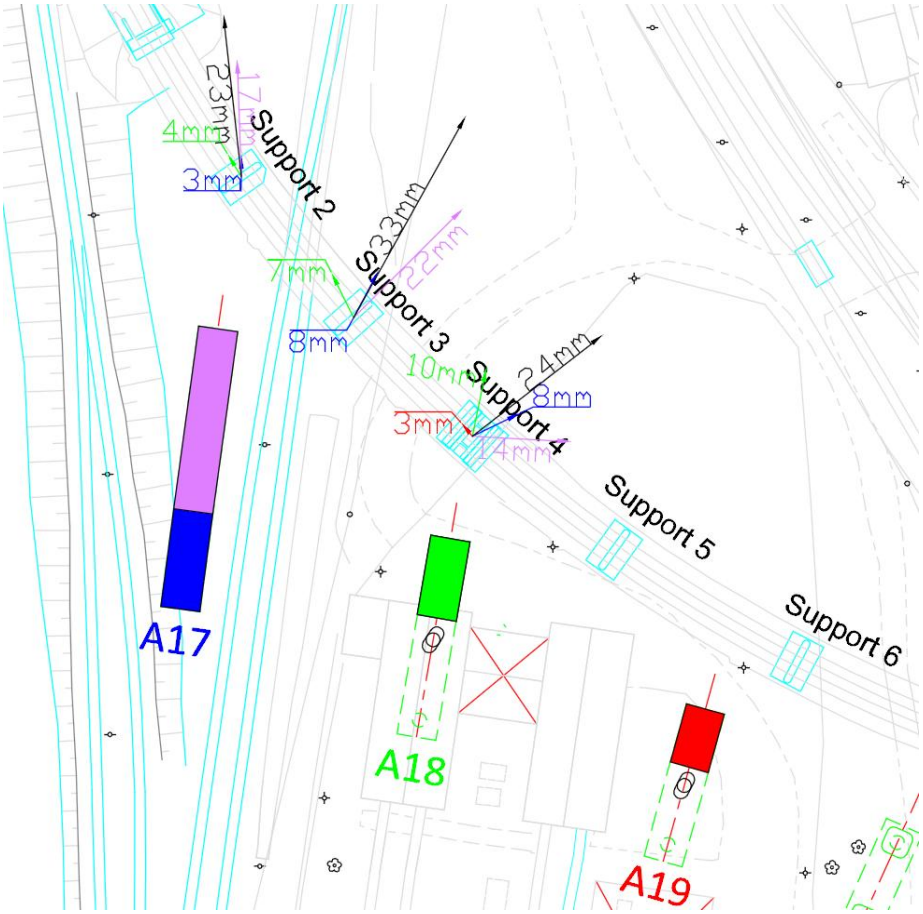

Figure 4.2 Horizontal surface displacement according to Hellman/Rehnman.

4.4 Soil displacements during piling

The measurements of soil displacements during piling were done once a day and compared to the predicted movements, which resulted in updated prognoses. Due to the locking of the bearings of Skäran, see Section 3.2, a precaution was that if half of the acceptable relative displacement (5 mm) was developed, measures were needed. Both measurements of horizontal and vertical displacements were done. The maximum horizontal displacement appeared at support 4 and measured 40 mm. The largest relative displacement was 6 mm which was below the limit but above the observational limit, half of the acceptable relative displacement.

The values used for comparison with the modelled displacements are the displacements after the different piling phases. In Figure 4.3 the measured displacements for support two to four for the first four phases are shown.

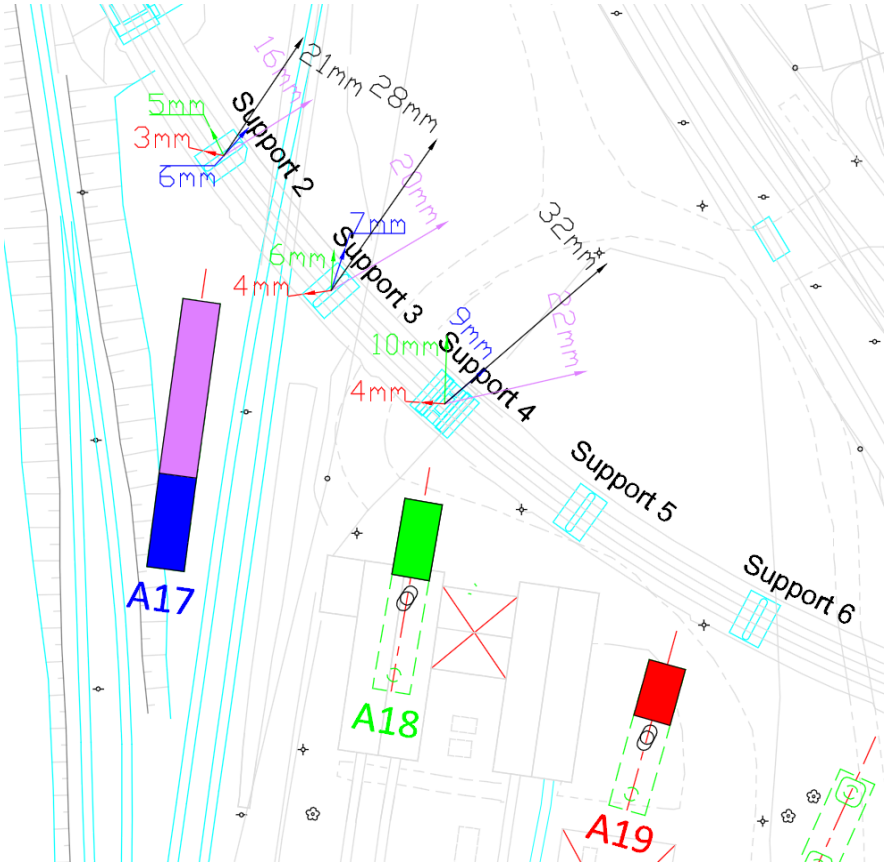

Figure 4.3 Measured horizontal displacements at the surface.

Table 3 shows the measured heave for the corresponding phases.

Table 3 Measured heave for the first four pile driving stages in millimeters.

	Stage 1	Stage 2	Stage 3	Stage 4	Total
Support 2	-3	1	3	3	4
Support 3	-2	2	3	8	11
Support 4	-2	5	4	4	11

5 Study of a Less Complicated Case

When modelling in PLAXIS Foundation 3D it is important to work with a simplified model and to make sure that the model captures the real behaviour of the soil. This is due to the complexity of the calculations and the prolonged calculation time. Therefore, a study was done on a less complicated case where effects of changing soil parameters and geometry could be studied. The direct effect of the changes is easier to ensure when there are fewer disturbances in the surrounding. The studied object is another support for Partihallsbron, A11, which is located in an area without prior constructions. During the construction of this support extensive measurements of the ground movements were done. This includes both surface movements and movements down to a depth of 45 meters. The measurements were done on the north and south side of the support. Due to uncertainty in the measurements with depth, an interval of the displacement is defined.

The studied support has 60 piles in total. Instead of modelling each pile individually, three super piles are used to symbolize 20 piles each with a length of 65 meters. The increase of volume in the ground, caused by the piles, is simulated by an expansion of a chosen volume in PLAXIS. So called clusters are drawn in the geometrical model to symbolize the super piles. A cluster is defined by lines and specifies the area for e.g. a floor, a horizontal load or a locally refined mesh.

5.1 Comparison of material models

In the study linear elastic and Mohr-Coulomb material models were compared. When calculating the horizontal displacements at the surface, both models give acceptable results, see Figure 5.1. Closer to the piling area, the Mohr-Coulomb material model corresponds slightly better with the measured horizontal displacements.

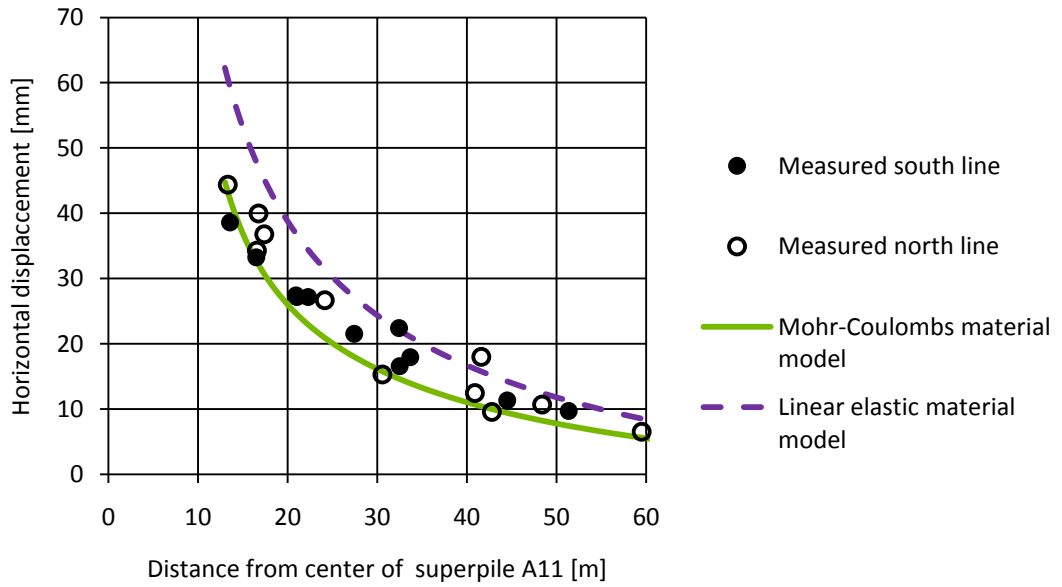

Figure 5.1 Comparison of material models, horizontal displacement at the surface.

There is a notable difference between the linear elastic and the Mohr-Coulomb material model when studying the horizontal displacement with depth. The Mohr-

Coulomb material model corresponds better to the measured horizontal displacement near the surface than the linear elastic material model, see Figure 5.2. The Mohr-Coulomb model captures the plastic behaviour of the soil close to the superpile, which results in a large heave and reduces the horizontal displacements. Therefore the deformation is larger for the linear elastic model near the surface. Below 10 meters the models give equally good results, with the Mohr-Coulomb model giving a lower bound and linear elastic model an upper bound solution. Below 40 meters, both of the models show very large displacements compared to the measured. The inclinometer that measures the movements below the surface is installed 17 meters from the centre of the piling area.

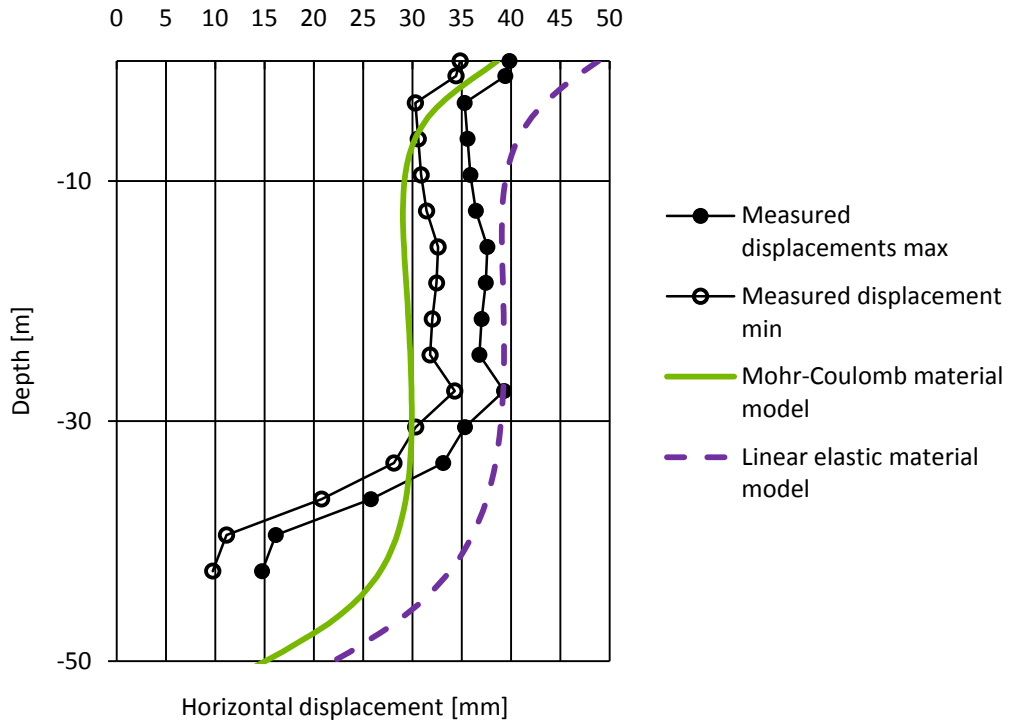

Figure 5.2 Comparison of material models, horizontal displacements with depth at 17 meters distance.

5.2 Comparison of geometrical models

In the geometric analysis three different approaches, using Mohr-Coulombs material model, were compared. The area of the cluster symbolizing the super pile was varied, and the volumetric expansion factor was adjusted accordingly. In the first approach the area of one superpile was equal to the area of 20 actual piles, which means that the volume increase of the cluster was 100 percent. In the second analysis, a larger area of the superpile and a volume increase of 10 percent were used. Thirdly, the area of the three superpiles was set to equivalent to the total support area and the volume increase to 4.38 percent. The third approach is the one where the soil behaviour corresponds best with the measured displacements, both in the surface and below, see Figure 5.3 and Figure 5.4.

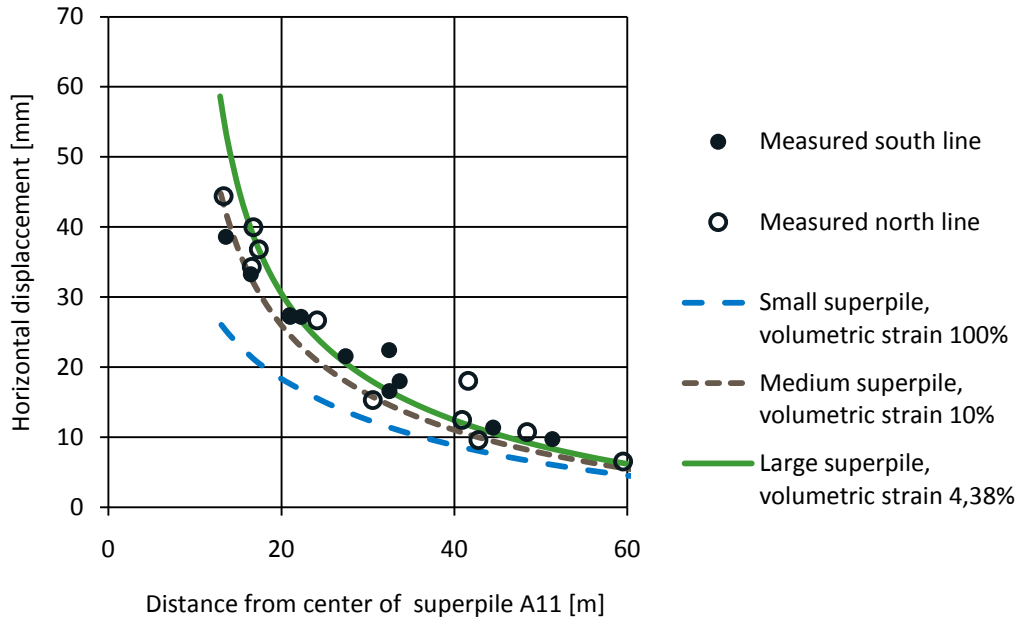

Figure 5.3 Comparison of geometrical models, Mohr-Coulomb, horizontal displacements at the surface.

The reason that the large model with small volumetric expansion corresponds best with measured values could be that a large volumetric expansion causes high stresses near the expanded cluster which in turn causes large localized heave in the area around the superpile. If a larger part of the expanded volume contributes to the heave, the horizontal displacements decrease. For figures with comparison of the heave, see Appendix 4.

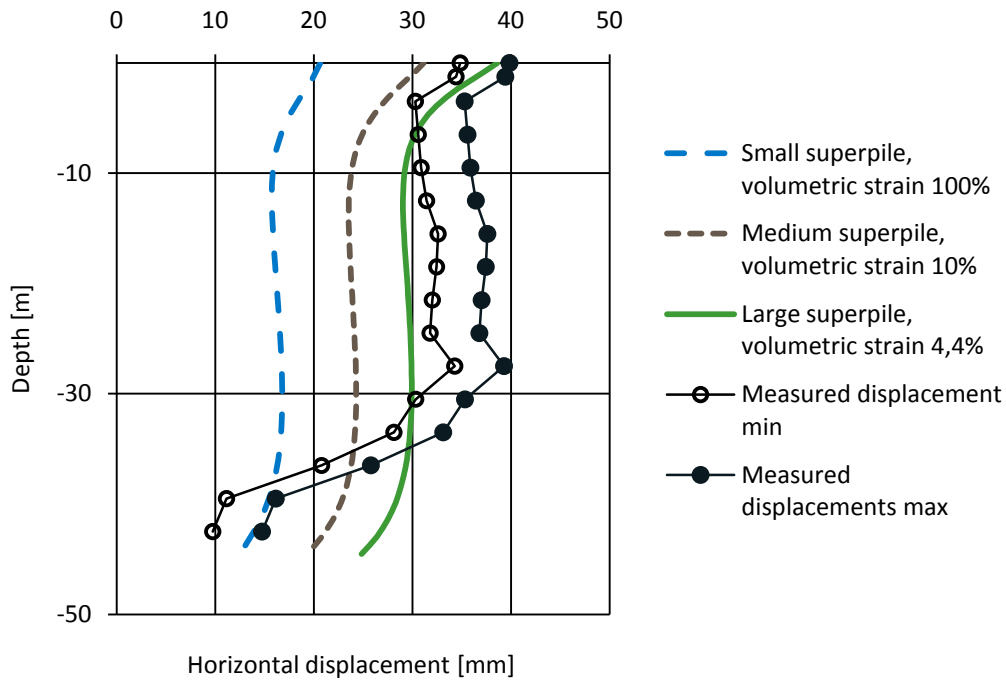

Figure 5.4 Comparison of geometrical models for Mohr-Coulombs material model, horizontal displacements with depth at 17 meters distance.

The same analysis was also done using a linear elastic material model; however the results were more or less independent of the geometrical model as is shown in Figure 5.5 and Figure 5.6.

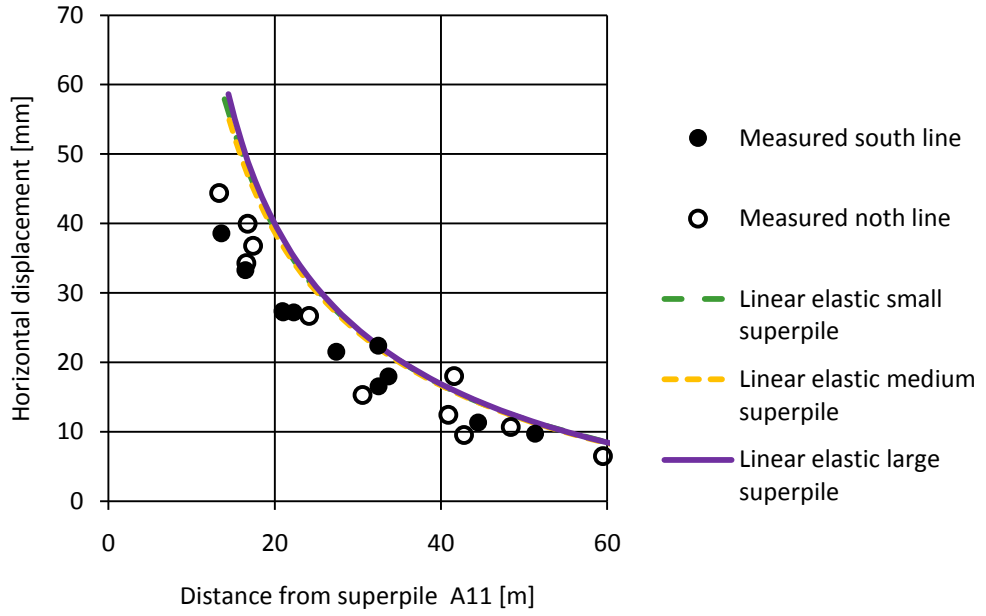

Figure 5.5 Comparison of geometrical models for the linear elastic material model, surface displacement.

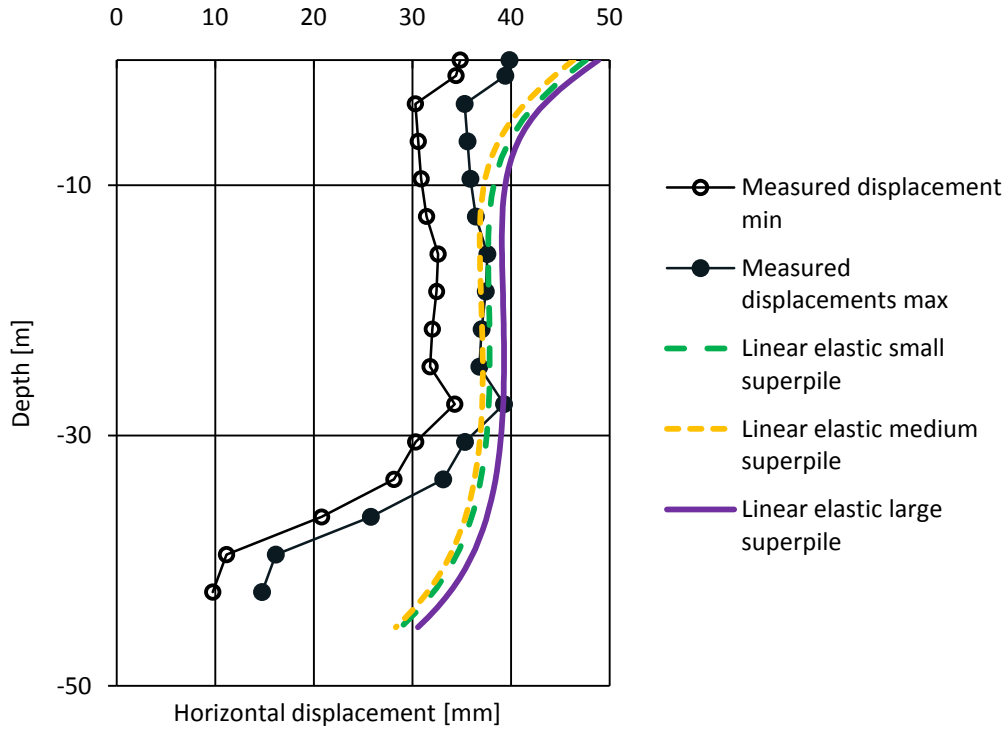

Figure 5.6 Comparison of geometrical models for the linear elastic material model, displacements with depth at 17 meters distance from the center of the superpile.

6 Model in PLAXIS 3D Foundation

As mentioned in Section 2.4.3 the finite element program used in this thesis is PLAXIS 3D Foundation. It is a program for geotechnical application with three main steps; input, calculation and output. In Section 6.4 the geometrical model created in the input step is described and in Section 6.5 the calculation phases defined in the calculation step are presented. The output is presented in the next chapter, Chapter 7.

6.1 Choice of soil model

From the analysis of a simpler case in Chapter 4 it becomes clear that a linear elastic material model, i.e. with a one phase material, of the soil gives the same accuracy as the more complex material model, Mohr-Coulomb. Therefore the linear elastic material model has been used in the analysis of the movements of Skäran.

The linear elastic model represents Hooke's law of isotropic linear elasticity and can be defined with two input parameters involving the stiffness, Young's modulus, *E*, or shear modulus *G*, and Poisson's ratio *v* (Brinkgreve et al. 2007). The linear elastic material is not affected by the pore water so a drained analysis can be done in this case.

The rest of the input parameters for the soil model are shown in Table 4. The shear modulus *G* is used instead of Young's modulus *E* but the incremental modulus $E_{incremental}$ is calculated according to equation (6.1) (Brinkgreve et al. 2007) and used as input, since $G_{incremental}$ cannot be used as input in PLAXIS 3D Foundation.

$$E_{incremental} = 2 \cdot (1 + \nu) \cdot G_{incremental} \tag{6.1}$$

The y_{ref} value is the depth where the modulus starts increasing.

Table 4 Input parameters for the linear elastic soil model.

Material type	γ **[kN/m^3]**	G_{ref} **[kN/m^2]**	E_{inc} **[kN/m^2/m]**	y_{ref} **[m]**	v **[-]**
Drained	16,5	1100	358,8	4,5	0,495

Poisson's ratio is chosen to simulate an incompressible material, which is true for clay in the short term scenario, see Section 2.1.1, but since the value 0.5 causes numerical problems in PLAXIS it is chosen to 0.495 (Brinkgreve et al. 2007).

6.2 The Skäran bridge

Since a model of the whole of Skäran with all its supports would be too complex to model in PLAXIS under the present conditions, supports 2, 3 and 4 have been chosen as the ones to be studied, see Figure 6.1. They are closest to the piling phases modelled for Partihallsbron, see chapter 6.3, and support 4 shows the largest total displacements.

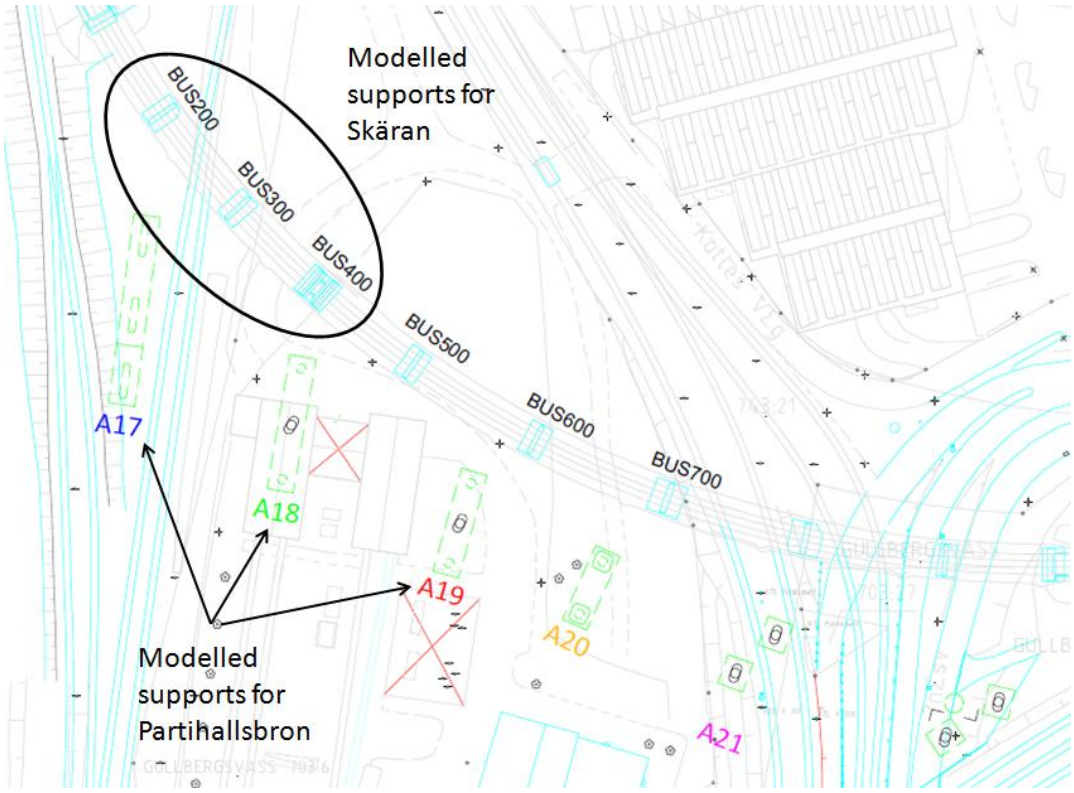

Figure 6.1 Parts of Skäran and Partihallsbron included in the FE-model.

The decision to study support 2, 3 and 4 was also based on the fact that there is a joint in support 4 which indicates that the movements of the two "halves" of the bridge are somewhat independent of each other, see Section 3.2.

6.2.1 **Foundation**

To model the piles in the foundation of Skäran the predefined structural element *embedded pile* in PLAXIS 3D Foundation is used. The *embedded piles* consist of linear elastic beam elements and interface elements to model the pile itself and the soil-pile interaction respectively. The piles can be placed in an arbitrary direction in the soil, and pass through the finite elements at any place. Inside the finite elements three additional nodes are created along the beam representing the pile, as shown in Figure 6.2. The interaction may include both skin resistance and foot resistance. The interface elements describing the skin friction along the pile are based on elements with pairs of nodes, where one node belongs to the beam element and one to the soil element. In Figure 6.2 the node pairs can be seen, where the black nodes belong to the beam and the blank gray circles to the soil. (Brinkgreve et al., 2007).

Each pile is modelled individually to ensure a correct response in the piles. This is important since the response in the piles is what is studied in the thesis. The piles are square, reinforced concrete piles with dimensions 275 mm x 275 mm. The input parameters for the piles are shown in Table 5. The inclination of the piles is included in the model in a slightly simplified manner where the direction of the inclination has been adjusted so that all the piles are inclined either in the direction of the centreline of the pile cap or perpendicular to it.

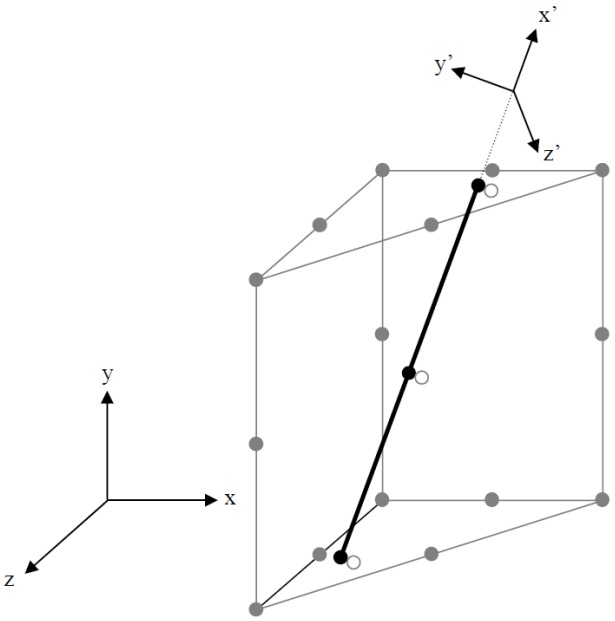

Figure 6.2 Illustration of finite element with embedded beam element denoted by solid line. (Brinkgreve et al., 2007)

A *floor* element is used to model the pile caps. Clusters are created for the three modelled pile caps and the *floor* element added to these clusters. The *floor* elements are defined by thickness, unit weight and stiffness, see Table 5, and in contrast to the embedded pile elements no interface elements are created along floors.

Table 5 Input parameters for the foundation of Skäran.

Structural element	**Element in PLAXIS**	***d* [m]**	***A* [m^2]**	***E* [kN/m^2]**	***γ* [kN/m^3]**	***ν* [-]**
Piles	Embedded pile	-	$0{,}275^2$	$3 \cdot 10^7$	24	-
Pile cap	Floor	1,3	-	$3 \cdot 10^7$	25	0,15

The attachment of the piles to the pile cap is modelled as rigid and the skin resistance of the piles has been approximated as linearly increasing with depth. The skin resistance T_{skin} is 11 kN per meter at the surface and increases to the shear strength of the soil at the bottom of the piles. This means that the skin resistance at the bottom of the piles vary with the length.

6.2.2 **Bridge**

Since PLAXIS 3D Foundation is a program for geotechnical applications there are some limitations of how the bridge can be modelled. The bridge itself is therefore simplified and modelled as a system of columns and beams using *vertical* and *horizontal beam* elements. These elements are given approximately the same stiffness, area and unit weight as the actual bridge to emulate its behaviour as well as possible, see Table 6. The calculations can be found in Appendix 5. In PLAXIS the beams and

columns have rigid connections, which is not the case in the actual bridge. But because of the fixation of the bearings with locks, see Section 3.2, this approximation is considered acceptable.

Table 6 Input parameters for Skäran.

Structural element	**Element in PLAXIS**	A **[m^2]**	E **[kN/m^2]**	γ **[kN/m^3]**	I_3 **[m^4]**	I_2 **[m^4]**
Bridge column	Vertical beam	5,84	$3 \cdot 10^7$	25	18,41	18,41
Bridge deck	Horizontal beam	6,22	$3 \cdot 10^7$	25	1,14	15,41

Because only a part of the bridge is modelled, see Figure 6.3, boundary conditions must be found for the vertical beams beyond support 2 and 4. The way this can be achieved in PLAXIS 3D Foundation is either with line fixities or with springs. The line fixities can be fixed in x-, y- or z- direction, or any combination of these. The springs can be given a specified stiffness and placed in any direction to simulate a partially fixed joint. Different alternatives were compared to see which results in movements that correspond best with that of the actual bridge. Since the results were not improved, see Appendix 6, the bridge was left free at support 2 and 4. The actual conditions, with adjacent supports partially fixing the studied part of the bridge, but also moving themselves, cannot be modelled in a simplified way in PLAXIS 3D Foundation.

Figure 6.3 Modell of support 2, 3 and 4 of Skäran.

6.3 Foundation of Partihallsbron

The pile-driving for the foundation of Partihallsbron is modelled in the same way as for the less complicated case studied in Chapter 4, which is by drawing clusters and expanding them laterally. This will result in equal horizontal stresses but no vertical stresses, compare with Figure 2.2. Each stage of the pile-driving is modelled separately so that the effect of each stage can be studied. The areas that represent the various stages are chosen to correspond as well as possible with the actual piling area. The resulting volumetric expansions are show in Table 7.

Table 7 Input data for pile-driving stages 1-4.

Pile driving stage	**Support**	**Area [m^2]**	**Depth [m]**	**Volumetric strain [%]**	**Pre-augering [m^2]**	
					min	**max**
1	A17 south	80,4	59,3	2,26	-	-
2	A18 north	65,5	65,6	2,77	1,21	2,42
3	A19 north	49,1	58,7	3,70	2,65	4,46
4	A17 north	136,4	63,5	2,66	-	3,63

The volumetric expansions are between 2.26 and 3.70% which correspond quite well with the "large superpile" geometrical model in Chapter 5, but since we use a linear elastic model for the soil the effect of the geometric model on the results is quite small, see Section 5.2.

Because of the sensitivity to movements of Skäran, measures had to be taken to decrease the soil movements when piling for Partihallsbron and this was done by pre-boring with auger bores, see Section 4.2. The pre-augering has been taken into account in two different ways; reduction of expansion and excavation. The pre-augering for the piles has been simulated by not having any volumetric expansion above the depth 10 meters. The effects of the slits that were bored around some of the supports are accomplished by excavating areas corresponding to the amount of pre-augering, down to 10 meters. The areas for the two pre-augering alternatives, as discussed in Section 4.2, are shown in Table 7. The excavations have been placed in approximately the same area as where the slits were made. Because of the uncertainty of the exact amount and the effectiveness of pre-augering a sensitivity analysis has been made and the results are shown in Section 7.3.

6.4 Mesh generation

To perform a finite element calculation the geometry is divided into elements and the elements compose a finite element mesh. When generating the mesh in PLAXIS 3D Foundation, the difficulty is to find a mesh fine enough to give accurate results but not so fine that the calculation time becomes unreasonable or that the model becomes to extensive for the computers RAM. When creating the mesh in PLAXIS 3D Foundation, a two-dimensional mesh is first generated in the work plane. When this is

satisfactory the three-dimensional mesh is created by extruding the two-dimensional mesh in the direction of the depth.

The horizontal, two-dimensional mesh consists of six node triangles. It is based on a triangulation procedure and results in a so-called unstructured mesh which give better results than regular, structured meshes. (Brinkgreve et al., 2007) These triangles are then extruded into 15-node wedges, see Figure 6.4. In case there are any non-horizontal layers in the model, special care must be taken when generating the mesh.

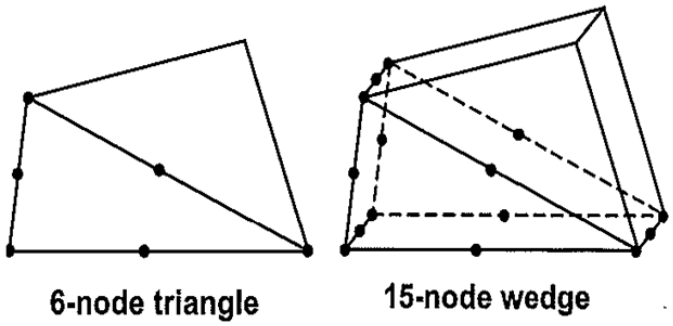

Figure 6.4 Mesh elements in PLAXIS. (Brinkgreve et al., 2007)

The horizontal mesh can be refined globally, in an area defined by a cluster, along lines or in geometrical points. The vertical mesh can be refined by adding work planes, but every work plane will have the same horizontal mesh. Therefore the vertical mesh cannot be refined in just a certain area.

6.5 Calculation phases

When defining the calculation phases in PLAXIS 3D Foundation the order of the pile-driving is followed. The type of calculation chosen is *Plastic calculation* which performs an elastic-plastic deformation analysis, which is appropriate for most geotechnical applications (Brinkgreve et al., 2007). The *staged construction* approach is used to specify the different construction stages.

In the initial phase the initial stresses in the soil are calculated. This can be done with either *Gravity loading* or the *K0 procedure*. With *Gravity loading* the soil weight, and weight of structures if any, is applied and the initial stresses are calculated by means of finite element calculation. In this analysis *K0 procedure* is chosen and works well because of the homogenous soil with horizontal surface. When this option is adopted, PLAXIS generates vertical stresses that are in equilibrium with the soil, but it does not take weight of structures into consideration. (Brinkgreve et al., 2007)

In the next phase, Phase 1, the existing bridge, Skäran, is put in place. This is done by activating the structural elements in the bridge, the piles, pile caps and columns and beams that correspond to the bridge. It is important to choose the option *set displacements to zero* in the following phase, to eliminate the effects of installation of Skäran, since it was constructed a long time ago, and these effects are therefore not relevant in the analysis.

In Phase 2 to 7 the installation of the piles for Partihallsbron and the pre-augering is executed following the actual schedule, see Table 8.

Table 8 Input for the calculation phases in PLAXIS.

Phase	**Calculation type**	**Construction phase**
Initial	K0 procedure	Initial stresses
Phase 1	Plastic analysis	Installation of Skäran
Phase 2	Plastic analysis	Reset displacements to zero Piling of A17 S
Phase 3	Plastic analysis	Pre-augering A18 N
Phase 4	Plastic analysis	Piling of A18 N
Phase 5	Plastic analysis	Pre-augering A19 N
Phase 6	Plastic analysis	Piling of A19 N
Phase 7	Plastic analysis	Piling of A17 N

7 Parametric Study

To investigate the sensitivity of the model the impact of the chosen parameters has been analyzed. The effect of refining the mesh is studied to ensure that the mesh used in the final analysis is sufficiently refined. The linear elastic material model is compared to Mohr-Coulombs material model to examine if there is cause to use the somewhat more complex model, or if the simplification is satisfactory. As mentioned in Section 4.2 the amount of pre-augering in the area has not been fully recorded and this might be a source of error in the analysis. Therefore the effect of pre-augering has been studied in Section 7.3. The results without any pre-augering are compared to results with the minimum amount, alternative 1, and the maximum amount, alternative 2, see also Table 7 in Section 6.3.

7.1 Coarseness of the finite element mesh

As mentioned in Section 6.4 it is important that the finite element mesh is fine enough to capture the real behaviour of the soil and structures, but not so fine that the calculation time becomes unreasonable. To find a suitable mesh size several calculations with progressively refined meshes were performed. The calculation times are plotted against the number of elements in Figure 7.1 and the displacement in support 3 after four pile driving phases against number of nodes in Figure 7.2.

Since the calculation time varies almost linearly with the number of elements in the finite element mesh, the objective is to find the coarsest mesh that give satisfactory results.

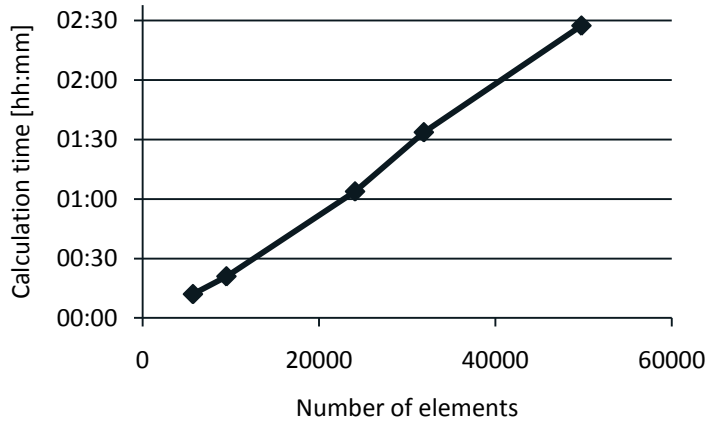

Figure 7.1 Number of elements in the finite element mesh against calculation time in PLAXIS 3D Foundation.

Since the resulting displacement in the analysis is almost constant from 20400 to about 50000 elements, see Figure 7.2, it can be assumed that the mesh with 20400 elements gives acceptable results and does not need to be refined further.

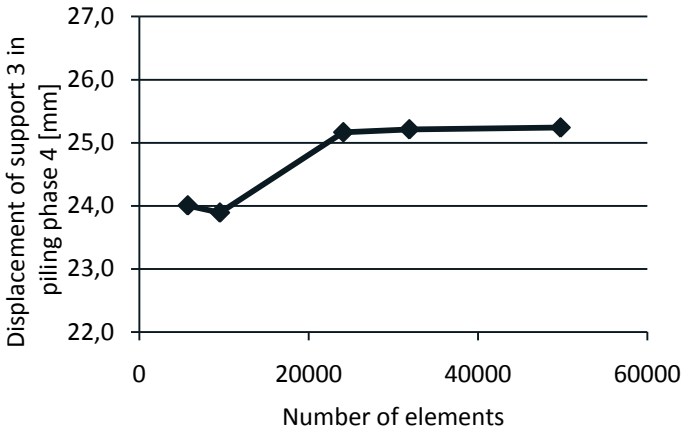

Figure 7.2 Number of elements plotted against the displacement of support 3 after the fourth pile driving phase.

7.2 Mohr-Coulomb soil model

For the main analysis in this thesis a linear elastic material model was intended to be used for the soil. Since soil is a more complicated material than that, a comparison was made with the Mohr-Coulomb material model to ensure the accuracy of the results from the simpler linear elastic analysis. The input parameters for the two material models can be seen in Table 9. The parameters that differ between the models are shown in bold.

Table 9 Input parameters for linear elastic and Mohr-Coulomb material models.

	Linear elastic	**Mohr Coulomb**
Material type	**Drained**	**Undrained**
γ [kN/m^3]	16,5	16,5
G_{ref} [kN/m^2]	1100	1100
$\boldsymbol{E_{inc}}$ **[kN/m^2/m]**	**358,8**	**324**
c [kN/m^2]	-	**11**
$\boldsymbol{c_{increment}}$ [kN/m^2]	-	**1,5**
y_{ref} [m]	4,5	4,5
v **[-]**	**0,495**	**0,35**
$k_{x,y,z}$ [m/day]	$8{,}64\cdot10^{-5}$	$8{,}64\cdot10^{-5}$
φ [˚]	-	**0**
ψ [˚]	-	**0**

The displacements for the four pile driving phases, with the minimum amount of pre-augering, were modelled and the horizontal displacements in the surface are compared in Figure 7.3 to Figure 7.5. For all three supports the displacements are almost identical for the first three pile driving phases. For the fourth phase there is some difference in the results, but only about 3 mm, which is considered acceptable. The heave is practically identical for the two models; a comparison is shown in Appendix 7.

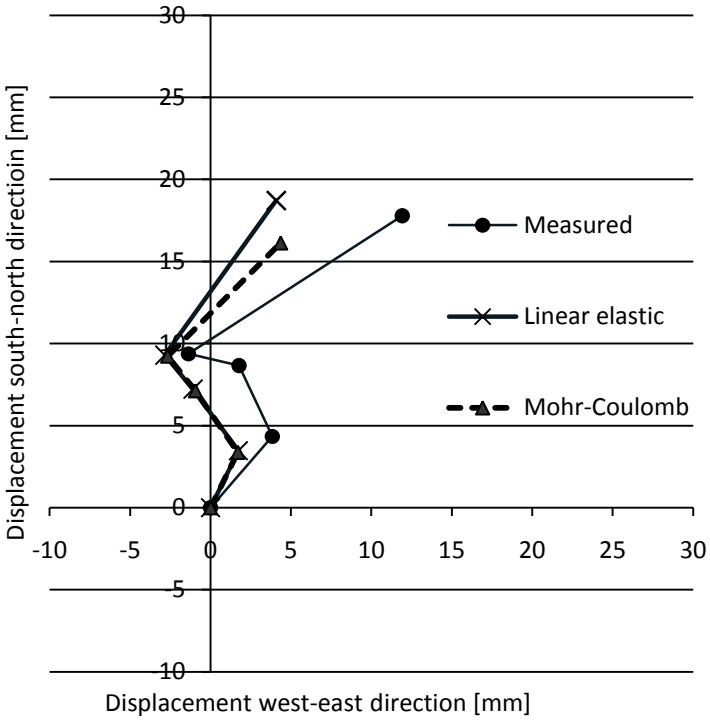

Figure 7.3 Support 2: Measured and modelled horisontal displacements. A comparison of linear elastic and Mohr-Coulombs material models.

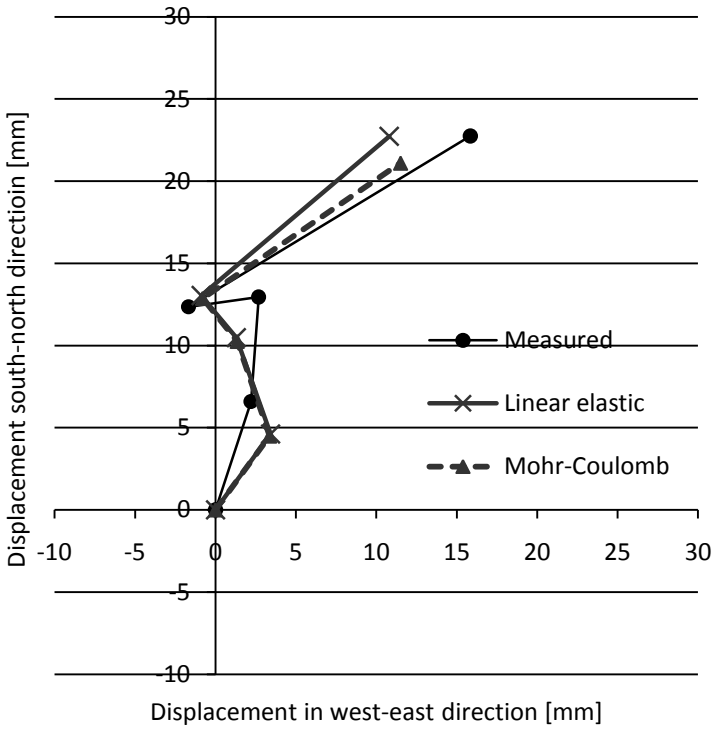

Figure 7.4 Support 3: Measured and modelled horisontal displacements. A comparison of linear elastic and Mohr-Coulombs material models.

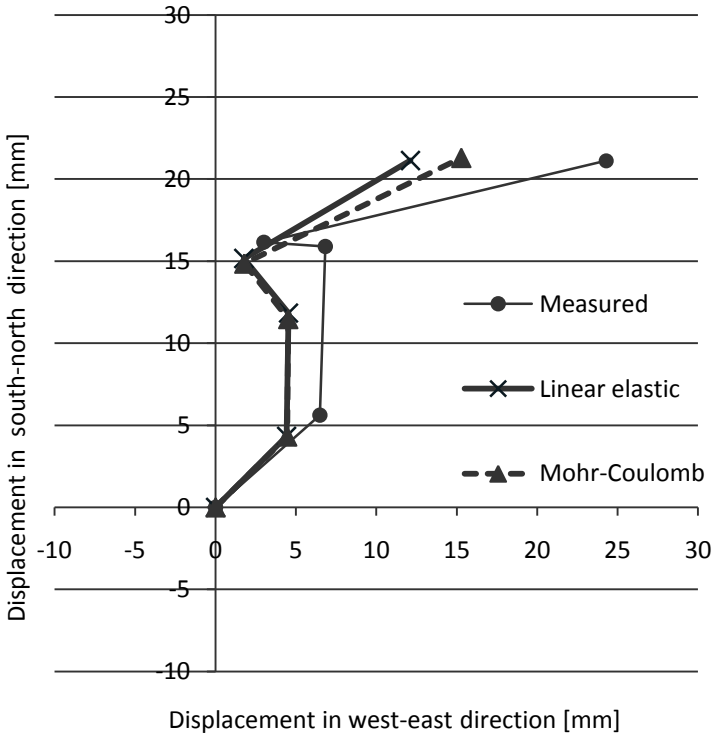

Figure 7.5 Support 4: Measured and modelled horizontal displacements. A comparison of linear elastic and Mohr-Coulombs material models.

The horizontal displacements with depth at support 3 are compared in Figure 7.6. This support is the one where the modelled displacements seem to correspond best with the measurements and it is therefore suitable for further studies. The figure shows how the displacements in the soil have developed during the four stages of pile driving. In

the fourth stage the pile driving takes place much closer to the support than in stage one to three which explains the larger displacements. The results from the two models are practically identical in stage one to three but the results differ somewhat in the fourth stage, just as the horizontal displacements in the surface. This implies that the linear elastic model is a satisfactory approximation in this thesis. In stage 4, at depth -20 meters, there is an anomaly in the graph and this is most likely due to the coarseness of the mesh.

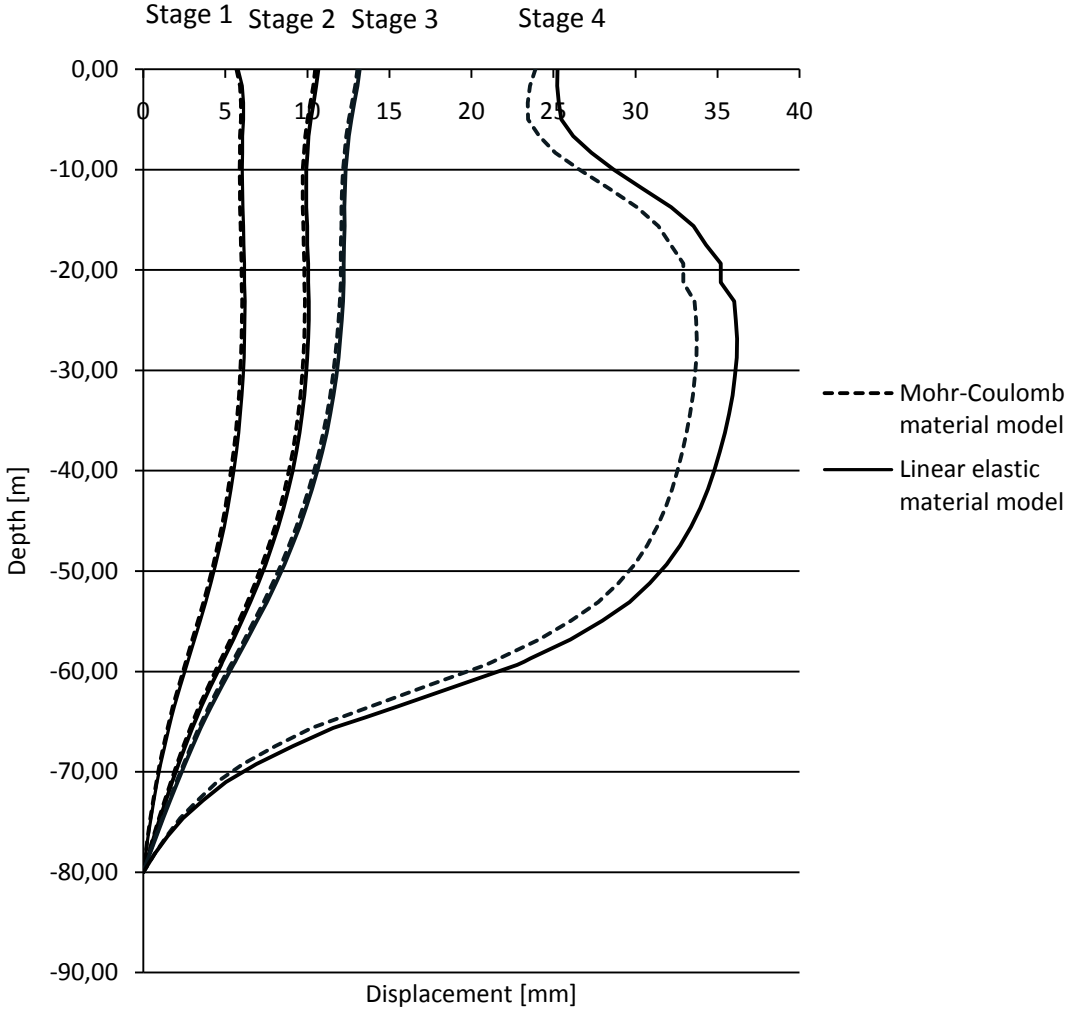

Figure 7.6 Horizontal displacements with depth at support 3. The progression of the displacements are shown for the first four piling stages.

These results correlate quite well with the analysis of the simpler case done in Chapter 5, both for the displacements at the surface and in the soil profile, which also verify the results.

7.3 Pre-Augering

As mentioned in Section 4.2, there is a lack of information about the pre-augering in the project. The two alternatives concerning pre-augering, see Section 4.2, and an alternative where no pre-augering was considered were compared.

For all three studied supports, there is no difference between alternative 1 and alternative 2 concerning surface displacements, see Figure 7.7, Figure 7.8 and Figure 7.9. There are larger displacements without pre-augering which shows that the pre-augering somehow is efficient. Only the magnitude of the displacements changes when taking pre-augering into account, and not the direction of the displacements. The alternatives with pre-augering correlate better with the measured displacements and alternative 1 is the alternative chosen for further analyses.

Concerning heave, there is no difference between the three models. The figures showing the comparison of the heave can be found in Appendix 8.

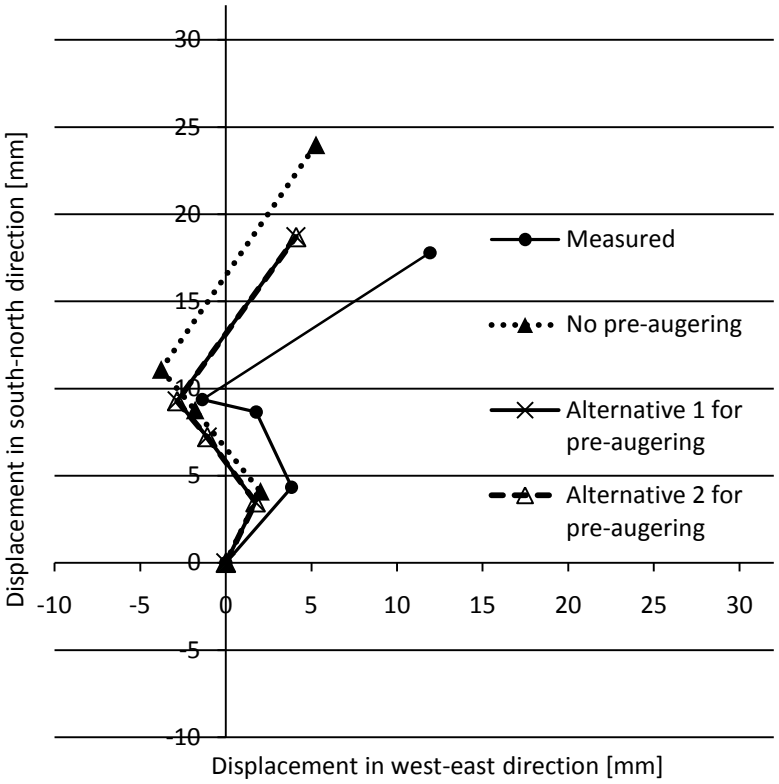

Figure 7.7 Support 2: Measured and modeled horizontal displacements. An analysis of the influence of pre-augering.

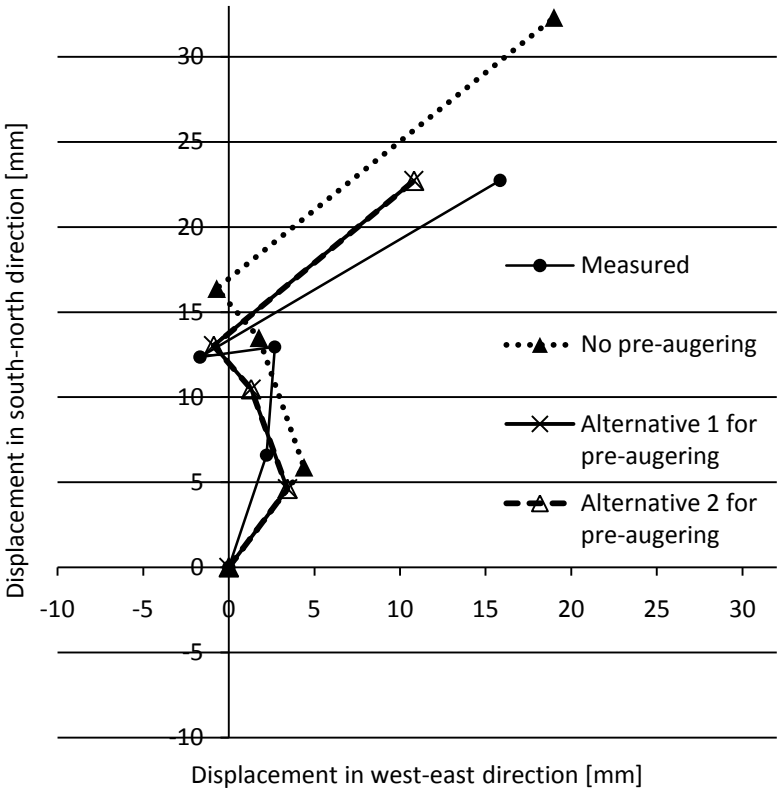

Figure 7.8 Support 3: Measured and modelled horizontal displacement. An analysis of the influence of pre-augering.

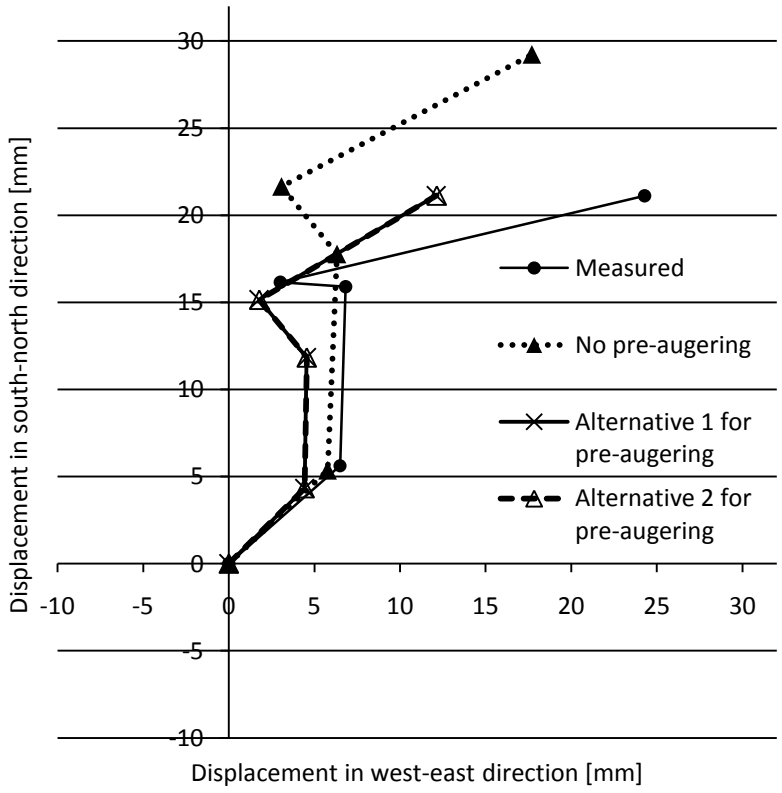

Figure 7.9 Support 4: Measured and modeled horizontal displacement. An analysis of the influence of pre-augering.

In Figure 7.10 the horizontal displacements, for support 3, with depth are compared. Alternative one, with minimum pre-augering, is compared to the alternative with no pre-augering. It shows that the pre-augering has effect to about -25 meters and below this the curves converge. Since there are no measurements for the displacements below the surface for Skäran this cannot be used to verify the model directly.

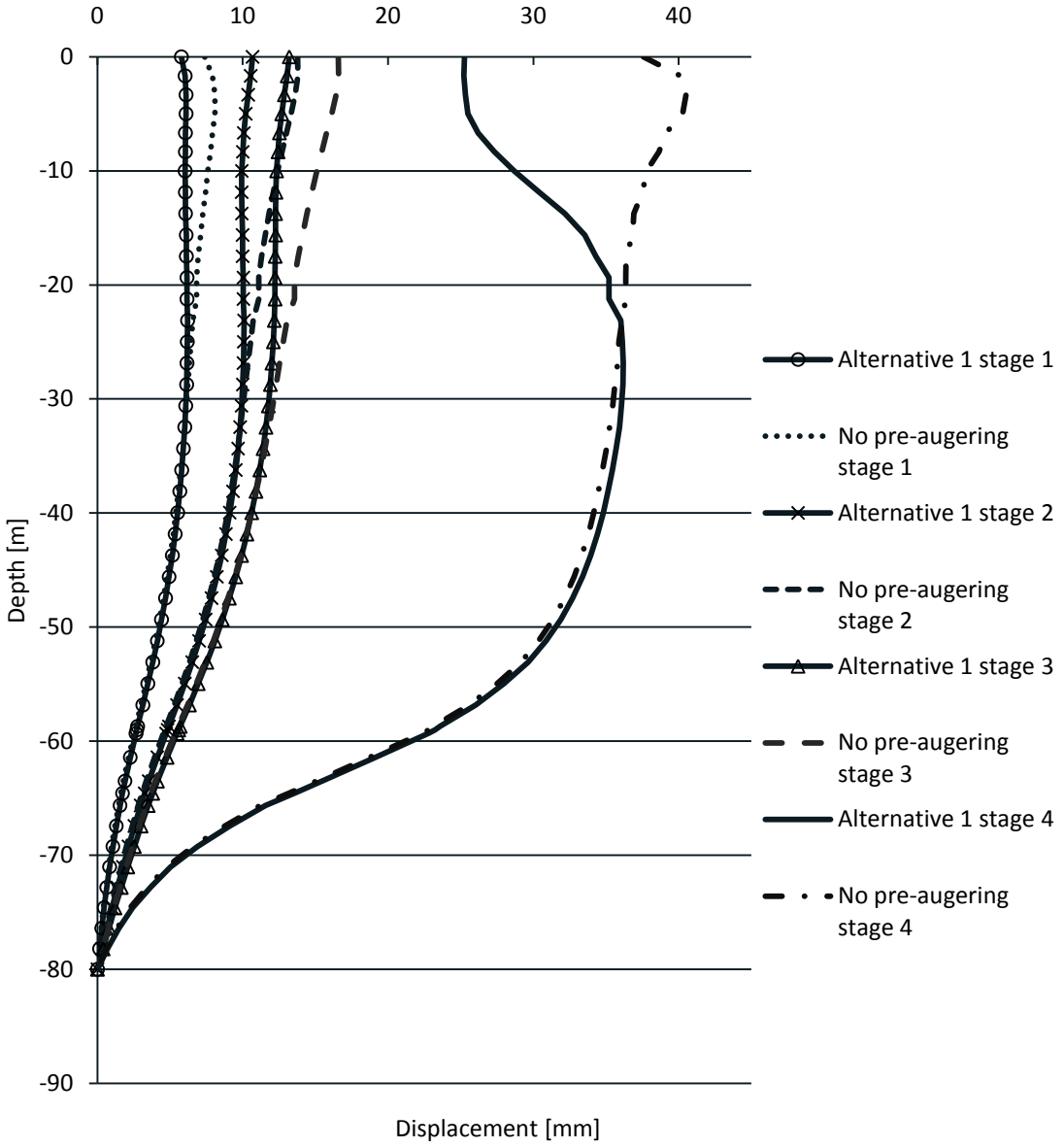

Figure 7.10 Horizontal displacement with depth for support 3. Alternative 1, with minimum pre-augering is compared to an alternative with no pre-augering for the first four piling stages.

8 Results and Evaluation

In this chapter the results from the analyses are presented. The soil movements in the surface are shown in Section 8.1. In Section 8.2 the effects on the foundation of Skäran and the bridge itself are presented. In Section 8.3 the results from the finite element analysis in PLAXIS 3D Foundation are compared to the different hand calculation methods. The simplifications and sources of errors in the analyses are discussed in Section 8.4.

8.1 Soil movements

The soil movements in the surface, both horizontal movements and heave, are here compared to the actual movements of the bridge supports 2, 3 and 4. The modelled movements below the surface, with and without including the piles and support of Skäran, are shown, but since no measurements with depth were made, these cannot be compared to real displacements.

8.1.1 **Surface displacement**

The modelled horizontal surface displacements in support 2, 3 and 4 are shown in Figure 8.1 to Figure 8.3 together with the measured displacements. The movements for the first four piling stages are shown, represented by vectors with the x-axis in west-east direction and the y-axis in south-north direction.

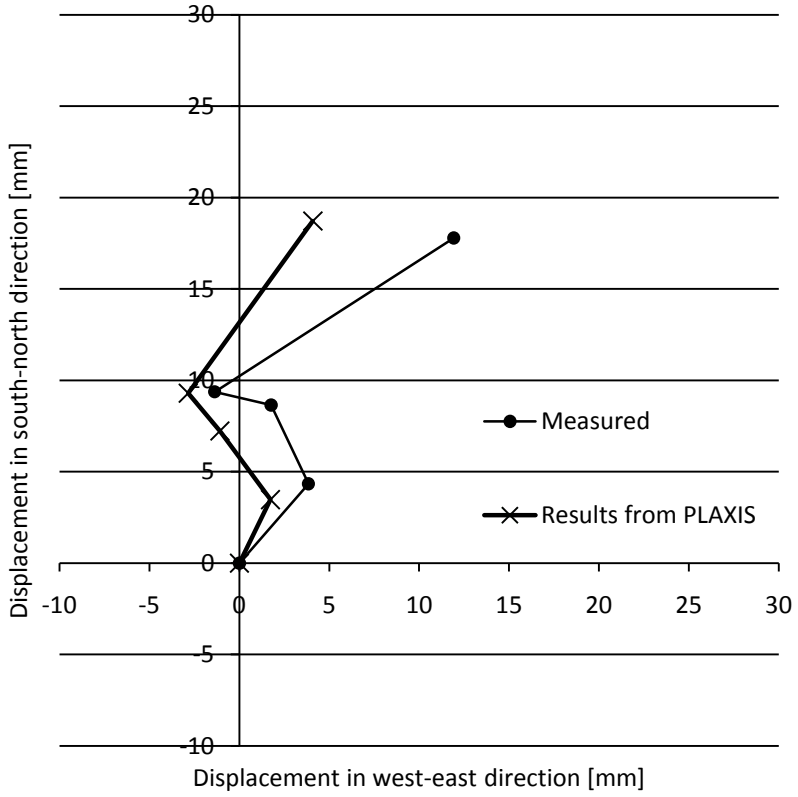

Figure 8.1 Support 2: Measured and modelled horizontal displacement.

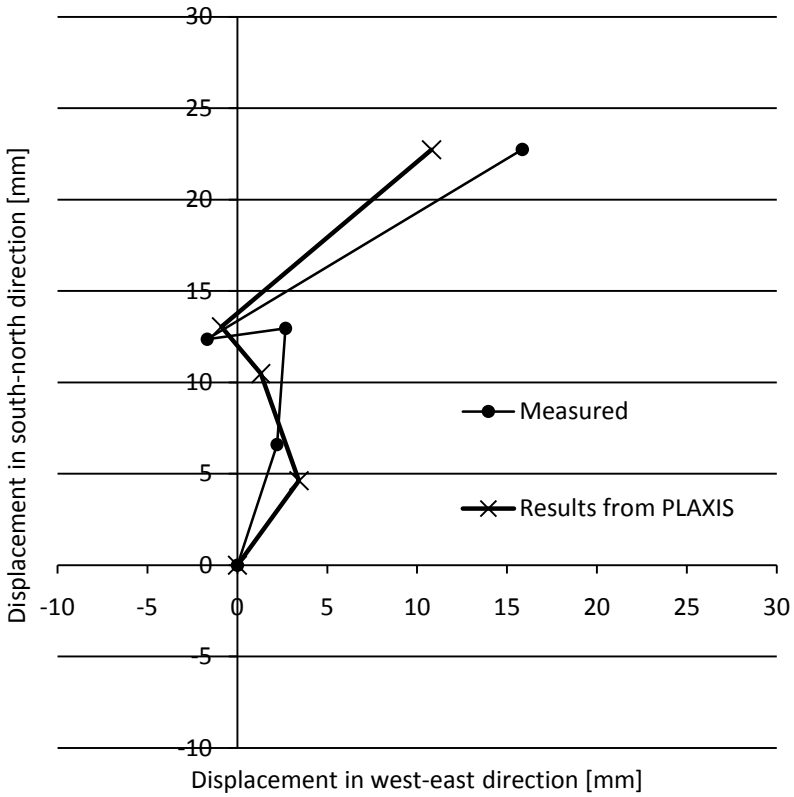

Figure 8.2 Support 3: Measured and modelled horizontal displacement.

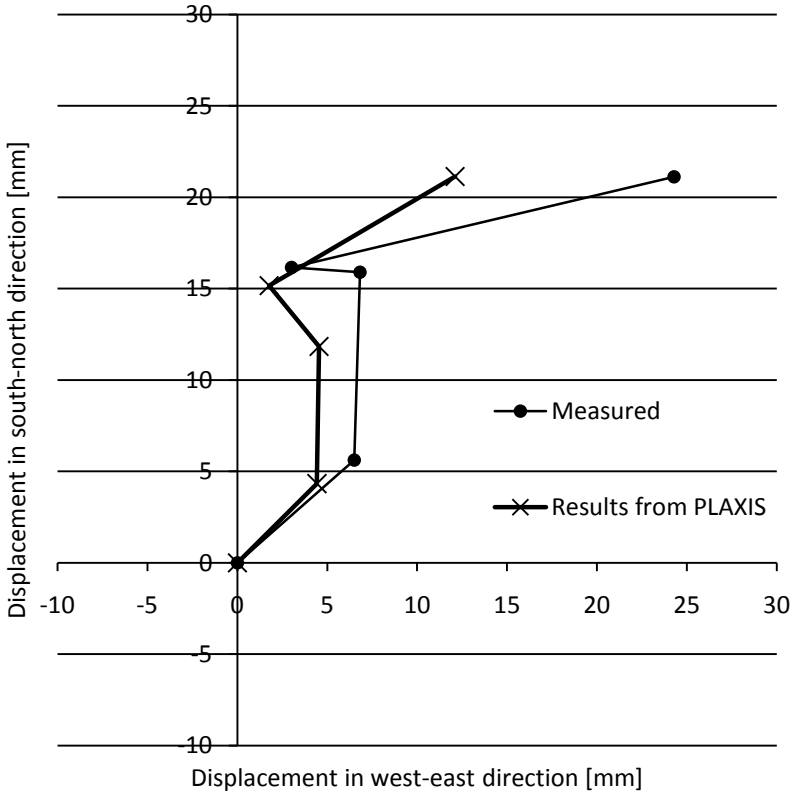

Figure 8.3 Support 4: Measured and modelled horizontal displacement.

8.1.2 **Heave**

The results for the vertical displacements at support 2, 3 and 4 are shown in Figure 8.4, Figure 8.5 and Figure 8.6 with the measured displacements. According to the measurements there is an initial settlement of about 2 mm in all three supports. This behaviour is not what is expected, nor what the model shows. This could be due to an error in the measurements or a reaction in the soil due to the disturbance caused by the sudden activity in the area. If the clay is sensitive to agitation the shear strength can decrease which leads to decreased bearing capacity of the piles, which can cause settlements (Sällfors, 2001).

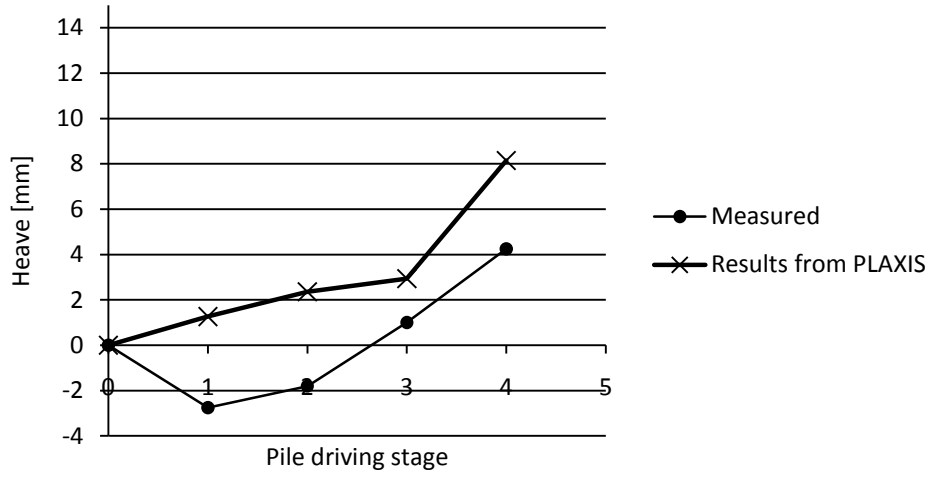

Figure 8.4 Support 2: Measured and modelled heave.

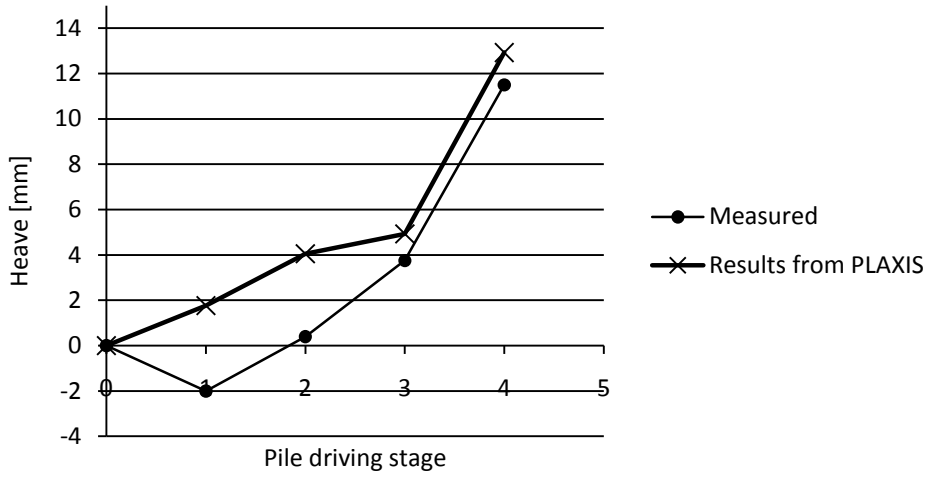

Figure 8.5 Support 3: Measured and modelled heave.

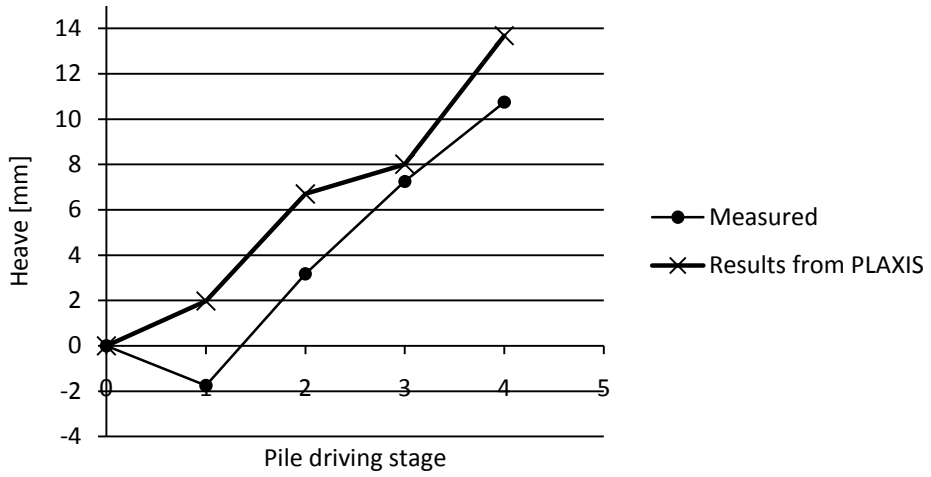

Figure 8.6 Support 4: Measured and modeled heave.

8.1.3 **Effect of piles in the ground**

To analyze which effects the foundation of Skäran has on the movements in the soil the analysis was repeated but without activating the elements representing Skäran. The resulting horizontal soil movements with depth, with and without Skäran, are shown in Figure 8.7. Only the movements at support 3, and for the four phases, are studied.

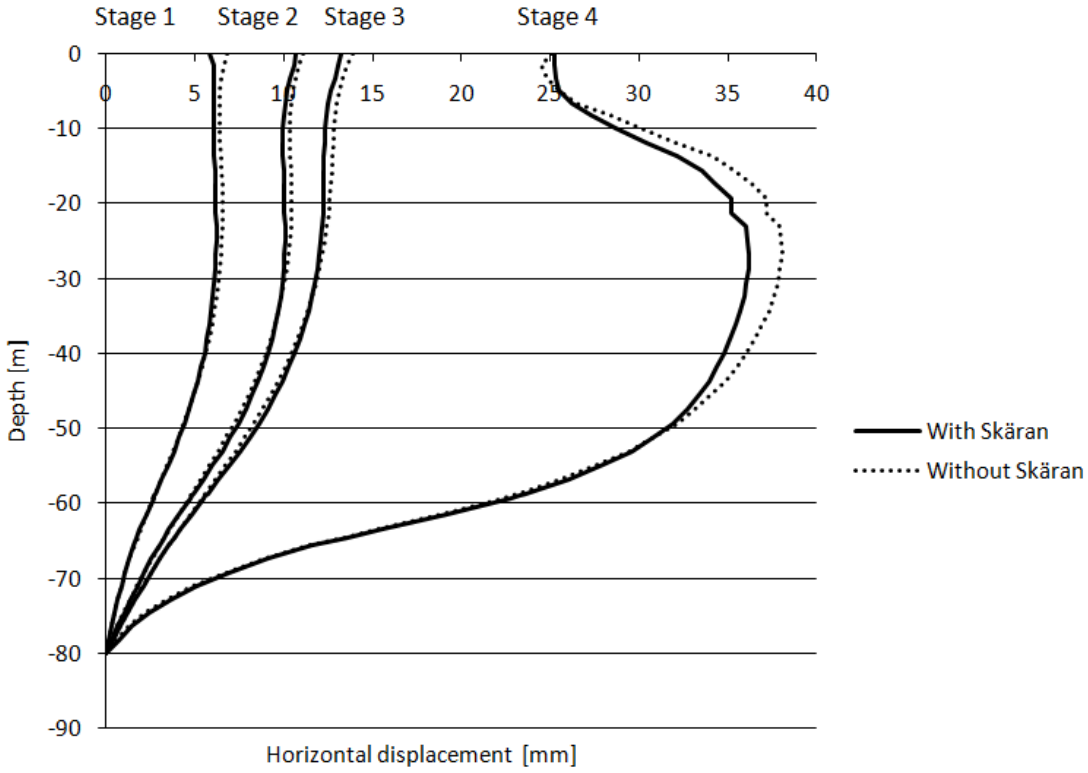

Figure 8.7 Horizontal displacement in the soil with depth at support 3 with and without the support and piles of Skäran. The progression of the displacements is shown for the first four piling stages.

The effect on the horizontal movements is quite small, and it seems that the piles cannot restrain the soil movements in any significant way.

In Figure 8.8 the heave for support 3 is shown for the four stages; with and without Skäran. The vertical displacements are about halved when including the foundation of Skäran. Since piled foundations are primarily designed to take vertical loads, this considerable effect is expected.

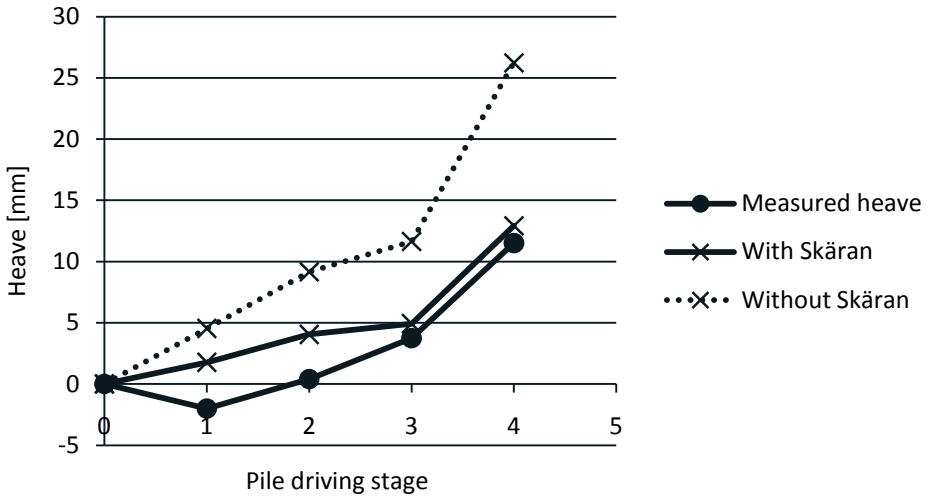

Figure 8.8 Modelled heave at support 3, with and without including the foundation of Skäran in the model.

8.2 Effects on the foundation of Skäranbron

For the analysis of the effects on the foundation of Skäran piles in support 3 has been chosen, see Figure 8.9. The soil movements at this support correspond best with the measurements and the simplification of boundary conditions has the least effect. The studied piles have been chosen due to the direction of the inclination. The displacements of the piles have been studied as well as moments, shear- and axial forces in the piles.

This study has been done for four pile stages and does not take the final displacement into account. However the major part of the displacement has already propagated in the four studied phases; for the horizontal 65 percent displacement and 76 percent for the heave. If the total effects on the piles are of interest, this must be taken into account.

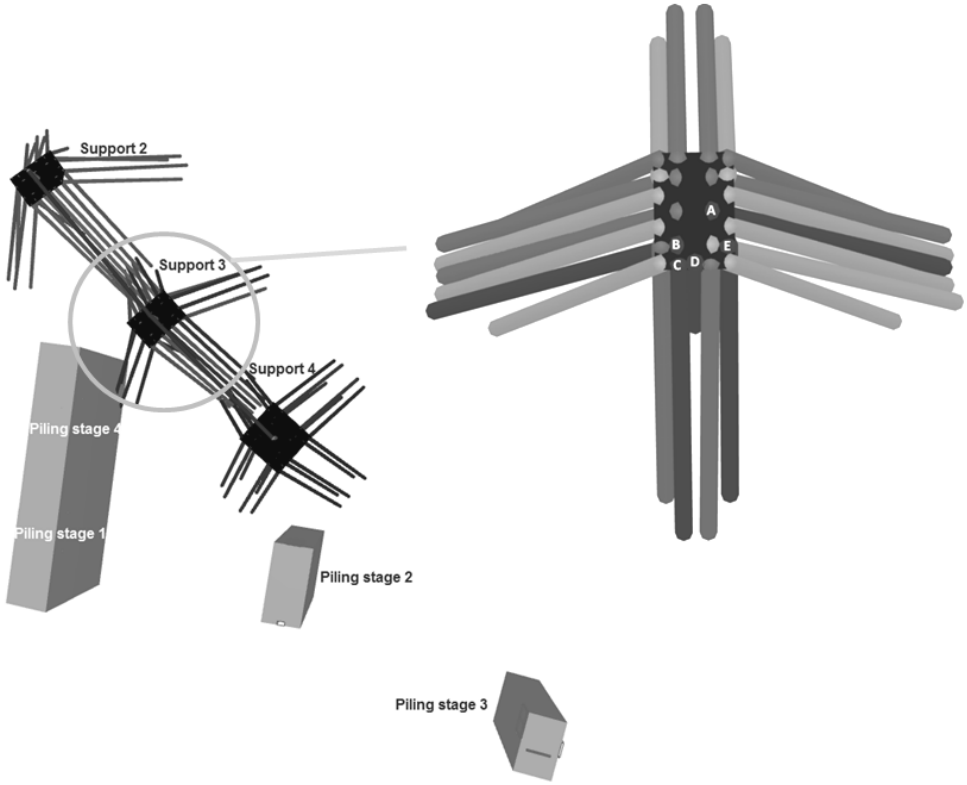

Figure 8.9 Studied supports of Skäran and piling stages for Partihallsbron. The darkest gray piles in support 3 are the ones chosen for analysis, pile A-E.

The capacity of the piles before cracking is calculated according to the equations in Section 2.5 and is shown in Table 10. The concrete quality is K50 which correlate to C40/50. The tensile strength used in the calculations is $f_{ctk0,05}$= 2,5 MPa. The moment capacity is reduced in the event of present tensile force in the piles, see Section 8.2.4. The yield strength for the reinforcement used in the calculation is f_{yk}=590 MPa.

Table 10 Cracking moment, axial and shear force for the pile.

M_{cr} (N=0) [kNm]	V_{cr} [kN]	N_{cr} [kN]	$N_{Rd,tensile}$ [kN]
9	126	189	533

8.2.1 **Displacement of the piles**

The displacements for the piles after 4 piling stages can be found in Figure 8.10. The shape of the curve resembles the displacement curve in Figure 8.7. The S-shape can also be found in the displacement curve in the "less complicated case" in Chapter 5.

The top of the piles have almost equal displacements due to the connection in the pile cap. However, the foot of the piles have different displacements. This is mainly due to the difference in distance to the piling area. The closer the pile is to the piling area the more effects on the pile. The foot of pile C is inside the piling area, which is modelled as an expansion of the soil. This causes the irregularity in the displacement curve. Pile A, B and D has almost equal distance to the piling area which explains the similarity of the displacement curves. Furthermore, pile A has the longest distance to the piling area, which results in the smallest displacements. Another explanation to the small

displacement for pile A is that the pile is partially hidden by the piles surrounding it in the pile group.

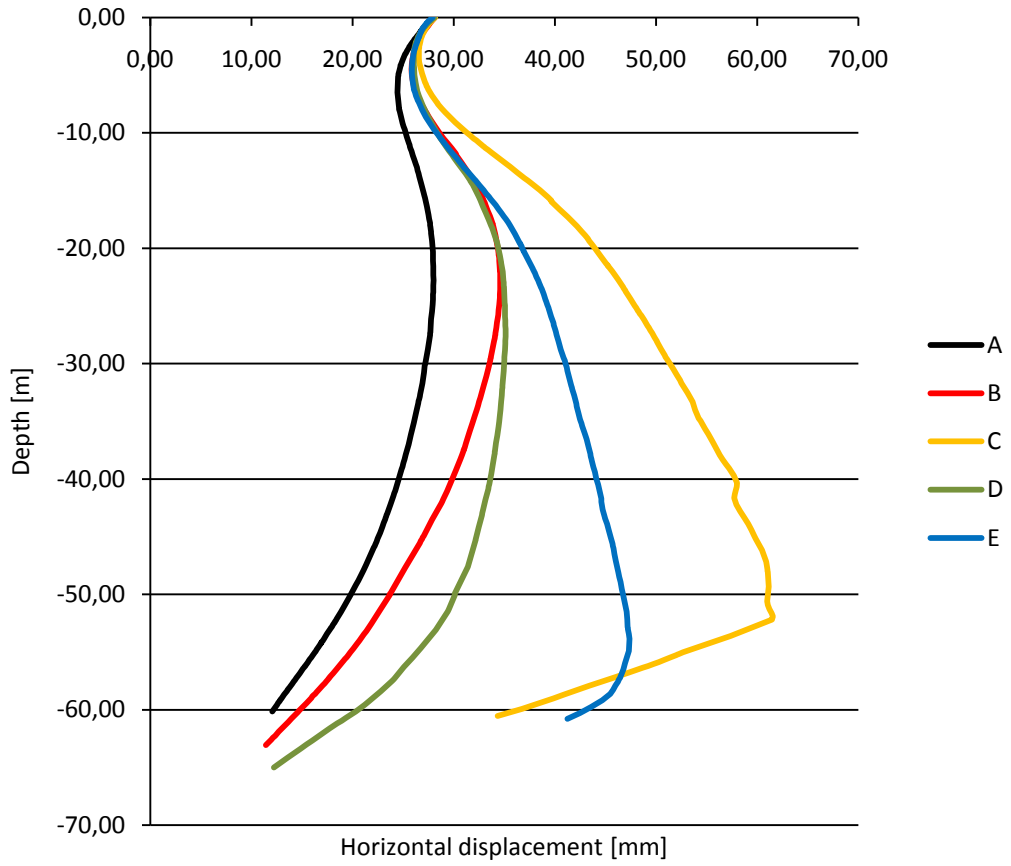

Figure 8.10 Horizontal displacements of piles in support 3.

Since the connection between the piles and the pile cap are not totally rigid, a comparison of the two types of connections; rigid and hinged, have been done, see Figure 8.11. The result shows that there is no difference between the two types of connection. In reality a pile with hinged connection could not get the curvature in the upper part of the pile.

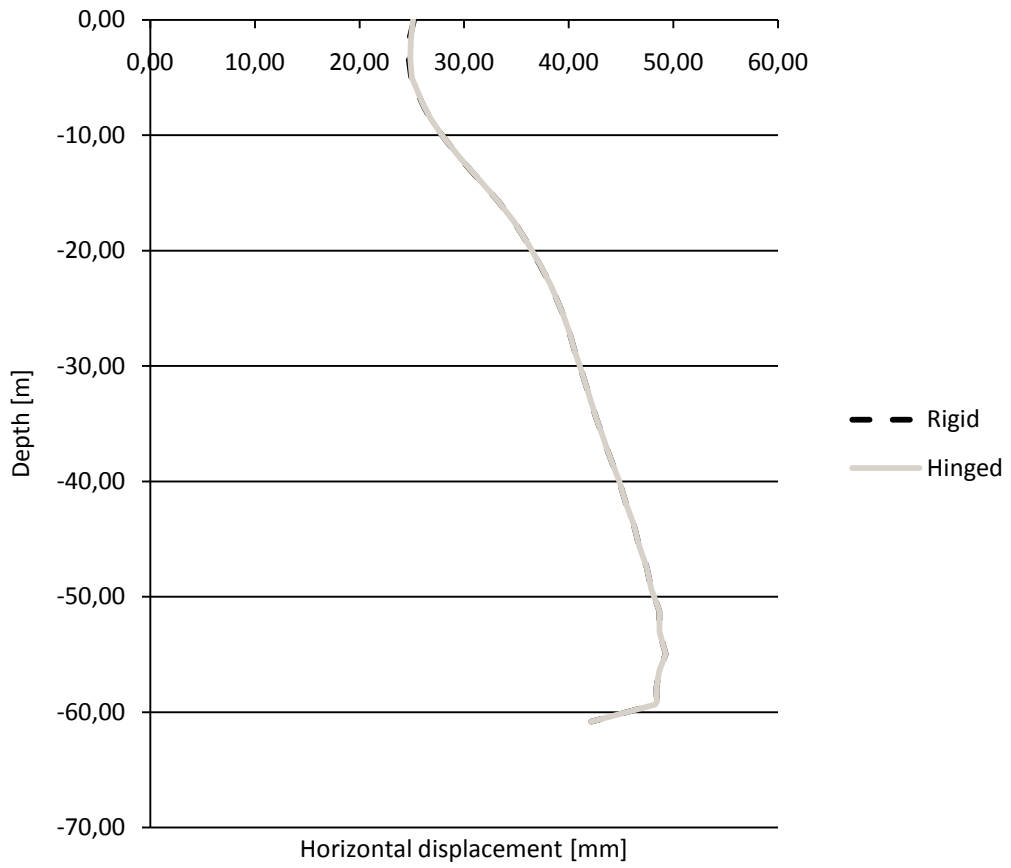

Figure 8.11 Comparison of the displacement with different properties for the connection pile-pile cap in the model in PLAXIS 3D.

8.2.2 **Moments**

To evaluate the moments, the displacements along the piles were simplified to a polynomial function of six degrees. The second derivative of this function gives the moments according to the equation of the elastic line, see Section 2.5. Since the polynomial function cannot take the form of a straight line, it cannot describe the displacements near the foot of the pile in a satisfying way. The displacement diagrams have been evaluated and divided into one part that coincides well with the polynomial approximation, see Appendix 9, and an end part, near the foot, that does not. The part of the moment diagrams corresponding to the end part of the displacement diagrams have been approximated as linearly decreasing to zero, since moment at the foot of the pile is zero. For the analyses used to evaluate the moments, the connections between piles and pile cap are modelled as rigid to get results on the safe side.

Figure 8.12 shows the approximated moment distributions for piles A to E in support 3. The larges moments occur where the radius of curvature for the displacement curve is the smallest, which is at the top of the piles.

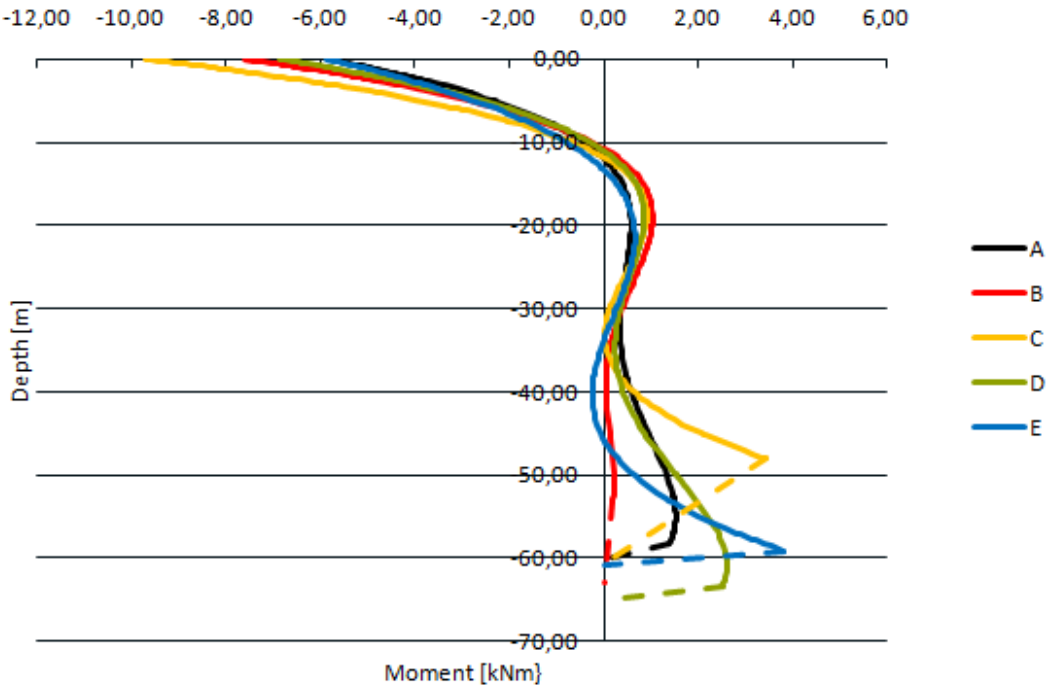

Figure 8.12 Moment distributions in piles in support 3 of Skäran.

The pile with largest moment is pile C which is closest to the fourth piling stage, and inclined towards it. As mentioned in Section 8.2.1 the foot of the pile is actually placed within the super pile representing piling stage 4. The largest moment is the fixed end moment and it is 9,7 kNm which is higher than the cracking moment, M_{cr}= 9 kNm. In reality the pile is only partially fixed to the pile cap, so the actual moment at the top of the pile is lower, but there is reason to investigate this further. For the other piles the fixed end moment is below the cracking moment.

When calculating the cracking moment, the axial force in the piles must also be taken into account. If there are tensile forces in the piles the moment resistance with regard to cracks must be reduced. This is discussed further in Section 8.2.4.

8.2.3 **Shear forces**

The shear force is calculated as the derivative of the moment distribution. Since the function of the moment does not describe the real behavior at the foot of the pile, neither will the function of the shear force describe the real behavior at the foot. In reality, the shear force will be zero at the foot of the pile. The shear capacity before cracking is 126 kN and the largest shear force in the piles, see Figure 8.13, are well below the capacity.

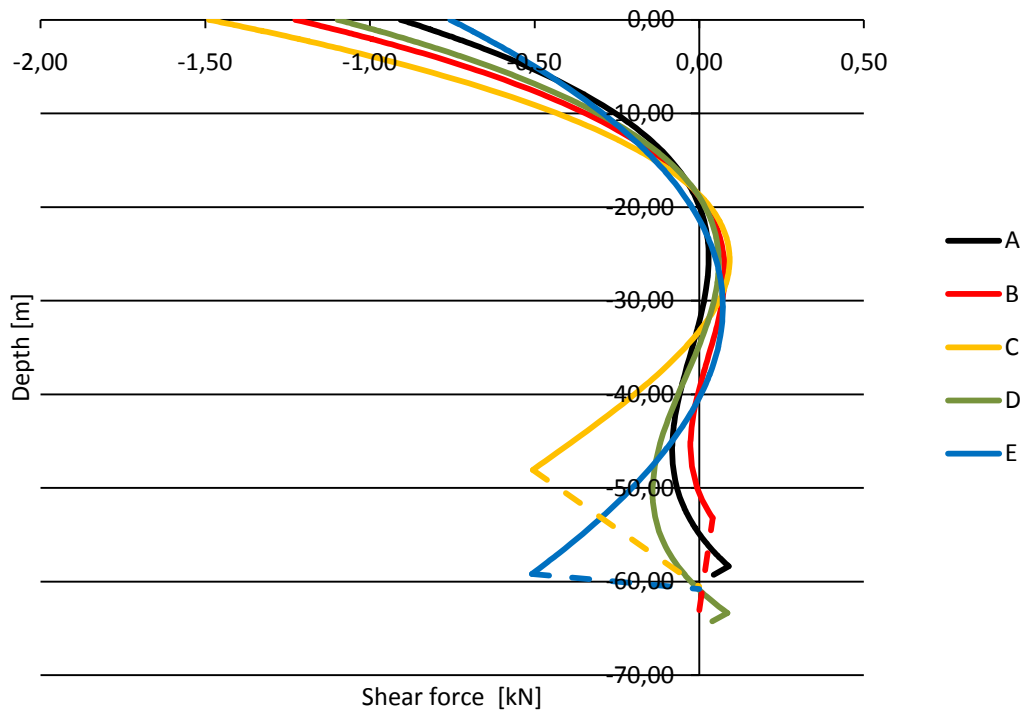

Figure 8.13 Shear forces in piles in support 3 of Skäran.

8.2.4 **Axial forces**

As with the displacements, the axial forces in the piles depend on the proximity to the piling area but also the inclination of the pile. The piles that are inclined with the foot towards the expansion, pile C and E, will be pushed towards the pile group and pile cap by the soil movements. This will cause compression at the top of the pile, but since the soil at the foot will have less displacement than the soil near the surface, see Figure 8.7, there will be a tensile axial force in the bottom part of the pile.

For the piles inclined perpendicular to the expansion, pile A and B, the soil movements will cause a tensile axial force in the whole pile as the soil pulls the pile along, away from the pile cap. Pile D is vertical.

In Figure 8.14 the axial forces in pile A-E are shown after four piling stages. The axial force created by the weight of the bridge is included and the results are taken directly from PLAXIS. For pile B the tensile force created by the soil movements is so large that it cancels out the compression caused by the loading from the bridge.

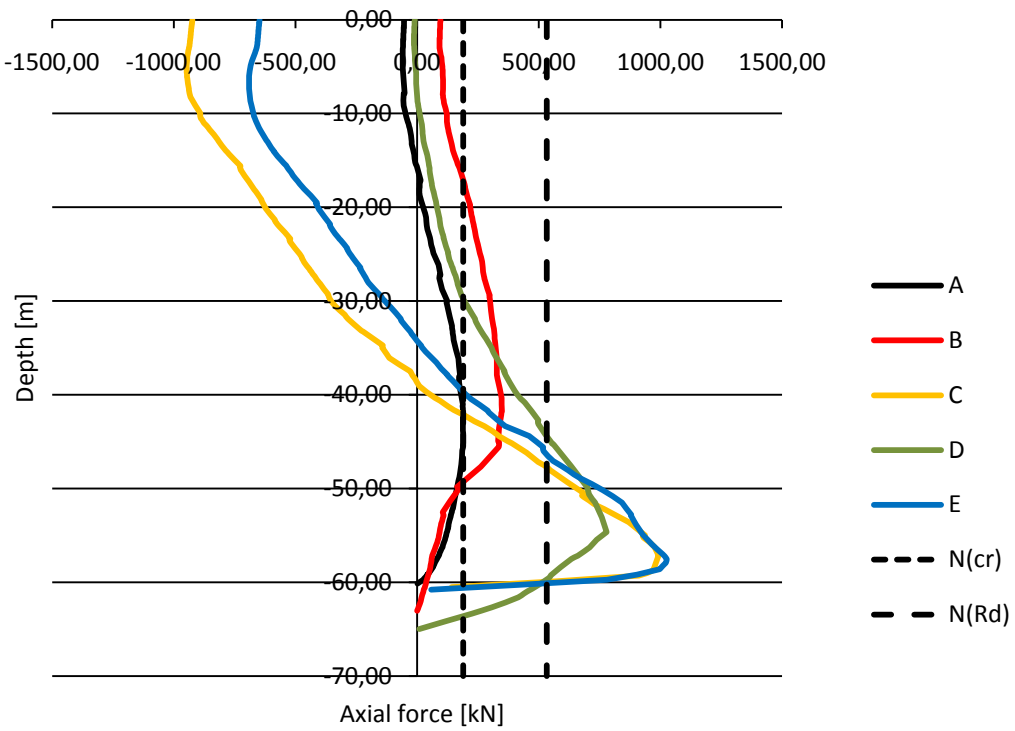

Figure 8.14 Axial forces in piles in support 3 of Skäran, negative is compression and positive is tension.

The capacity of the piles before cracking is 189 kN which is less than the maximum axial force in the piles.

Since the pile is modelled as a linear elastic material the behaviour after cracking is not shown. In Figure 8.15 below, the behaviour of a reinforced concrete member in pure tension is shown. State I is the response of the uncracked cross-section and state II of the cracked cross-section. At N_{cr} the concrete cracks and the tension is resisted by the reinforcement bars that have a lower stiffness than the total cross-section. Since the element is modelled as linear elastic the behaviour is that in State I. No cracking occurs in the model and the axial force in the piles is only correct until it reaches N_{cr}. After this the program cannot predict the correct behaviour of the piles.

The tensile capacity of the reinforcement is 533 kN. However, whether yielding occurs or not cannot be investigated since the response in the piles after cracking is not captured in the model. It is therefore not possible to study the combination of moments and axial force in this analysis.

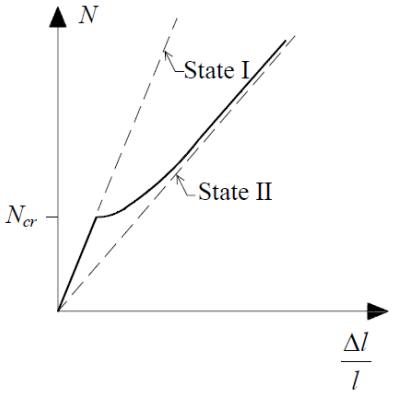

Figure 8.15 Typical behaviour of a reinforced concrete member in pure tension, based on the assumption of a linear stress-strain relationship for concrete and reinforcement. (Engström, 2010)

Since there are ongoing settlements in the area, the piles will be subjected to down drag. An estimation of the compression due to down drag can be found in Appendix 10. This has not been taken into account in the analysis. The total effect on the piles in this case will be only a small tensile axial force near the foot of the analysed pile.

8.3 Comparison of different calculation methods

In this section the results from the finite element calculations are first compared to the two hand calculation methods mentioned in Section 2.4, the Hellman/Rehnman method and the Sagaseta method. A comparison of the results from two PLAXIS applications, 3D Foundation and 3D 2010, is also done.

8.3.1 Finite element analysis compared to hand calculation methods

To evaluate the worth of spending the extra effort on a more complicated method for evaluation of soil movements, the results from the finite element analysis are compared to those from hand calculation methods. As mentioned earlier, the amount and effect of pre-boring is somewhat uncertain and since the different methods have different ways of taking the pre-boring into account, the results without considering pre-boring are compared. The results when including the minimum alternative for pre-boring are shown in Appendix 11.

The resulting horizontal soil movements at support 3 for the four first pile driving stages are compared in Figure 8.16. The measured displacements are also shown. Since the pre-boring is not taken into account the resulting displacements are larger than the measured. The results from PLAXIS and Hellman/Rehnman are similar, both in direction and size. The results from Sagaseta have a somewhat different direction but the size of the displacements is comparable.

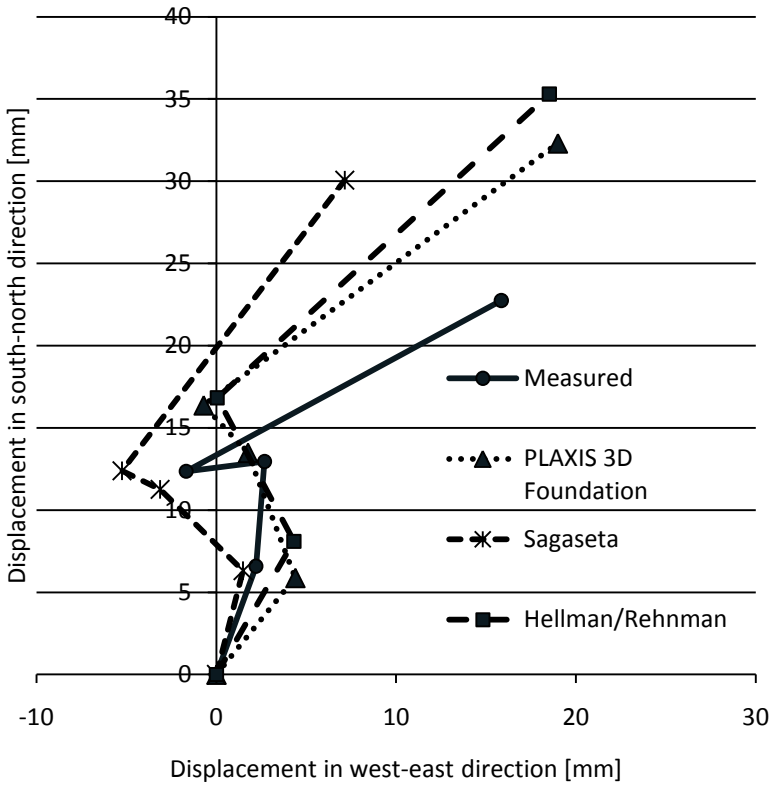

Figure 8.16 Comparison of horizontal movements at the surface at support 3. Measured displacement compared to results from PLAXIS, Sagaseta method and Hellman/Rehnman method, without considering pre-boring.

Figure 8.17 shows the resulting heave. Note that, as for the horizontal displacements, the pre-boring is not considered. The results from PLAXIS and Sagaseta correspond well with the measurements, except for the first phase where the measurements show settlements. The Hellman/Rehnman method predicts a heave four times larger than the actual one.

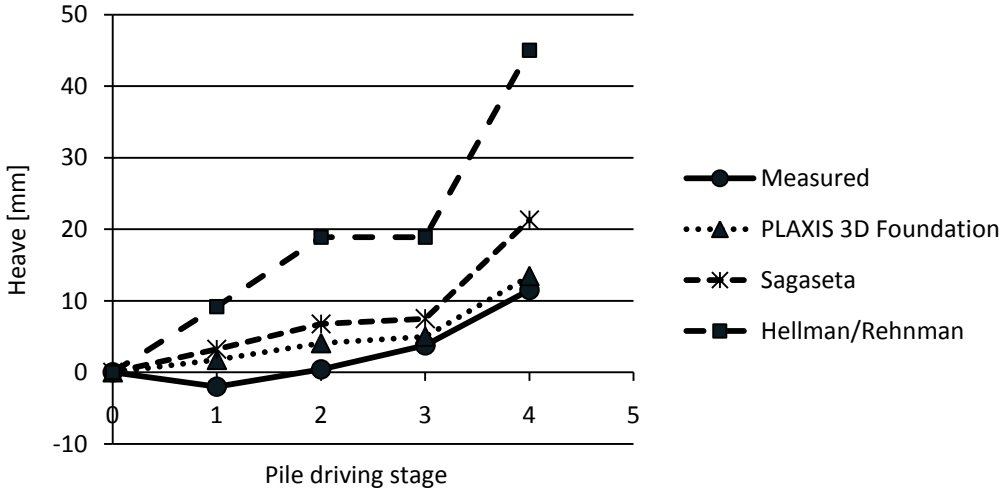

Figure 8.17 Comparison of heave at the surface at support 3. Measured displacement compared to results from PLAXIS, Sagaseta method and Hellman/Rehnman method, without considering pre-boring.

Worth noting about the results from the Hellman/Rehnman method is that the calculation method is somewhat open to interpretation. The distance to the piling area

is a parameter in the equation for the displacement, see Section 2.4.1, but it is not clearly stated how this distance is defined. Along the sides of the piling area the definition is straightforward, but in the corner regions the distance could be measured either as the actual distance from the piling area, or as the perpendicular distance to thought "extensions" of the sides of the piling area. The heave factors in the equation are also difficult to define and they have all been set to 1 in the calculations in this thesis. Since this corresponds to a light building this is an explanation to the large heave. The heave factor can vary between 0 and 1 and in this case 0.25 would give good results. However, the method has very limited recommendations of how to determine the weight of the structure and needs further development.

8.3.2 PLAXIS 3D Foundation compared to PLAXIS 3D 2010

In the study of the piles, both PLAXIS 3D Foundation and PLAXIS 3D have been used. Therefore, a comparison of the two programs has been done, see Figure 8.18. In the figure, the displacements of pile E have been compared. In PLAXIS 3D the finite element mesh is finer than in PLAXIS 3D Foundation which probably causes the differences in the results. The difference in the mesh is larger in the top and the end of the pile likewise the difference in the displacement.

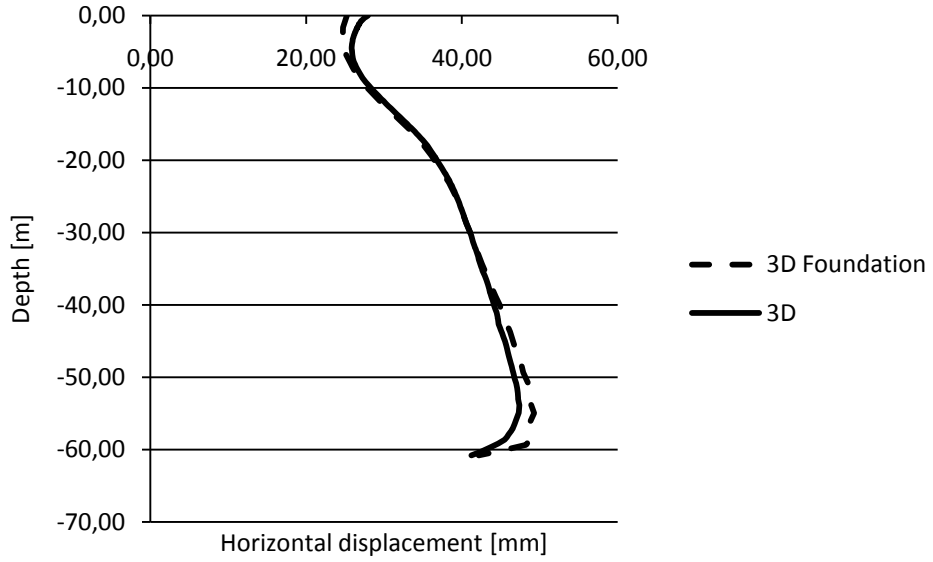

Figure 8.18 Comparison between PLAXIS 3D Foundation and PLAXIS 3D.

8.4 Simplifications and sources of error

To get a model that is practical to work with, certain simplifications have to be made. Before mentioned are that only part of both of the bridges have been modelled and the use of a linear elastic soil model. Other simplifications that may have impact on the results must also be considered in the evaluation of the results.

In the area where the pile driving is done several older buildings have been demolished prior to the start of the construction. At least one of these, an old transformer station, had a piled foundation, and the remaining piles in the ground may influence the direction and magnitude of the soil movements caused by the pile

driving for Partihallsbron. The demolished buildings can be seen in the plan drawing in Figure 3.1 and they are placed close to support A18 and A19. These piles were not considered in the analyses but an initial effort was made to include them in the finite element model. Unfortunately, no simple and accurate way to include them was found. A trial was made with stiffer clusters representing the existing piles, but this does not capture the true soil pile interaction and only gives a rigid body movement of the stiffer cluster. In addition, the analysis of the effects of the piles in the ground shows that there is no major influence on the horizontal movements. In the final analysis the existing piles were disregarded.

Another simplification was to disregard the inclination of the piles of Partihallsbron. The piles were simulated by lateral expansion of clusters approximately corresponding to the area of the pile caps and this does not take into consideration the inclination of the piles. One way of including the inclination is to model the expansion in several clusters, increasing their area with depth to correspond with the outermost piles. This would give a stepwise pyramid shape that would better correspond with the actual shape of the pile group. To accomplish this in PLAXIS 3D Foundation a horizontal layer, or work plane, would need to be added at each step of the pyramid. This would greatly increase the amount of finite elements and consequently the calculation time. There is also a limit to the number of elements due to the limitation of the RAM. However, the analysis of a simpler case in Chapter 5 showed that for a linear elastic material model, the area of expansion had little influence on the results. Therefore it is assumed that the simplification is acceptable.

A source of error that must be considered is that of the measurements of the displacements. Because of the construction and traffic in the area there could be some unwanted effects on the results of the measurements that have nothing to do with the pile driving that is studied in the thesis. There might also be disturbances to the measuring equipment. As mentioned before in Section 8.1.2 the vertical displacement for the first piling stages is negative, indicating settlements have occurred. This is not what is expected according to the theory of soil displacement due to pile driving, which might point to an error in the measurements. But there could be other explanations for the movements, e.g. disturbance of the soil decreasing the shear strength and causing settlements.

There might also be some sources of error in the modelling and finite element program. As mentioned in Section 8.2.1 the foot of pile C is placed inside the expanded cluster representing pile driving stage 4. This results in an irregular displacement curve near the foot, which probably does not coincide with the actual response in the pile. Therefore this pile is not chosen for further analysis. Because of difficulties with the output from PLAXIS, especially concerning the embedded pile elements, the moments and shear forces have been evaluated using a polynomial approximation of the displacement curve and the derivatives of this. If there are errors in the displacement curve, they will therefore also transfer to the moments and shear force. One indication of problems in the program is the fact that piles modelled with different connection to the pile cap; hinged and rigid, have the same displacement curve and moment distribution. This is not the case in reality, since a hinged connection is moment free.

It must also be kept in mind that the soil displacements below the surface have not been verified since no measurements of this were made.

9 Conclusion

The results in this thesis show that using Plaxis 3D Foundation to predict ground movement result in good correlation with measured values of the movements at the surface. Since the measurements have been done during construction there is a risk of disturbances. However, due to frequent measurements during an extended period of time and the correspondence with the theory of soil movements, the accuracy of the values can be confirmed, with one exception; the settlements in the beginning of the pile driving. According to the theory of soil movements due to pile driving heave is expected due to the added volume, but the activity in the area could cause unexpected settlements due to sensitivity of clay. The outcome is that Plaxis 3D Foundation in an accurate way can predict the actual surface displacements.

The results from the study of a simple case show that the calculated displacements correlated well with the measurements also for the soil movements below the surface. The comparison of the soil movements with and without including Skäran show that the horizontal soil movements are not affected in any significant way. However, the influence on the heave is considerable. The piles are designed to resist vertical loads but are slender and relatively flexible in transversal direction, which explains the behaviour, see Section 2.5.

The analysis of the piles shows that cracking can occur due to fixed end moment. Since the connection between pile and pile cap is not fully fixed in reality, the moment near the pile cap is overestimated, but in combination with axial tension, cracks may appear. The maximum axial tension occurs near the foot of the pile, in piles close to and inclined towards the piling area. The tension is large enough to cause cracks in the concrete and there is also a risk of yielding of the reinforcement. However, when taking the down drag due to settlements into consideration the piles will be in compression. There is no considerable risk for the foundation even if yielding would occur in the lower part of the piles. Due to the anaerobe environment the reinforcement will not corrode.

The comparison of the different calculation methods shows that the finite element analysis gives the best accordance with measured surface soil displacements. For horizontal displacements Hellman/Rehnman give results comparable to the FE-analysis but this method greatly overestimates the heave. The outcome from the Sagaseta method is reasonable both for horizontal movements and heave. The advantage of a three dimensional finite element analysis, such as in Plaxis 3D Foundation, is that the whole area can be studied, both at the surface and below. For Hellman/Rehnman and Sagaseta the calculations must be carried out for each studied point individually. The advantages with the hand calculation methods are that they are simple to use, not very time consuming and do not demand special program licenses or high capacity computers.

When choosing method the demanded accuracy and the amount of time and resources available are decisive. The hand calculation methods are fast and simple, but with a relatively simple model in Plaxis, a more advanced analysis can be done without an unreasonable time effort.

10 Future research

In the studied case there was an uncertainty about the amount of pre-boring. Pre-boring is a subject with need for more research. In this report it can be seen that there will be a difference in the results when considering pre-boring but the efficiency of pre-boring needs more analysis. The results show that the pre-boring has effect down to 25 meters, but since there are no measurements with depth this cannot be confirmed. Also the most efficient position to pre-bore could be investigated. Furthermore, the efficiency of the method using auger bore for pre-boring could be analyzed. The amount of clay removed by the bore is likely to vary with the consistency and shear strength of the clay, and also with the actual procedure when pre-boring.

An interesting continuation of this study would be to model the piles more accurately in a program where the actual cross-section and the non-linear response after cracking could be modelled, and not only the linear elastic. Since the piles crack due to the soil movements the linear elastic approximation does not show the real response.

The installation effects of the pile driving for Partihallsbron are not considered in the model since the soil movements are approximated by expansions of soil volumes. It would be interesting to study this case with installation effects included, and investigate how the piling order within the pile groups influence the soil movements.

The movements of the supports create moments and forces in the bridge deck and columns of Skäran, and stresses in the locks used for the bearings. These could not be analyzed in the model used in this thesis due to the simplification of the bridge, but it would be interesting to investigate how much stress the bridge and locks are subjected to. Will Skäran "push back" the soil movements and return to its original location now that the construction of Partihallsbron is finished?

References

Alén, Claes (2009). *Pile foundations – Short handbook.* Course Literature in Geotechnics BOM045 2010, Chalmers University of Technology, Göteborg. Sweden.

Al-Emrani, M. et al. (2008a). *Bärande konstruktioner del 1.* Chalmers University of Technology. Göteborg. Sweden.

Al-Emrani, M. et al. (2008b). *Bärande konstruktioner del 2.* Chalmers University of Technology. Göteborg. Sweden.

Binkgreve, R.B.J. et al. (2007). *PLAXIS 3D Foundation, version 2.* PLAXIS, Netherlands.

Edstam, T. et al. (2010). *Partihallsbron – Ingen koloss på lerfötter.* SGF. Grundläggningsdagen 2010: Geoteknik att grunn(d)a på, Stockholm. Sweden.

Edstam, T. & Kullingsjö, A. (2010). *Ground displacements due to pile driving in Gothenburg clay*. Proc. 7th European Conference on Numerical Methods in Geotechnical Engineering, Trondheim, Norway.

Edstam, Torbjörn (2010). *SBUF-ANSÖKAN Skäranbron – rörelser vid pålslagning för den närliggande Partihallsbron*.

Engström, Björn (2010). *Design and analysis of continious beams and columns.* Chalmers University of Technology. Göteborg. Sweden.

Kompetenscentrum (-). *En kortkurs om TRIAXIALFÖRSÖK på främst normalkonsoliderade och svagt överkonsoliderade leror.* Available at: www.ag-programutveckling.se/UserFiles/kurskompendie%20triaxkurs.pdf [2011-05-10]

Kullingsjö, Anders (2007). *Effects of deep excavations in soft clay on the immediate surroundings – Analysis on the possibility to predict deformations and reactions against the retaining system.* Diss. Chalmers University of Technology. Göteborg. Sweden.

Larsson, R. et al. (2007). *Skjuvhållfasthet- utvärdering i kohesionsjord.* Statens geotekniska institut (Information 3), Linköping.

Larsson, Rolf (2008). *Jords egenskaper*. Statens geotekniska institut (Information 1), Linköping.

Lundh, Hans (2007). *Grundläggande hållfasthetslära*. KTH, Stockholm.

Meijer, K. & Åberg, A. (2007) *Krypsättningar i lera – en jämförelse mellan två beräkningsprogram.* Chalmers Reproservice, Göteborg.

Olsson, C. & Holm, G. (1993). *Pålgrundläggning.* AB Svensk Byggtjänst och Statens geotekniska institut, Stockholm, Sweden.

Poulos, Harry G. (1973). *Analysis of Piles Undergoing Lateral Movement.* Journal of the Soil Mechanics and Foundations Division, ASCE, vol 99, pp. 391-406.

Poulos, Harry G. (2005). *The influence of construction "Side effects" on existing pile foundations.* Journal of Southeast Asian Geotechnical Society, April 2005, pp. 51-67.

Sagaseta, C. et al. (1997). *Deformation analysis of shallow penetration in clay.* International Journal for Numerical and Analytical Methods in Geomechanics, vol. 21, pp. 687-719.

Sagaseta, C. & Whittle, A. (2001). *Predictions of Ground Movements due to Pile Driving in Clay*. Journal of Geotechnical and Geoenviromental engineering, ASCE, vol. 127, issue 1, pp 55-66.

Sällfors, Göran (1993). *Handledning till laborationer i Geoteknik – Laboratorieundersökningar*. Chalmers University of Technology, Göteborg, Sweden.

Sällfors, Göran (2001). *Geoteknik, Jordmateriallära-Jordmekanik.* Göteborg, Sweden.

Sällfors, Göran (2008). *Basic concepts- Repetition*. Course literature in Geotechnics BOM045 2010. Chalmers University of Technology, Göteborg, Sweden.

White, D. t al. (2008). *Behavior of Slender Piles Subject to Free-Field Lateral Soil Movements.* Journal of Geotechnical and Geoenviromental engineering, ASCE, vol. 134, issue 4, pp 428-436.

Appendices

APPENDIX 1: EVALUATION OF SOIL TESTS

APPENDIX 2: FOUNDATION OF SKÄRAN

APPENDIX 3: DISPLACEMENTS ACCORDING TO HELLMAN/ REHNMAN

APPENDIX 4: HEAVE, COMPARISON OF GEOMETRICAL MODELS, A11

APPENDIX 5: CALCULATIONS OF THE PROPERTIES OF THE BRIDGE DECK AND COLUMNS OF SKÄRAN

APPENDIX 6: BOUNDARY CONDITIONS FOR THE BRIDGE SKÄRAN IN THE MODEL

APPENDIX 7: HEAVE, COMPARISON OF MATERIAL MODELS

APPENDIX 8: HEAVE, INFLUENCE OF PRE-AUGERING

APPENDIX 9: POLYNOMIAL APPROXIMATION OF DISPLACEMENTS

APPENDIX 10: EFFECT OF DOWN DRAG

APPENDIX 11: COMPARISON OF CALCULATION METHODS CONSIDERING PRE-BORING

Appendix 1. Evaluation of soil tests

Triaxial shear test

This equation can be used to determine the shear modulus from a triaxial shear test.

$q = 3G\varepsilon_q$ (Kullingsjö, 2007)

The result from the triaxial shear test is a graph describing how the deviator stress, $2\tau = (\sigma_1' - \sigma_3')$, varies with the vertical deformation, ε_v.

$$\varepsilon_q = \frac{2}{3}\sqrt{\frac{1}{2}\left((\varepsilon_{11}-\varepsilon_{22})^2 + (\varepsilon_{11}-\varepsilon_{33})^2 + (\varepsilon_{22}-\varepsilon_{33})^2 + 6\cdot(\varepsilon_{12}^2+\varepsilon_{13}^2+\varepsilon_{23}^2)\right)}$$

(Kulllingsjö, 2007)

$\varepsilon_p = \varepsilon_{11} + \varepsilon_{22} + \varepsilon_{33} = 0\ (undrained)$

$\varepsilon_{11} = \varepsilon_v$

$\varepsilon_{22} = \varepsilon_{33} \ \rightarrow \ \varepsilon_{22} = \varepsilon_{33} = -\frac{1}{2}\varepsilon_v$

$\varepsilon_{12} = \varepsilon_{13} = \varepsilon_{23} = 0$

$$\varepsilon_q = \frac{2}{3}\sqrt{\frac{1}{2}\left(\varepsilon_v + \frac{1}{2}\varepsilon_v\right)^2 + \left(\varepsilon_v + \frac{1}{2}\varepsilon_v\right)^2}$$

$\varepsilon_q = \varepsilon_v$

$$q = \sqrt{\frac{1}{2}\left((\sigma_{11}-\sigma_{22})^2 + (\sigma_{11}-\sigma_{33})^2 + (\sigma_{22}-\sigma_{33})^2 + 6\cdot(\sigma_{12}^2+\sigma_{13}^2+\sigma_{23}^2)\right)}$$

(Kullingsjö, 2007)

$\sigma_{12} = \sigma_{13} = \sigma_{23} = 0$

$\sigma_{11} = \sigma_v$

$\sigma_{22} = \sigma_{33} = \sigma_h$

$$q = \sqrt{\frac{1}{2}(\sigma_v - \sigma_h)^2 \cdot 2} = \sqrt{(\sigma_v - \sigma_h)^2} = \sigma_v - \sigma_h = 2\tau$$

$$2\tau = 3G\varepsilon_v \ \rightarrow G = \frac{2\tau}{3\varepsilon_v}$$

The shear modulus can also be determined by the following expression:

$E = 2G(1+\nu) \ \rightarrow G = \frac{E}{2(1+\nu)}$ (Larsson, 2008)

Direct shear test result evaluation

From the test result we get the τ-γ curve, which we want to translate into a q-ε_q curve to solve q=3Gε_q (Kullingsjö, 2007).

$$\varepsilon_q = \frac{2}{3}\sqrt{\frac{1}{2}([(\varepsilon_{11}-\varepsilon_{22})^2 + (\varepsilon_{11}-\varepsilon_{33})^2 + (\varepsilon_{22}-\varepsilon_{33})^2 + 6\cdot(\varepsilon_{12}^2+\varepsilon_{13}^2+\varepsilon_{23}^2)])}$$

In the direct shear test the specimen is subjected only to shear strain in one direction, ε_{12}. The other strains are zero.

$$\varepsilon_{11} = \varepsilon_{22} = \varepsilon_{33} = 0$$

$$\varepsilon_{13} = \varepsilon_{23} = 0$$

$$\varepsilon_{12} = \varepsilon_{21}$$

$$\varepsilon_{12} + \varepsilon_{21} = \gamma_{12} \implies \varepsilon_{12} = \frac{1}{2}\gamma_{12}$$

$$\varepsilon_q = \frac{2}{3}\sqrt{\frac{1}{2} \cdot 6 \cdot \left(\frac{1}{2} \cdot \gamma_{12}\right)^2} \Leftrightarrow \varepsilon_q = \frac{1}{\sqrt{3}} \cdot \gamma_{12}$$

In the same way all stresses except for one is equal to zero.

$$q = \sqrt{\frac{1}{2} \cdot [(\sigma_{11} - \sigma_{33})^2 + (\sigma_{11} - \sigma_{22})^2 + (\sigma_{22} - \sigma_{33})^2 + 6 \cdot (\sigma_{12}^2 + \sigma_{23}^2 + \sigma_{31}^2)]}$$

$$\sigma_{11} = \sigma_{22} = \sigma_{33} = 0$$

$$\sigma_{23} = \sigma_{31} = 0$$

$$\sigma_{12} = \tau_{12}$$

$$q = \sqrt{\frac{1}{2} \cdot 6 \cdot \tau_{12}^2} = \sqrt{3}\tau_{12}$$

$$q = 3 \cdot G \cdot \varepsilon_q \implies G = \frac{q}{3 \cdot \varepsilon_q} = \frac{\sqrt{3}\tau_{12}}{3 \cdot \frac{1}{\sqrt{3}} \cdot \gamma_{12}} = \frac{\tau_{12}}{\gamma_{12}}$$

So from the curves from the test, the modulus G_{50} is found as the gradient of the line from (0,0) through the point $0{,}5 \cdot \tau_{fu}$.

Appendix 2. Foundation of Skäran

Table A- 1 Pile lengths in the three modelled supports of Skäran

Support:	No. piles	Pile length [m]
2	**12**	**71**
	11	**69**
3	**11**	**65**
	12	**62**
4	**10**	**59**
	12	**63**

Appendix 3. Displacements according to Hellman/ Rehnman

Phase 1, Southern part of A17

Input:

Number of piles:	24	
Width:	0,275	m
Length (d):	59,33	m
Width of pre-boring:	0,275	m
Length of pre-boring:	10	m
Effectivity	1	
Pre-bored volume:	0,76	m^3
Number of pre-boring holes:	24	

V_{piles}: 108 m^3

$V_{pre\text{-}boring}$: 18 m^3

Geometry of the piling area:

Length (l): 14,1 m

Width (b): 5,7 m

Heave factors	
α	1,0
β	1,0
γ	1,0
δ	1,0
η:	1,0

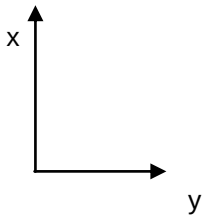

η*(V_{piles}-$V_{pre\text{-}boring}$)= 90

($\alpha+\beta$)*(l/2+d/3): 54

y($\gamma+\delta$)*(b/2+d/3): 45

(b*l)/d: 1,4

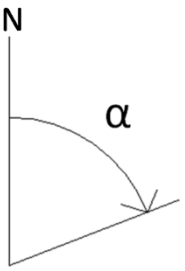

x=(h*(Vpiles-Vpre-boring))/(d*((a+b)*(l/2+d/3)+(g+d)*(b/2+d/3)+(b*l)/d)) 0,015 m

Heave in the center of the piling area

					Horizontal displacement		
Distance [m]	**Heave [mm]**		**Heave [mm]**	**Support**	**α [°]**	**Δx**	**Δy**
51,12	2	S2, corner 1	3	S 2	1	3,1	0,1
47,57	3	S2, corner 2					
42,70	4	S2, corner 3					
46,29	3	S2, corner 4					
33,56	7	S3, corner 1	8	S 3	28	6,7	3,6
30,38	7	S3, corner 2					
24,98	9	S3, corner 3					
28,16	8	S3, corner 4					
28,22	8	S4, corner 1	8	S 4	64	3,3	6,8
34,41	6	S4, corner 2					
30,40	7	S4, corner 3					
24,20	9	S4, corner 4					

Phase 2, Phase 3 and Phase 4 are calculated in the same manner.

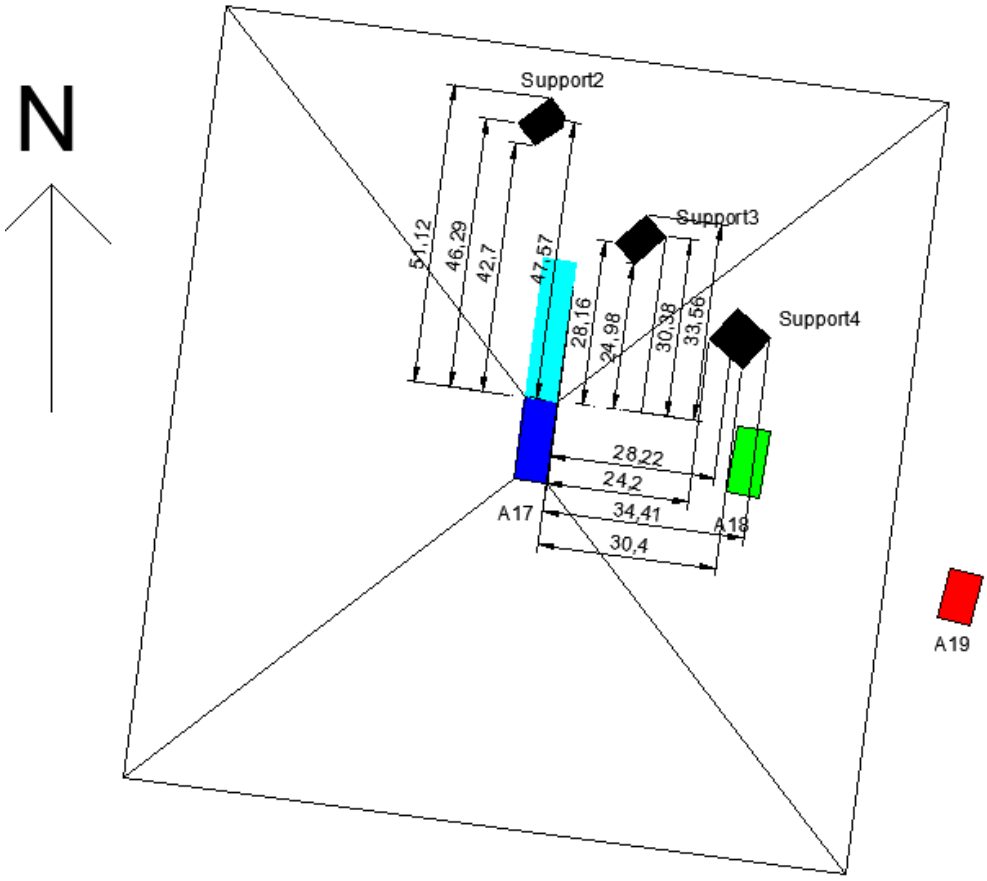
N
Support2
Support3
Support4
51,12
46,29
42,7
47,57
28,16
24,98
30,38
33,56
28,22
24,2
34,41
30,4
A17
A18
A19

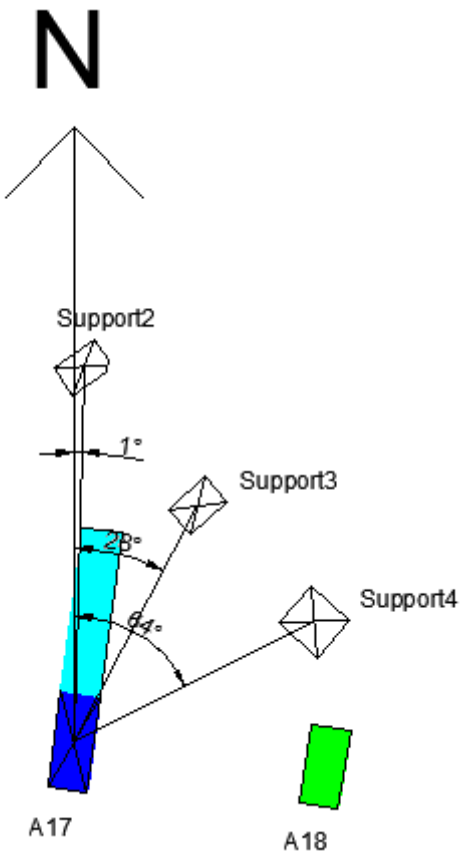
N
Support2
1°
Support3
28°
64°
Support4
A17
A18

Heave [mm]

		Phase 1	Phase 2	Phase 1+2	Phase 3	Phase 1+2+3	Phase 4	Total:
Support 2	2	3	4	7	0	7	17	24
Support 3	3	8	7	15	0	15	22	37
Support 4	4	8	10	18	3	20	14	34

Horizontal displacement

	Phase 1				Phase 2				Phase 1+2			
	Δx	**Δy**	**horizontal displacement**	**α**	**Δx**	**Δy**	**horizontal displacement**	**α**	**Δx**	**Δy**	**horizontal displacement**	**α**
Support 2	3,15	0,05	3,15	1,00	3,30	-1,98	3,84	-31,00	6,44	-1,92	6,72	-16,63
Support 3	6,73	3,58	7,63	28,00	6,51	-3,18	7,25	-26,00	13,25	0,40	13,25	1,75
Support 4	3,34	6,85	7,62	64,00	9,93	-0,69	9,95	-4,00	13,26	6,15	14,62	24,88

	Phase 3				Phase 1+2+3				Phase 4			
	Δx	**Δy**	**horizontal displacement**	**α**	**Δx**	**Δy**	**horizontal displacement**	**α**	**Δx**	**Δy**	**horizontal displacement**	**α**
Support 2	0,00	0,00	0,00	0	6,44	-1,92	6,72	-16,63	16,75	-0,58	16,76	-2,00
Support 3	0,00	0,00	0,00	0	13,25	0,40	13,25	1,75	15,57	15,57	22,01	45,00
Support 4	2,00	-1,68	2,62	-40,00	15,27	4,47	15,91	16,32	-0,74	14,12	14,14	-87,00

	Total			
	Δx	**Δy**	**horizontal displacement**	**α**
Support 2	23,19	-2,51	23,32	-6,18
Support 3	28,81	15,97	32,94	29,00
Support 4	14,53	18,59	23,60	52,00

Appendix 4. Heave, comparison of geometrical models, A11

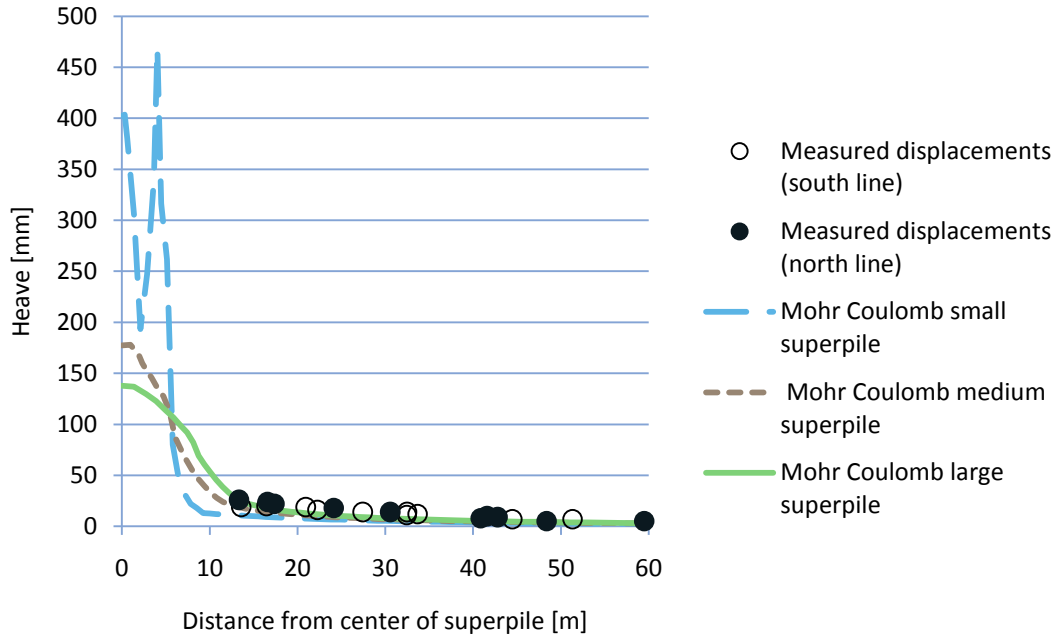

Figure A- 1 Comparison of heave, different geometrical models.

Appendix 5. Calculations of the properties of the bridge deck and columns of Skäran

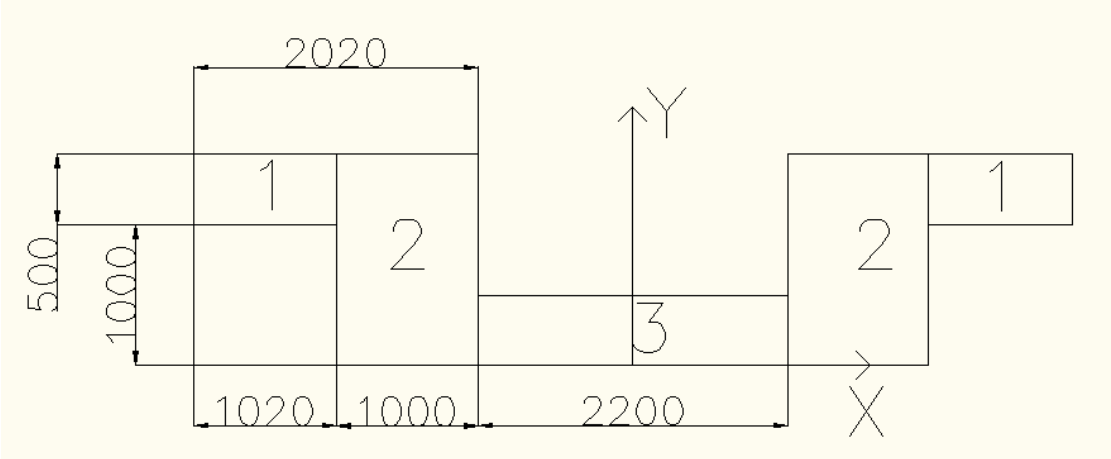

Figure A- 2 Simplified geometry of the bridge deck of Skäran.

Bridge deck

	Part 1	Part 2	Part 3		
b_x	1,02	1,00	2,20		
h_x	0,50	1,50	0,50		
x_{tp}	2,61	1,60	0,00		
b_y	0,50	1,50	0,50		
h_y	1,02	1,00	2,20		
y	1,25	0,75	0,25		
y_{tp}	0,51	0,01	-0,49	y_{tot}	0,742188

I_{x1}	0,14	
I_{x2}	0,28	
I_{x3}	0,29	
I_x	**1,14**	**Corresponds to I_3 in PLAXIS**

I_{y1}	3,52	
I_{y2}	3,97	
I_{y3}	0,44	
I_y	**15,41**	**Corresponds to I_2 in PLAXIS**

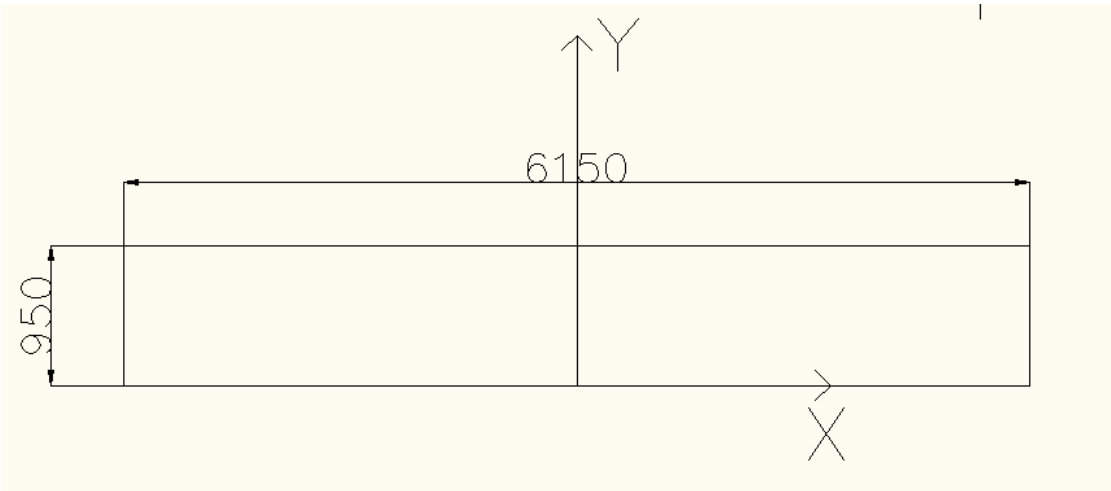

Figure A- 3 Simplified geometry of the columns of Skäran.

Columns

b_x	6,15
h_x	0,95
b_y	0,95
h_y	6,15
A	5,84

I_x	**0,44**
I_y	**18,41**

Appendix 6. Boundary conditions for the bridge Skäran in the model

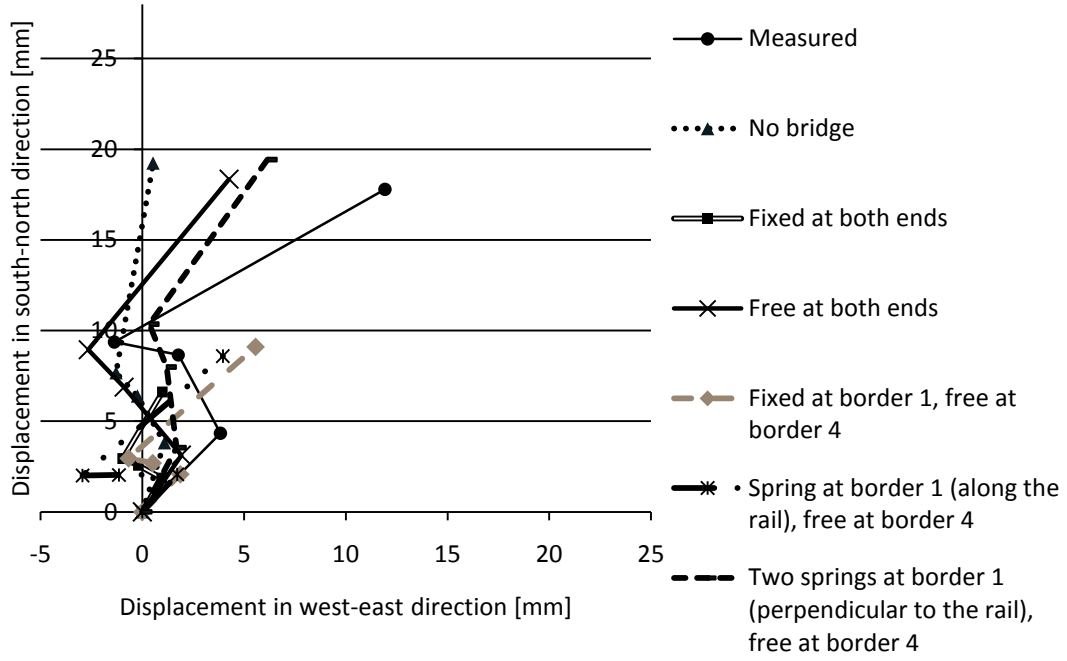

Figure A- 4 Support 2, boundary conditions for the bridge Skäran.

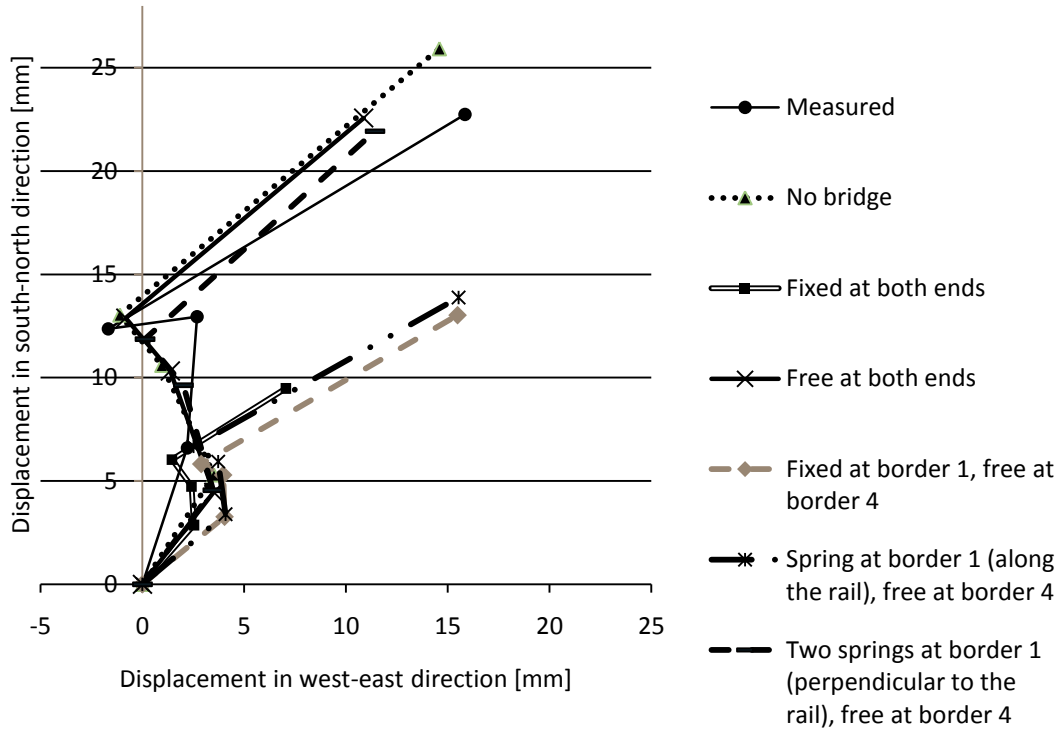

Figure A- 5 Support 3, boundery conditions for the bridge Skäran.

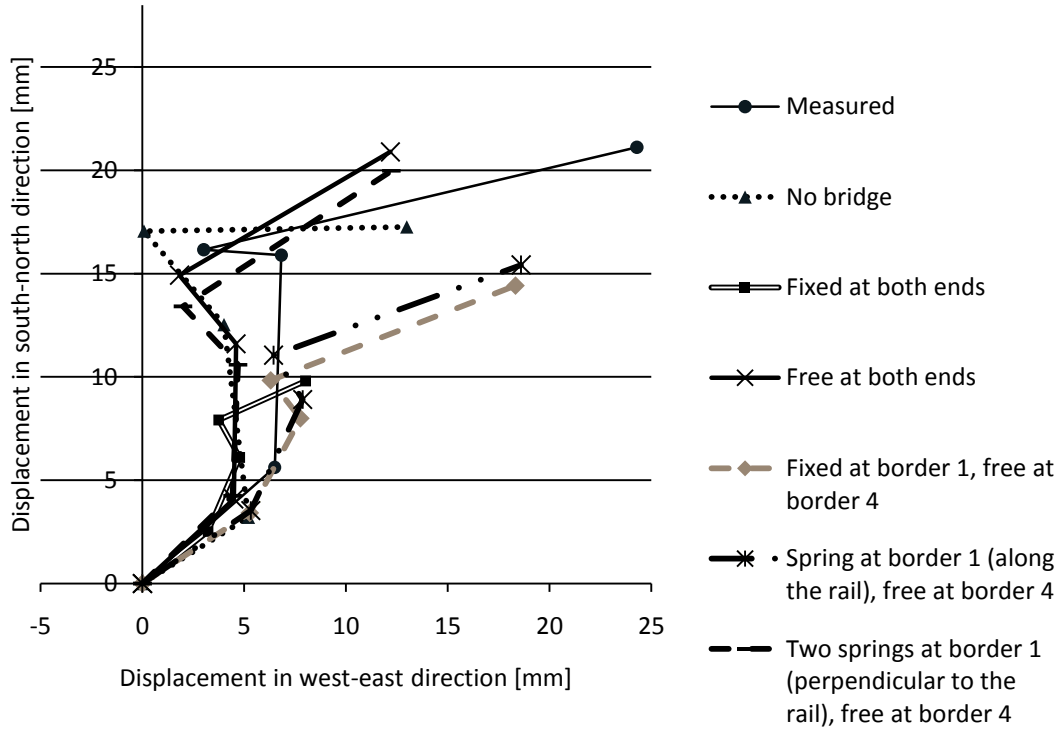

Figure A- 6 Support 4, boundary conditions for the bridge Skäran

Appendix 7. Heave, comparison of material models

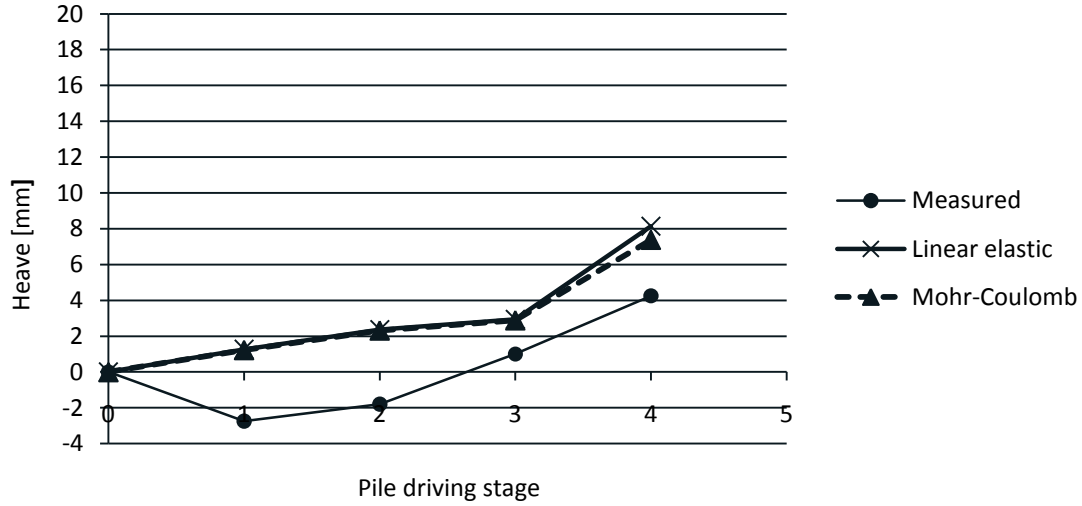

Figure A- 7 Support 2: Heave, comparison of material models.

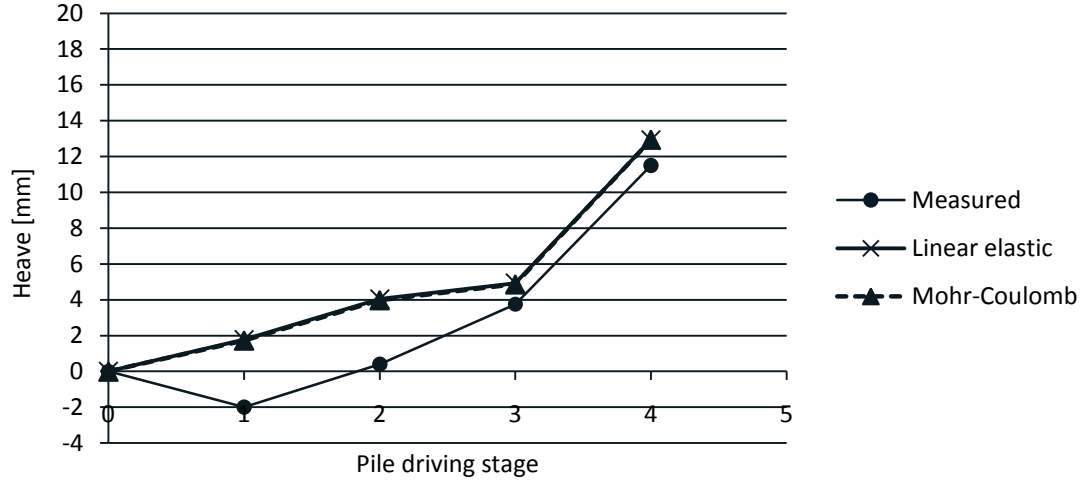

Figure A- 8 Support 3: Heave, comparison of material model.

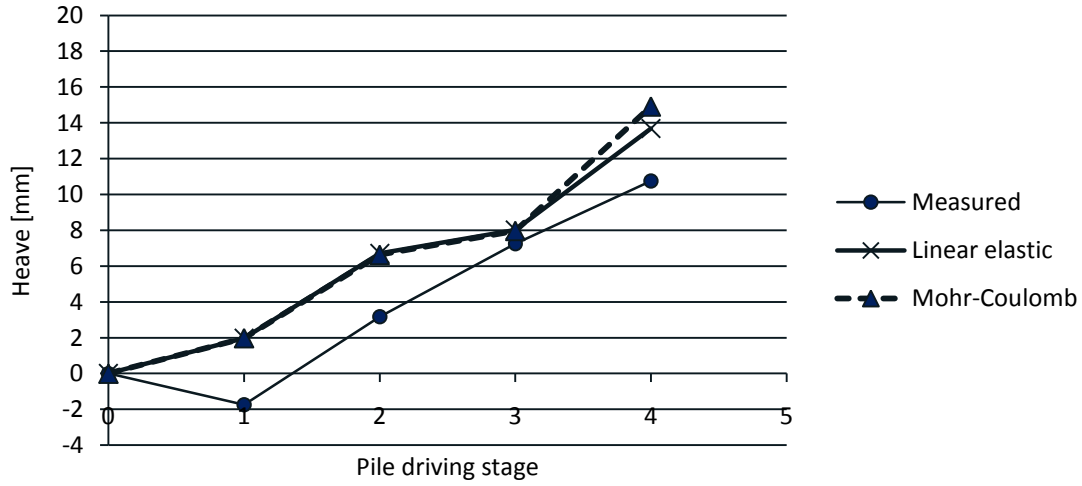

Figure A- 9 Support 4: Heave, comparison of material models.

Appendix 8. Heave, influence of pre-augering

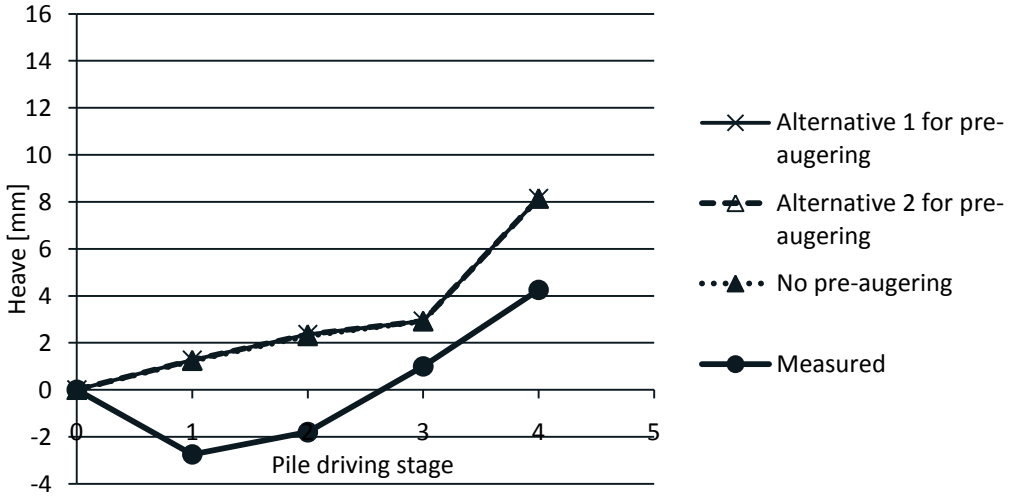

Figure A- 10 Heave at support 2, with and without pre-augering.

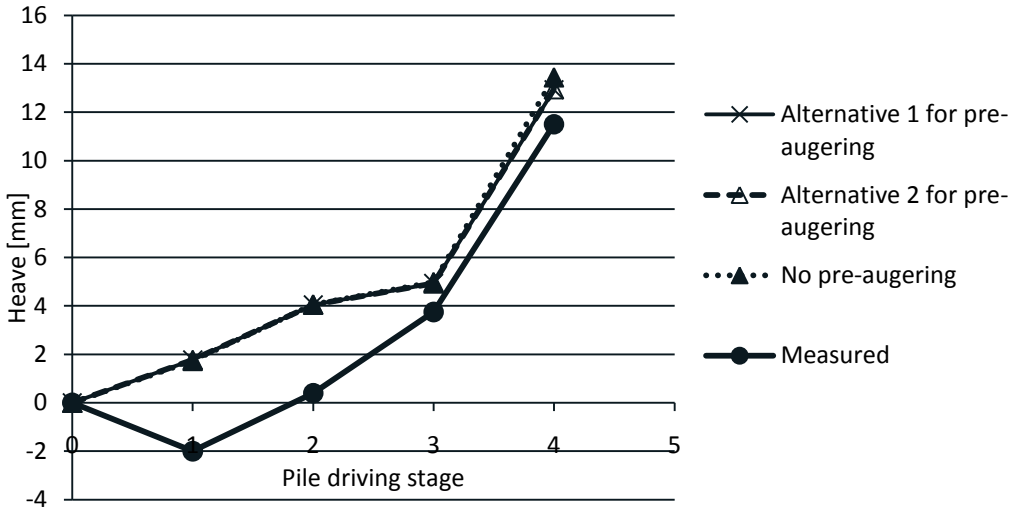

Figure A- 11 Heave at support 3, with and without pre-augering.

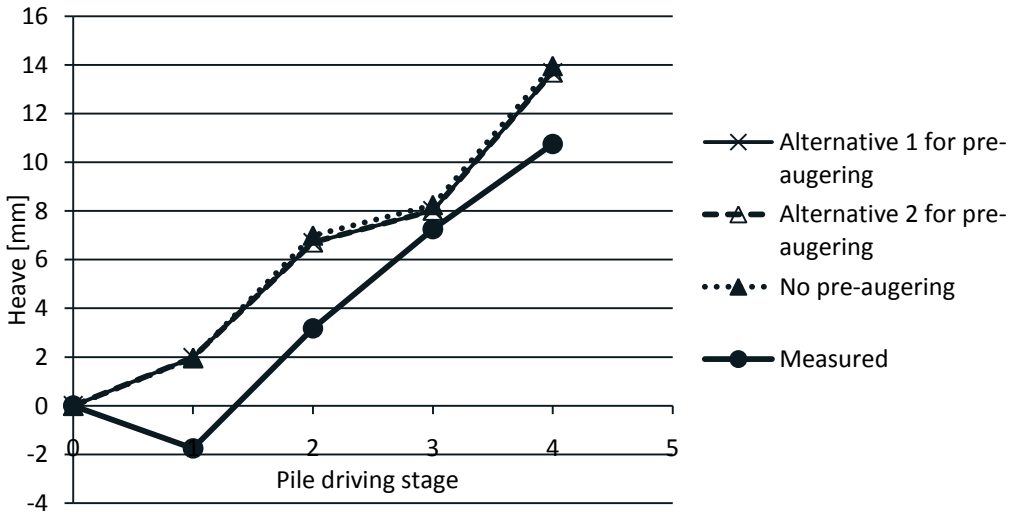

Figure A- 12 Heave at support 4, with and without pre-augering.

Appendix 9. Polynomial approximation of displacements

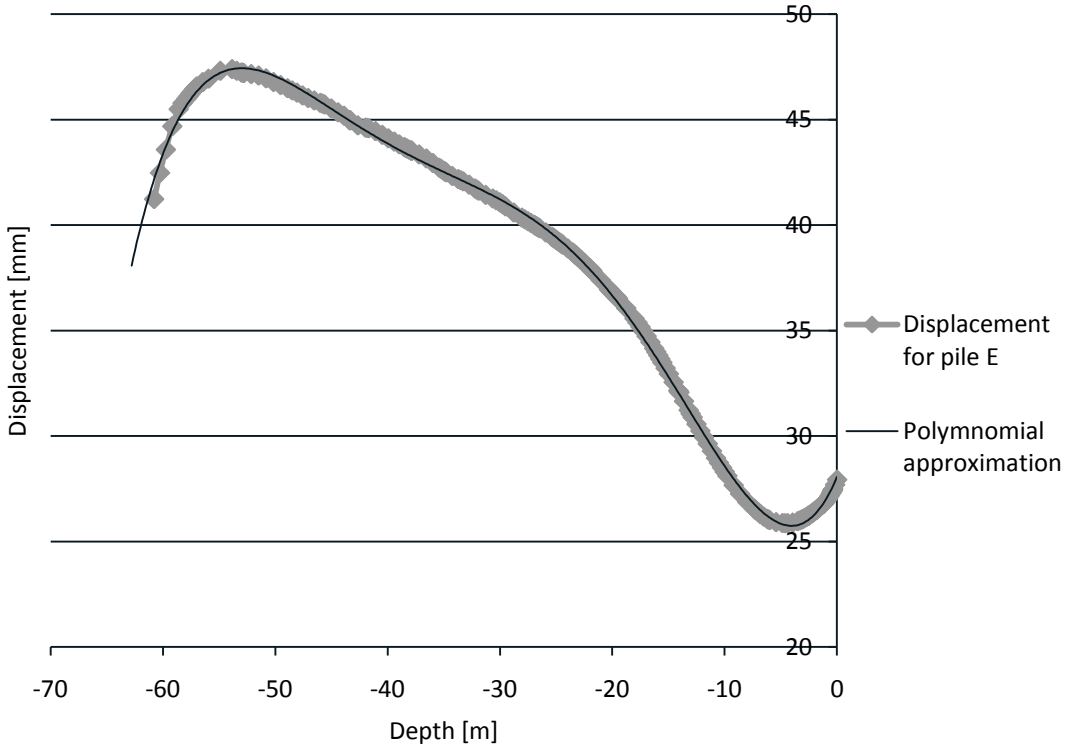

Figure A- 13 Polynomial approximation for the displacements of pile E.

The equation for the polynomial is:

$$y = 1{,}6 * 10^{-9}x^6 + 1{,}2 * 10^{-6}x^5 + 1{,}6 * 10^{-4}x^4 + 8{,}8 * 10^{-3}x^3 + 2{,}0 * 10^{-1}x^2 + 1{,}3x + 28{,}1 \quad \text{A-1}$$

The approximations for pile A, B, C, and D were done in the same way.

Appendix 10. Effect of down drag

$z := 0..65$

$L := 65$

$u := 4 \cdot 0.275$

$$E(z) := \int_0^z 11 + 1.5u \, du$$

$$R(z) := \int_z^L 11 + 1.5u \, du$$

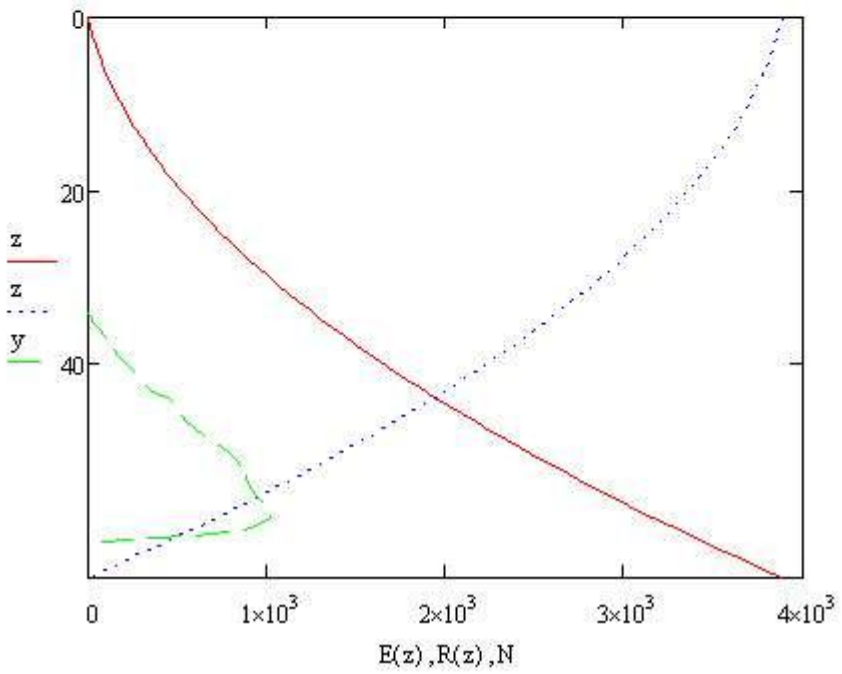

Figure A- 14 Effect of down drag (continuous line to neutral layer and then dotted line) according to Alén (2009) compared to tensile force (dashed line) in pile E

The effect of down drag, compression, is larger than the tensile force in the pile except near the foot of the pile. The total effect on the pile is the difference between the two forces, and only small tensile forces will occur.

Appendix 11. Comparison of calculation methods considering pre-boring